Master Thesis in Reservoir Chemistry

Influence of Residual Oil on Polymer Injectivity

Jørgen Gausdal Jacobsen

Department of Chemistry

uniCIPR

Centre for Integrated Petroleum Research

University of Bergen

June 2017

Acknowledgement

First of all, I would like to express my sincere gratitude towards my supervisor, Professor Arne Skauge, for his excellent guidance and support during the course of this thesis.

Both Nematollah Zamani and Iselin Salmo have provided me with sound advice and technical support throughout my simulation work, and I will always be grateful for their help.

I would also like to thank the Centre for Integrated Petroleum Research for providing me with a great working environment.

Furthermore, I would like to thank my fellow students Lars Christian Kjær and Tonje Nielsen for countless discussions, on and off topic, the past year. They have made my final year as a master student much better than I could ever have hoped for.

Finally, I would like to thank my family and friends for their motivation and encouragement, where special thanks go to my mother and father who have always supported and believed in me.

Jørgen Gausdal Jacobsen

Bergen, June 2017

Abstract

Because a significant fraction of the world's light oil reservoirs has already been produced, the technical and economic challenges of developing heavy oil fields is now unavoidable [1]. Water flooding has proven to be a less than adequate recovery mechanism for heavy oil fields, due to the unfavorable mobility ratio between water and oil, resulting in poor volumetric sweep efficiencies and low ultimate recovery factors. Consequently, reservoirs containing viscous crudes have reported recoveries of less than 20% when utilizing water flooding as the recovery mechanism. Therefore, it is evident that there exists a huge potential for additional recovery by implementing improved oil recovery (IOR) projects, especially by employing enhanced oil recovery (EOR) methods.

Polymer flooding has gained increased attention during the last decades. Several field scale pilot projects have been implemented in heavy oil reservoirs with a varying degree of success [2] [3]. During polymer flooding, polymers are added to the injection brine to impart a viscosity increase of the corresponding polymer solution. This will increase the mobility of the drive fluid, and the mobility ratio between the displacing and displaced fluid will be more favorable. However, there are challenges concerning polymer flooding. The viscosity increasing feature of the polymer solution frequently induce large injection pressures and consequently may have detrimental effects on injectivity. Injectivity damage resulting from polymer flooding will in some instances require drilling of additional wells. This may negatively affect the economic feasibility of a polymer flood project [4].

Also, polymer loss due to retention mechanisms is a major economic expenditure in polymer flooding projects and will in most instances influence the decision making in relation to polymer flood implementation [5].

The synthetic polymer partially hydrolyzed polyacrylamide (HPAM) has been extensively used for polymer flood projects due to its low production costs and beneficial rheological properties [3], and is the only polymer investigated in this thesis.

The rheological properties of HPAM in porous media have been investigated extensively, where mechanical degradation has been established as very probable when being subjected to the high shear rates experienced in an injection well [6]. Most of the research on HPAM in porous media have been carried out in linear core plugs, where the results from these studies have been considered transferable to flow in radial geometries. Recent research however,

suggest that polymer flow is significantly different in linear versus radial models [7]. HPAM injectivity in porous media may therefore be underestimated based on linear core studies.

The principal aim of this thesis is to investigate effects of residual oil on polymer injectivity in radial models. In addition, the relationship between polymer concentration and rheological behavior in presence of residual oil will be assessed and compared to conditions in absence residual oil.

In this thesis, a polymer flood experiment conducted in a radial disc saturated with residual oil will be history matched. These results will subsequently be compared to previously history matched results from experimental conditions in absence of residual oil.

Three water floods and two polymer floods was history matched, whereas two different polymer concentrations (800 and 2000ppm) in the semi-dilute regime were investigated. A sequential order of alternating water and polymer floods enabled a permeability estimation both prior and post polymer flooding.

History match results were obtained using two different simulator tools: STARS and MRST, respectively. Results from both simulator tools was consistent and thus will increase the confidence of obtained results.

A sensitivity analysis was conducted to investigate the effect of different parameters on the STARS simulation tool. Several simulation model parameters such as grid block length and maximum timestep was investigated. In addition, polymer and fluid flow properties were assessed, which include: Molecular weight, viscosity, adsorption, adsorption reversibility, inaccessible pore volume, concentration, residual resistance factor and endpoint relative permeability.

Current literature suggests that if porous media is first contacted with a low concentration HPAM solution that satisfies retention, no significant additional retention occurs when exposed to higher concentrations. In contrast, permeability determination both before and after polymer flooding revealed that additional retention occurred when the porous media was exposed to a higher concentration solution.

In agreement with previously reported retention results in presence versus absence of residual oil, the amount of retention in presence of residual oil was reduced. However, this reduction was far greater than previous literature suggests.

Both polymer concentrations exhibited strong shear thinning and shear thickening behavior in presence of residual oil. The highest polymer concentration was mechanically degraded during porous media propagation and the shear thinning behavior was inconsistent with previous literature. An effect of concentration on HPAM rheology was to shift the onset of shear thickening towards higher values with increasing polymer concentrations. This occurrence is not in agreement with previously obtained results.

A comparison of bulk and in-situ viscosity of the highest concentration polymer was performed. Results revealed that in-situ viscosity was below bulk viscosity in the lower shear rate region. This is inconsistent with previously reported literature in the semi-dilute regime.

An increase in HPAM concentration resulted in reduced injectivity values. However, this reduction was expected based on polymer rheology and presence of residual oil did not amplify the effect of concentration on injectivity.

Simulation results showed that even though the absolute viscosity values of HPAM was severely reduced in presence of residual oil, the permeability decrease experienced during two-phase flow dominated. Thus, the overall effect of residual oil was to reduce injectivity of HPAM when varying flow conditions of the two experiments was not taken into consideration. However, since the isolated effect of residual oil on polymer injectivity was of primary concern in this thesis, injectivity in both absence and presence of residual oil was scaled according to corresponding brine injectivities, thus excluding experimental condition effects.

The isolated effect of residual oil was to increase injectivity of HPAM significantly. Based on results obtained in this thesis, it may seem that injectivity estimation based on results from core floods in absence of residual oil may underestimate polymer injectivity.

Nomenclature

Variables

A	Area	$[m^2]$
c	Concentration	[ppm]
D_e	Deborah number	dimensionless
$\frac{dP}{dx}$	Pressure drop over distance x	$[Pa \cdot m^{-1}]$
$\frac{dP}{dr}$	Pressure drop over radius r	$[Pa \cdot m^{-1}]$
$\frac{dV}{dr}$	Velocity gradient over distance	$[s^{-1}]$
E_A	Areal sweep efficiency	dimensionless
E_D	Microscopic displacement efficiency	dimensionless
E_R	Recovery factor	dimensionless
E_V	Vertical sweep efficiency	dimensionless
E_{vol}	Volumetric displacement efficiency	dimensionless
F	Force	$[N]$
g	Gravitational constant	$[m^3 \cdot kg^{-1} \cdot s^{-2}]$
h	Height	$[m]$
I	Injectivity	$[m^3 \cdot s^{-1} \cdot Pa^{-1}]$
I_s	Ionic strength	$[mole \cdot L^{-1}]$
K	Absolute permeability	$[m^2]$ $(1D = 0{,}98692 \cdot 10^{-12}\ m^2)$
K	Power law constant	dimensionless
$k_{e,i}$	Effective permeability of phase i	$[m^2]$ $(1D = 0{,}98692 \cdot 10^{-12}\ m^2)$
$k_{r,i}$	Relative permeability of phase i	dimensionless

L	Length	$[m]$
M	Mobility ratio	dimensionless
M^0	Endpoint mobility ratio	dimensionless
M_w	Molecular weight	[Da]
n	Power law index	dimensionless
N	Volume of oil originally in place	$[m^3]$
N_p	Volume of oil produced	$[m^3]$
N_{vc}	Capillary number	dimensionless
P	Pressure	$[Pa]$
p_e	Production well pressure	$[Pa]$
p_w	Injection well pressure	$[Pa]$
Q	Volumetric injection rate	$[m^3 \cdot s^{-1}]$
r	Radius	$[m]$
r_w	Injection well radius	$[m]$
R_F	Resistance factor	dimensionless
R_k	Permeability reduction factor	dimensionless
R_{RF}	Residual resistance factor	dimensionless
S	Saturation	dimensionless
t	Time	[s]
u	Darcy velocity	$[m \cdot s^{-1}]$
V	Volume	$[m^3]$
V	Velocity	$[m \cdot s^{-1}]$
z	Ionic valence	dimensionless
Δ	Difference	dimensionless

$\dot{\gamma}$	Shear rate	$[s^{-1}]$
θ_f	Relaxation time of the polymer fluid	$[s]$
θ_p	Duration time of a process	$[s]$
λ	Mobility	$[m^2 \cdot Pa^{-1}s^{-1}]$
λ^0	Endpoint mobility	$[m^2 \cdot Pa^{-1}s^{-1}]$
λ	Time constant (power law)	$[s]$
μ	Shear independent viscosity	$[cP]$ $(1cP = 10^{-3}Pa \cdot s)$
η	Shear dependent viscosity	$[cP]$ $(1cP = 10^{-3}Pa \cdot s)$
ρ	Density	$[kg \cdot m^{-3}]$
σ	Interfacial tension	$[N \cdot m^2]$
τ	Shear stress	$[Pa]$
Γ	Retention level	$[\mu g/g]$
Γ_m	Retention	$[lb/AF]$
ϕ	Porosity	dimensionless
α'	Shape parameter of pore structure	dimensionless

Subscripts

a	after
app	apparent
abs	absolute
b	bulk
b	brine
c	critical
D	microscopic

eff	effective
e	effective
e	disc
F	factor
g	gas
i	component (phase)
i	initial
i	irreducible
max	maximum
o	oil
p	polymer
p	pore
pm	porous media
r	radial distance
r	relative
r	residual
r	rock
res	residual
R	recovery
RF	resistance factor
vol	volumetric
w	water
w	well
∞	infinite

0	zero

Abbreviations

CDC	Capillary Desaturation Curve
CF	Capillary force
CIPR	Centre for Integrated Petroleum Research
CMG	Computer Modelling Group Ltd.
EnKF	Ensemble Kalman Filter
EOR	Enhanced oil recovery
IOR	Improved oil recovery
IPV	Inaccessible pore volume
IWF	Initial water flood
HPAM	Hydrolyzed polyacrylamide
MRST	MATLAB Reservoir Simulation Toolbox
MW	Molecular weight
NCS	Norwegian Continental Shelf
PF	Polymer flood
ppm	Parts per million
SWF	Secondary water flood
TDS	Total Dissolved Solids
TWF	Tertiary water flood
VF	Viscous force
WF	Water Flood

Table of Contents

List of Figures

List of Tables

1 INTRODUCTION

As global energy demand grows and conventional oil reserves are depleted, EOR is becoming increasingly important [3]. A large fraction of the sedimentary basins that might contain oil have already been explored. Since the reported global average recovery factor for oil is only about 22%, the necessity to employ EOR methods to satisfy future energy demands is therefore evident [8].

The average recovery factor on the Norwegian Continental Shelf (NCS) is estimated at 45% [9]. This is well above the global average and has been achieved mainly by employing secondary water flooding as the recovery mechanism. At present, a large quantity of the fields on NCS are either in the tail production phase or consist of reservoirs containing heavy oils. To extend the lifetime of these fields, EOR projects needs to be considered.

The terms IOR and EOR are often used interchangeably since the distinction between them is not very sharp and unambiguous. While IOR usually is defined in a very broad manner as all economic measures that are intended to improve the oil recovery factor and/or accelerate reserves, EOR is more related to the use of unconventional recovery methods [10]. A common definition of EOR may be stated as tertiary oil recovery by the injection of materials not normally present in the reservoir. This definition excludes water flooding from being classified as an EOR method.

It is essential to avoid a rapid pressure decrease during production to achieve a high recovery factor. For reservoirs containing light oils pressure maintenance is achieved mainly by secondary water injection. However, this mechanism is often not adequate for heavy oil reservoirs. Water flooding in heavy oil fields will often result in an unstable displacement due to unfavorable viscosity ratios and a consequent reduction in recovery factor is observed. To remediate the problems associated with unfavorable mobility ratios, the mechanism of polymer flooding may be implemented.

Because it has a higher success rate, polymer flooding is the most commonly applied chemical EOR technique [3]. Polymer flooding as an EOR method for oil recovery was first proposed by Pye and Sandiford in 1964, where they established the fact that when polymer (HPAM) was added in very small amounts to the brine used in water flooding, the consequent increase in viscosity was substantial [11]. The viscosity increasing feature of polymers gives rise to a more favorable mobility ratio between water and oil, resulting in a higher degree of sweep efficiency

and improved/accelerated recovery [12]. However, this viscosity increase will reduce polymer injectivity and is a major concern when considering polymer flood projects [13].

The two most commonly used polymers for polymer flooding purposes are HPAM and Xanthan [3], whereas HPAM will be the polymer exclusively investigated in this thesis.

The rheological behavior of HPAM has been extensively studied during the past few decades. These studies and their consequent conclusions has assumed that results obtained in linear models are transferable to radial models. However, recent research of polymer rheology in radial versus linear models have suggested that this transferability cannot be utilized [7]. Based on these recent results, injectivity have been suggested to be underestimated from linear core floods and the need to investigate this suggestion is evident.

The effect of residual oil on both polymer rheology and injectivity has been given little attention in the literature. It is therefore the objective in this thesis to investigate how polymer rheology and retention will be influenced by residual oil and on their collective effect on polymer injectivity.

2 BASIC THEORY

The purpose of this chapter is to introduce some basic theory required to fully understand this simulation thesis.

2.1 Enhanced Oil Recovery

A common aspect and major disadvantage for primary recovery mechanisms is rapid and inevitable decrease in reservoir pressure, resulting in both low production rates and recovery factors [12].

The most commonly applied secondary recovery method is water flooding, which has been especially successful for light oil reservoirs on the NCS [10]. The background for this choice of recovery mechanism is easy access to water offshore and low costs associated with its implementation, together with relatively high recovery factors [14]. A significant drawback of water flooding is poor displacement efficiency for higher viscous crudes and poor volumetric sweep efficiency in heterogenous reservoirs. For this reason, implementation of EOR techniques have gained increased attention over the past few decades.

The aim of EOR is to achieve an additional recovery of oil (10-35%) by remobilizing capillary trapped oil that remains in the reservoir after initial pressure depletion and secondary water injection, thus reducing residual oil saturation in both contacted and uncontacted zones [15]. The term EOR includes thermal techniques, non-thermal techniques such as electrical, miscible, steam or chemical techniques for enhanced recovery of oil remaining in place [16].

The recovery factor, E_R, is defined as the ratio of the volume of oil produced and oil originally in place [17]:

$$E_R = \frac{N_p}{N} = E_D \; x \; E_{vol} = E_D \; x \; E_A \; x \; E_V \tag{2.1}$$

Where:

N_p: Volume of oil produced

N: Volume of oil originally in place

E_D = Microscopic displacement efficiency = $\frac{volume\ oil\ displaced}{volume\ oil\ contacted}$

E_{vol} = Volumetric displacement efficiency = E_A x E_V = $\frac{volume\ oil\ contacted}{volume\ oil\ in\ place}$

E_A = Areal sweep efficiency = $\frac{Area\ contaced\ by\ displacing\ fluid}{Total\ area}$

E_V = Vertical sweep efficiency = $\frac{Cross-sectional\ area\ contacted\ by\ displacing\ fluid}{Total\ cross-sectional\ area}$

A schematic of volumetric sweep efficiency in a layered reservoir is shown in Figure 2.1.

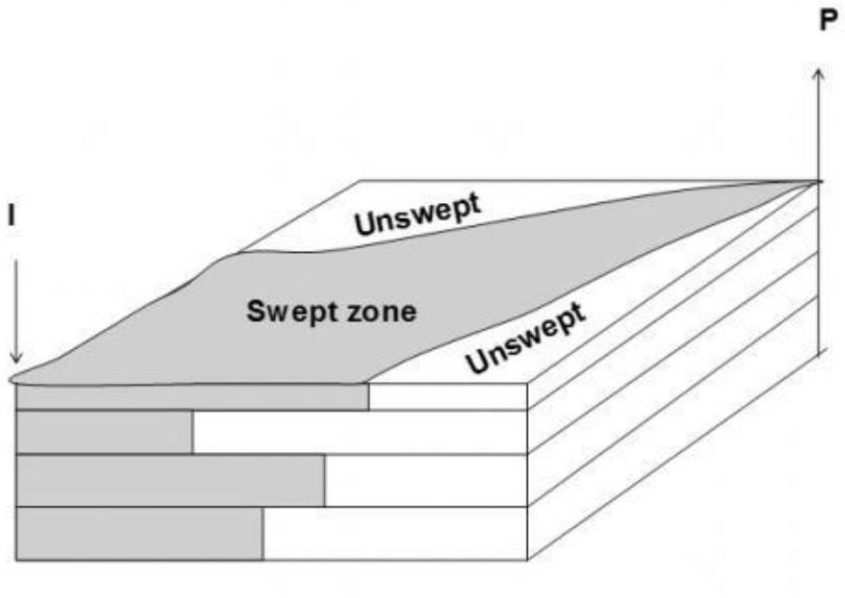

Figure 2.1: Sweep efficiency schematic (Skarestad, M. and Skauge, A.) [10].

Both areal and vertical sweep efficiencies may be significantly increased by adding polymers to the injection brine. However, microscopic displacement efficiency is not considered to be affected by polymer flooding although, recent research contradicts this assumption. Effects of polymer flooding on microscopic displacement efficiency will be discussed further in chapter 2.5.

2.2 Mobility

It is a necessity to introduce the idea of mobility ratio to appreciate how the situation for water flooding may be remedied using polymer [12].

Mobility is a measure of the flow of a fluid through a permeable formation [18]. In general, the mobility of a fluid is defined as the ratio between effective permeability and its viscosity [19]:

$$\lambda_i = \frac{k_{e,i}}{\mu_i} = \frac{Kk_{r,i}}{\mu_i}, i = water, oil, gas \quad (2.2)$$

Where λ_i is mobility, $k_{e,i}$ is effective permeability, μ_i is viscosity, K is absolute permeability and $k_{r,i}$ is relative permeability.

Mobility ratio, M, is defined as the mobility of the displacing to the displaced fluid, respectively:

$$M = \frac{\lambda_{displacing}}{\lambda_{displaced}} \quad (2.3)$$

For a water flood, mobility ratio may be written as:

$$M = \frac{\lambda_w}{\lambda_o} = \frac{k_{r,w}\mu_o}{k_{r,o}\mu_w} \quad (2.4)$$

Predominantly, mobility ratio is defined in terms of endpoint relative permeability values:

$$M^0 = \frac{\lambda_w^0}{\lambda_o^0} = \frac{k_{rw,or}\mu_o}{k_{ro,iw}\mu_w} \quad (2.5)$$

Where M^0 is endpoint mobility ratio, λ_w^0 and λ_o^0 is endpoint mobility for water and oil, respectively, and $k_{rw,or}$ and $k_{ro,iw}$ is endpoint relative permeability for water and oil, respectively. $k_{rw,or}$ is defined as relative permeability of water at residual oil saturation, i.e. only water is flowing. Likewise, $k_{ro,iw}$ is defined as the relative permeability of oil at irreducible water saturation, i.e. only oil is flowing.

Endpoint mobility ratio has a significant effect on the ultimate microscopic displacement efficiency due to its influence on water breakthrough [10]. It is common to distinguish between three different scenarios of endpoint mobility ratios, as illustrated in Figure 2.2.

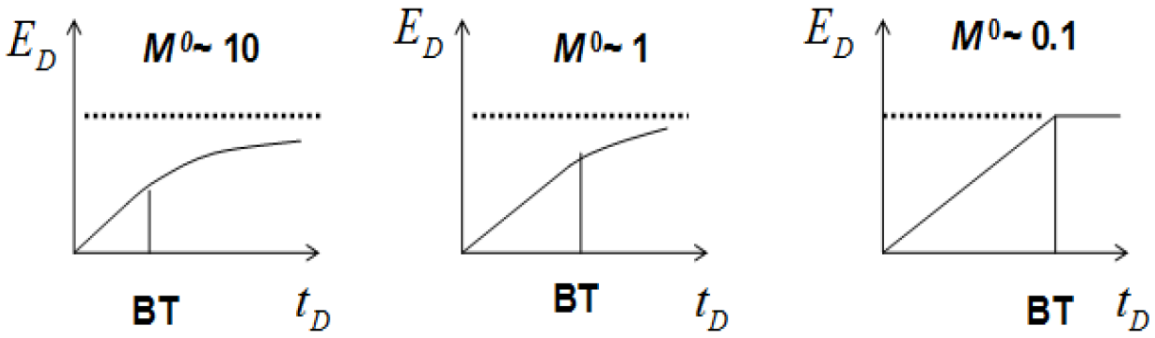

Figure 2.2: Illustration of the relationship between endpoint mobility ratio and microscopic displacement efficiency as a function of dimensionless time, where dashed lines represent ultimate microscopic recovery efficiency (Skarestad, M. and Skauge, A.) [10].

For high values of endpoint mobility ratio ($M^0 \sim 10$), water breakthrough will emerge at an early stage, resulting in a long tail production of oil. Intermediate values of endpoint mobility ratio ($M^0 \sim 1$) will lead to slower water breakthrough and a consequently smaller tail production of oil. The most desirable situation exists when endpoint mobility ratio is small ($M^0 \sim 0{,}1$), which will significantly delay water breakthrough and reduce tail production of oil.

The history matches performed in this thesis is based on an experiment where a radial disc saturated with residual oil was flooded alternatingly with water and polymer solutions. In total, five floods were conducted during the experiment, where two of them were polymer floods of varying concentrations. The viscosity of residual oil was equal to 250cP and is classified as a viscous crude.

Endpoint mobility ratio of all floods in the experiment was calculated (Table 2.1) using a reference viscosity value at 10 s^{-1}, obtained from bulk viscometric measurements (Table 7.3 and Table 7.4). Since all three water floods attained the same value of M^0, they are collectively referred to as Water Floods in Table 2.1.

Table 2.1: Endpoint mobility ratio of water and polymer floods in the history matched experiment.

M^0 Water Floods	M^0 800ppm HPAM Flood	M^0 2000ppm HPAM Flood
~ 13	~ 0,8	~ 0,1

As seen from Table 2.1, an unfavorable endpoint mobility ratio of 13 is obtained when flooding highly viscous oil with water. As mentioned, this will result in an early water breakthrough and a long tail production of oil. The left part of Figure 2.2 illustrates this situation.

The 800ppm HPAM flood resulted in an endpoint mobility ratio of approximately 0,8. An example of this situation is depicted in the center of Figure 2.2. This is a significant improvement compared to water floods and should result in a considerable improvement in both areal and vertical sweep efficiency. However, if a formation is significantly heterogenous, areal and vertical sweep efficiencies may still not be optimal.

The most favorable situation ensued when the disc was flooded with 2000ppm HPAM, where an endpoint mobility ratio of 0,1 was achieved. The right part of Figure 2.2 illustrates this situation. Even for heterogenous reservoirs, both areal and vertical sweep efficiencies should attain close to optimal values at an endpoint mobility ratio of 0,1.

Ultimate microscopic displacement efficiency, however low the M^0 might be, will be limited by the amount of residual oil present:

$$E_D^{\infty} = 1 - \frac{S_{orw}}{S_{oi}} \tag{2.6}$$

Where E_D^{∞} is ultimate microscopic displacement efficiency (marked by dashed lines in Figure 2.2), S_{orw} is residual oil saturation after water flooding and S_{oi} is initial oil saturation.

Since only residual oil is present in the experiment history matched in this thesis, ultimate microscopic displacement efficiency will be equal to zero, based on equation (2.6).

2.3 Residual Oil Saturation

After completing a recovery mechanism, a fraction of the original oil in place will remain in the reservoir as a residue, called residual oil. Residual oil saturation is defined as the fraction of total pore volume containing residual oil. Residual oil is immobilized as a result of capillary forces and consists of disconnected oil ganglia [12]. This trapping phenomenon can be explained in terms of two simplified, principal models: Pore doublet- and the snap-off model [10]. Figure 2.3 shows an illustration of the pore doublet model; oil remains as a residue due to bypassing water in a pore-doublet:

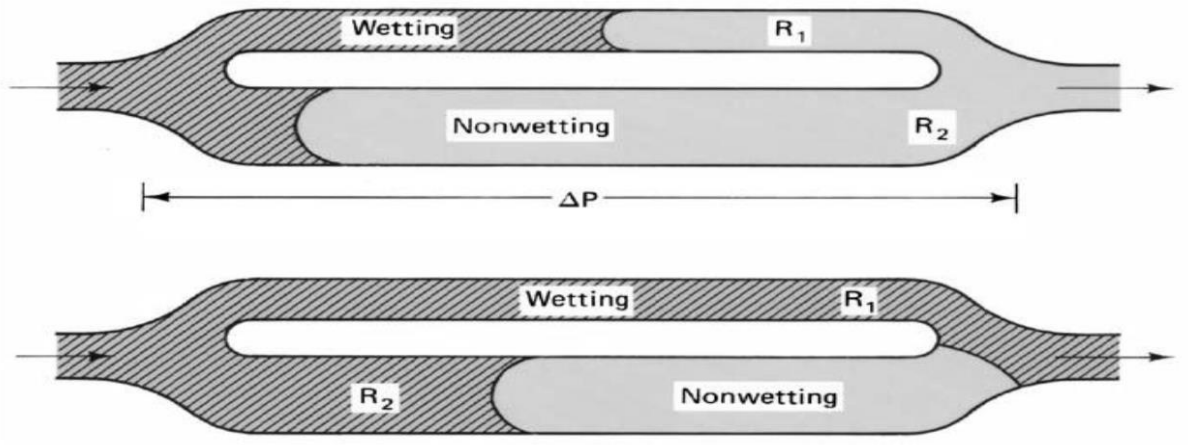

Figure 2.3: Trapping in a pore doublet model (Skarestad, M. and Skauge, A.) [10].

Figure 2.4 shows an illustration of the snap-off model; the oil phase snaps off into globules that are localized in pore bodies of the flow path.

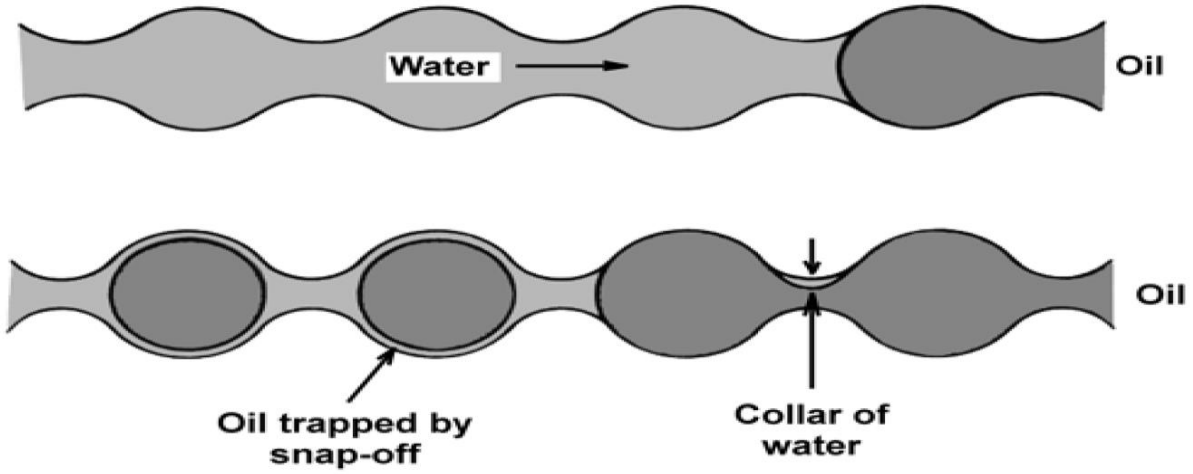

Figure 2.4: Trapping in a snap-off model (Skarestad, M. and Skauge, A.) [10].

2.4 Capillary Number and the Capillary Desaturation Curve (CDC)

The effectiveness of a flooding project using Newtonian fluids has proven to correlate well with the dimensionless capillary number, N_{vc}, defined as the ratio of viscous and capillary forces acting between the displacing and displaced fluid [10]:

$$N_{vc} = \frac{VF}{CF} = \frac{u\mu}{\sigma} \tag{2.7}$$

Where u is Darcy velocity of the displacing fluid, μ is the viscosity of the displacing fluid and σ is interfacial tension between the displacing and displaced fluid.

It has been observed in laboratory experiments performed at different injection velocities that the capillary number may be related to residual oil saturation. This relationship is called the Capillary Desaturation Curve (CDC), and is depicted in Figure 2.5.

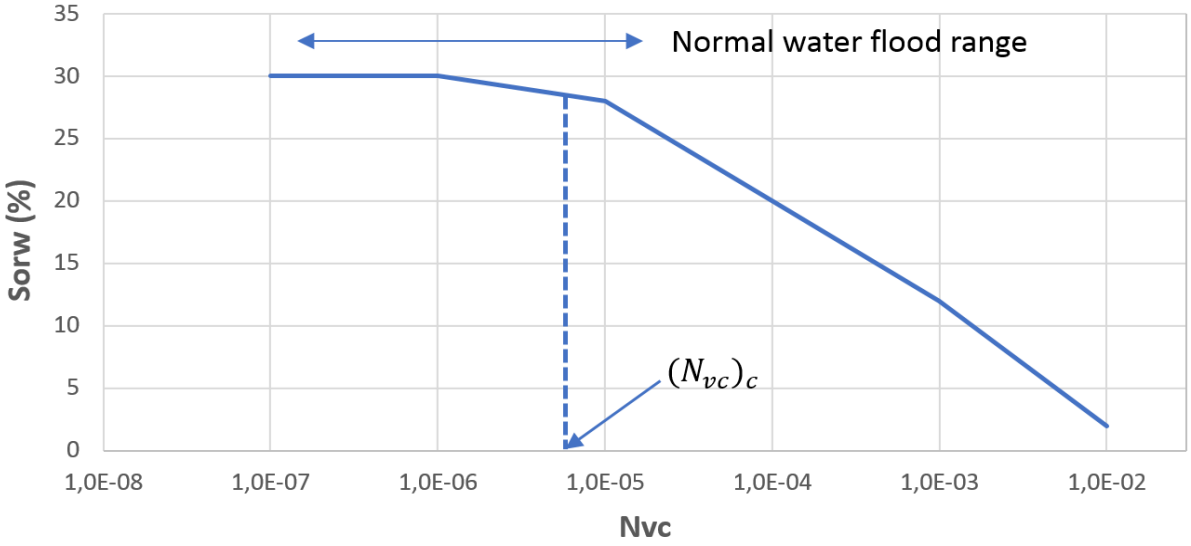

Figure 2.5: Illustration of Capillary Desaturation Curve, showing the relationship between capillary number and the percentage amount of residual oil saturation (modified from Skarestad, M. and Skauge, A.) [10].

From CDC, it is evident that at low values of N_{vc}, residual oil saturation is approximately constant at a plateau value. Increasing N_{vc}, will eventually lead to a knee in the curve and S_{orw} will start to decrease. This point is called the critical capillary number, $(N_{vc})_c$. Evident from Figure 2.5, to reduce S_{orw} significantly N_{vc} must be increased several orders of magnitude, and the normal water flood range is well within the plateau region of CDC.

Referring to equation (2.7), increasing the N_{vc} can be achieved by either increasing injection velocity or viscosity, or by lowering interfacial tension. Injection velocity is constrained by fracturing pressure, and is often already close to its maximum value in field operations.

However, both viscosity and interfacial tension can be altered by implementing EOR techniques such as polymer flooding and surfactant flooding, respectively. Adding a surfactant to the injection water is known to decrease interfacial tension by several orders of magnitude, which may result in significantly reduced residual oil saturations.

Polymers can be added to the drive fluid with a consequent increase in viscosity, but since injectivity damage may result from a too high viscosity increase, viscosity will often not be increased sufficiently to reduce N_{vc} required orders of magnitude. Based on CDC, residual oil saturation in contacted zones is not expected to decrease substantially during polymer flooding.

All water and polymer floods investigated in this thesis are conducted in radial geometry where Darcy velocities of injected fluids decrease in an exponential manner with distance from the injection well. Using equation (2.7), the critical capillary number for the water floods and both polymer floods are shown in Figure 2.6. Typical values of interfacial tension between water and oil are about 10-30 mN/m and a mean value of 20 mN/m was therefore utilized in equation (2.7) when a calculation of capillary numbers was performed [20]. The maximum velocity attained at the injection well of 2000ppm HPAM solution in porous media was chosen as a reference velocity for all floods (0,29 cm/min). Consistent with the history matched experiment, a brine viscosity of 0,96cP was used for water floods, while apparent viscosity at the reference velocity was used for polymer floods in the calculation of capillary numbers.

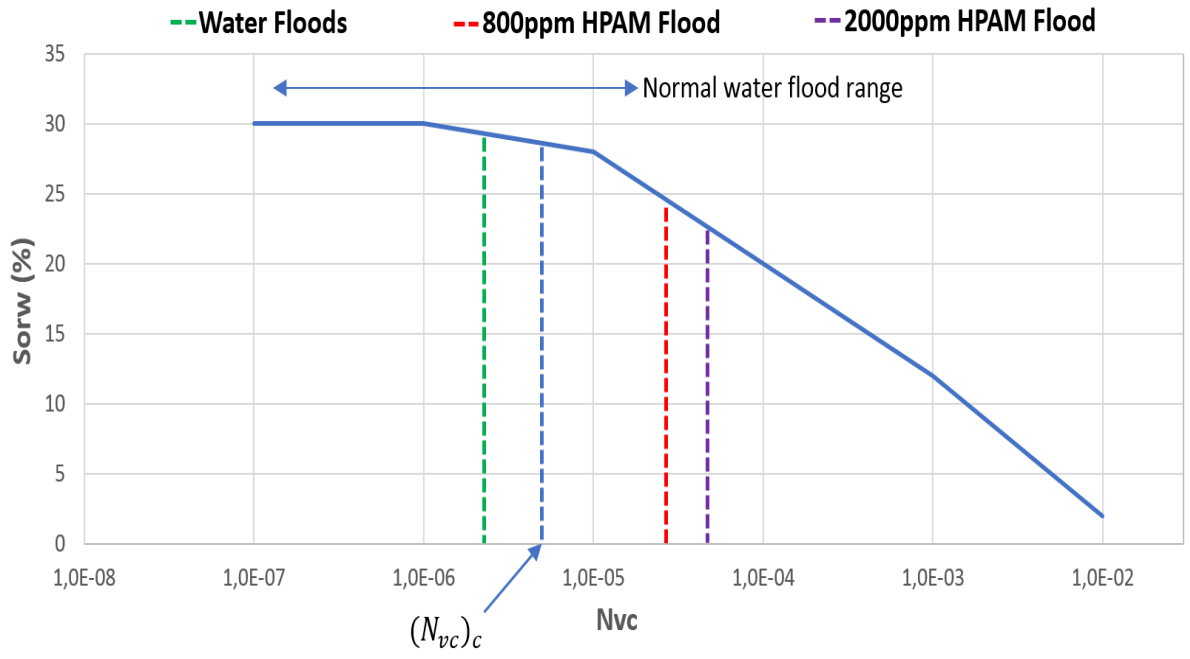

Figure 2.6: Capillary numbers of water and polymer floods history matched in this thesis.

Observable from Figure 2.6, water floods are clearly within the normal water flood range. Both 800 and 2000ppm HPAM floods exceeds the critical capillary number and are outside the normal water flood range.

Based on capillary numbers obtained for 800 and 2000ppm HPAM floods, residual oil saturations of approximately 22-24% are expected, respectively. Since residual oil saturation was initially at 22%, it is not expected that this saturation will decrease further after polymer flooding based on CDC. At least not within polymer concentrations encountered in this thesis. This expectation was confirmed during the experiment when no oil production was observed.

2.5 EOR with Polymer Flooding

As previously mentioned, polymer flooding is a chemically enhanced EOR technique in which addition of polymers aims at increasing water viscosity, consequently reducing the mobility ratio between water and oil.

As mentioned in chapter 2.1, recovery factor is a combination of microscopic displacement efficiency and volumetric sweep efficiency, where the latter may be decomposed into areal and vertical sweep efficiency.

Areal sweep efficiency is significantly affected by mobility ratio between oil and water. Figure 2.7 shows the distinction between areal sweep efficiency for an unfavorable water flood and a favorable polymer flood, respectively.

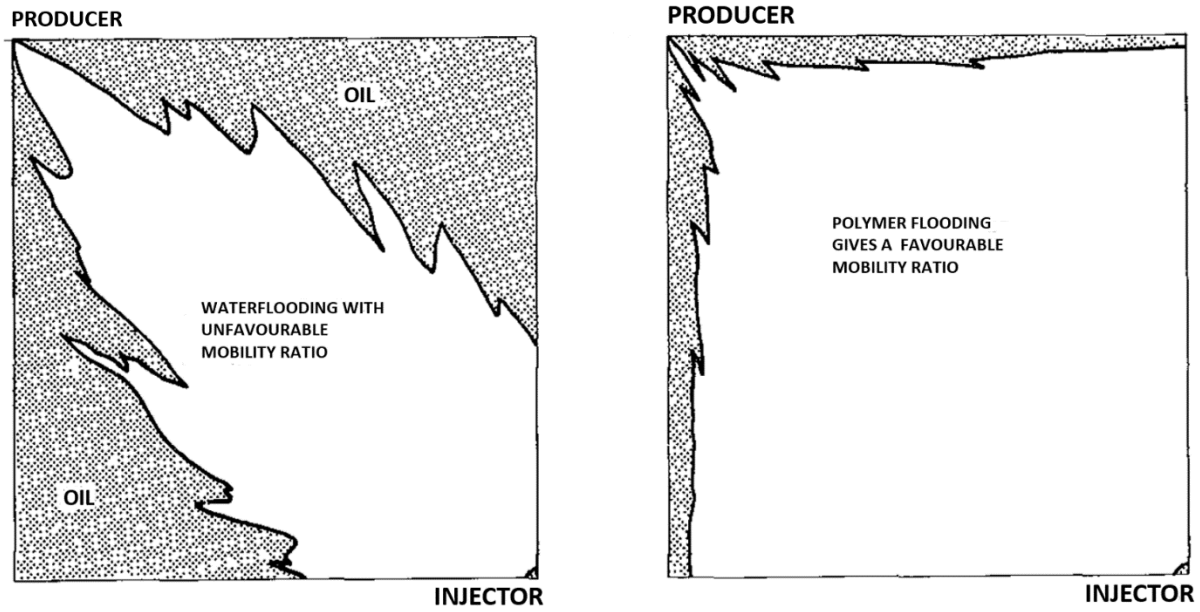

Figure 2.7: Schematic diagram of areal sweep improvements caused by polymer flooding in a five-spot system (modified from Sorbie, K. S.) [12].

The unfavorable water flood in the left part of Figure 2.7 exhibit a mobility ratio above unity, promoting early breakthrough followed by a significant tail production at increasing water cut, resulting in poor areal sweep efficiency. In addition, immiscible viscous fingering may negatively affect the efficiency of areal sweep. Polymer injection will therefore be much better suited for reservoirs containing high viscous oil compared to water injection.

The right part of Figure 2.7 shows an improved areal sweep efficiency imparted by a reduction in mobility ratio. This diverts injected polymer solutions into previously unswept areas in the reservoir and supresses the phenomenon of viscous fingering [12].

Vertical sweep efficiency is also affected by the mobility ratio between oil and water, but is also dependent on reservoir heterogeneity, i.e. reservoirs containing large-scale layering with severely contrasting permeabilities [12]. In these situations, water breakthrough of high permeable layers will dominate, leaving low permeable layers unswept. The remedy in these reservoirs may be to inject polymer to reduce effective permeability to injected fluids. In addition, polymers may block high permeable layers. Figure 2.8 shows the distinction between vertical sweep efficiency in a layered system for an unfavorable water flood and a favorable polymer flood, respectively.

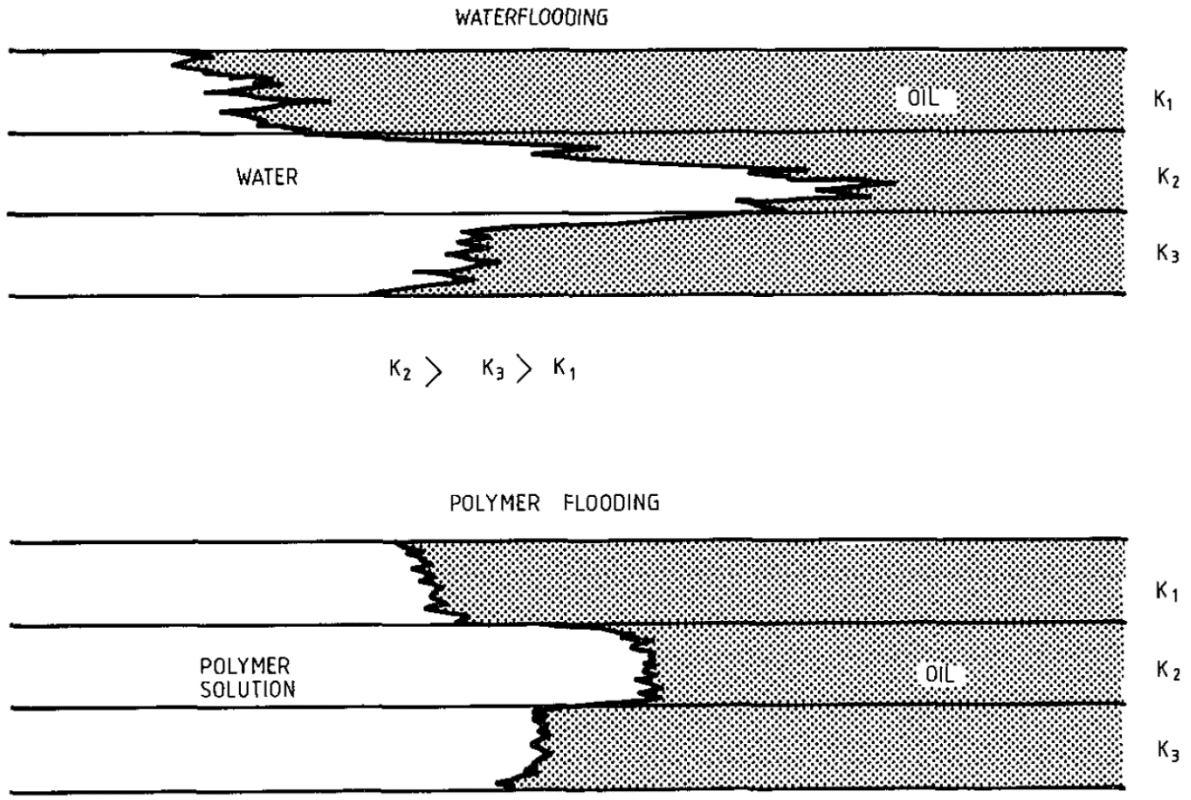

Figure 2.8: Schematic diagram of the improvement in vertical sweep efficiency caused by polymer in a layered system (from Sorbie, K. S.) [12].

Earlier literature suggest that the aim of polymer flooding is confined to increasing volumetric sweep efficiency, but does not change microscopic displacement efficiency in contacted zones. Thus, polymer flooding recovers any oil bypassed in a water flood, but does not include residual oil [12].

Numerous results in recent years do not support conclusions from earlier literature. It was observed by Wang et al. (2000) [21] that viscoelastic polymers can increase microscopic displacement efficiency in cores, i.e. reduce residual oil saturation in contacted zones. The types

of residual oil investigated by Wang et al. includes oil film on the rock surface, oil in "dead ends", oil in pore throats retained by capillary forces and oil unswept in microscale heterogeneous portions of the core. It was reported that flooding with viscoelastic polymers reduced all types of microscale residual oil. This achievement was attributed to the elastic nature of the polymer, where deviations from Newtonian velocity distribution in pores results in a "pulling effect" on different types of residual oil. CDC, originally defined for Newtonian fluids will therefore not necessarily be a suited model to assess residual oil saturations achieved in a polymer flood using elastic polymers.

As mentioned, the experiment history matched in this thesis showed no production of residual oil during polymer flooding. However, a small amount of residual oil was observed to propagate from the injection well to a small distance into the radial disc, but was not displaced far enough to be produced. Therefore, the assumption of completely immobile residual oil was implemented when history matching the polymer floods in this thesis.

3 PETROPHYSICAL PROPERTIES

This chapter introduces basic concepts and definitions concerning fluid flow in porous media, which is essential to fully understand the mechanisms of polymer flooding.

3.1 Porosity

A rock's porosity, or fluid-storage capacity, is a dimensionless parameter and is defined as the void part of a rock's total volume unoccupied by rock grains and mineral cement [17]. Porosity may be divided into two principal categories: Effective and residual porosity [22]. While effective porosity originates from interconnected pores which allows fluid flow, residual porosity originate from isolated pores which are unable to transmit fluids. Absolute porosity is defined as the ratio of total void volume, encompassing both interconnected and isolated pores, to the bulk volume of a rock sample, and can be expressed as the total sum of effective and residual porosity:

$$\phi_{abs} = \frac{V_{p,abs}}{V_b} = \phi_{eff} + \phi_{res} \tag{3.1}$$

Where ϕ_{abs} is absolute porosity, $V_{p,abs}$ is total void volume, V_b is bulk volume and ϕ_{eff} and ϕ_{res} is effective and residual porosity, respectively.

Effective porosity is defined as the ratio of void volume consisting of interconnected pores to the bulk volume of a rock sample:

$$\phi_{eff} = \frac{V_{p,eff}}{V_b} \tag{3.2}$$

Where $V_{p_{eff}}$ is the volume of interconnected pores.

Residual porosity refers to porosity of isolated pores in a rock sample which is unable to implement a fluid flow, and may be be defined as:

$$\phi_{res} = \frac{V_{p,abs} - V_{p,eff}}{V_b} \tag{3.3}$$

3.2 Saturation

A rock's saturation, S_i, is a dimensionless parameter and is defined as the fraction of pore volume occupied by a particular fluid [17]:

$$S_i \stackrel{\text{def}}{=} \frac{V_i}{V_p}, \quad i = 1, \ldots, n \tag{3.4}$$

Where V_i is the volume occupied by a particular fluid, V_p is pore volume and the subscript i denotes phase.

Consequently, the sum of individual saturations should be equal to unity:

$$\sum_{i=1}^{n} S_i = 1 \tag{3.5}$$

If a rock's pores consist exclusively of oil, gas and water, the pore content can be written in volumetric terms:

$$V_p = V_o + V_g + V_w \tag{3.6}$$

Where V_o, V_g and V_w is the volume of pores containing oil, gas and water, respectively.

If a rock's pores consist exclusively of oil, gas and water, the saturation may be written as:

$$S_i = \frac{V_i}{V_p}, \quad i = o, g, w \tag{3.7}$$

Where subscripts o, g and w denotes oil, gas and water, respectively.

3.3 Permeability

The permeability of a porous medium is the medium's capability to transmit fluids through its network of interconnected pores [17]. Consequently, the permeability of a porous medium will be proportional to its effective porosity. There exist three distinct types of permeability: Absolute, effective and relative permeability.

Absolute permeability is a characteristic of porous media and can be defined as a constant property if only a single (incompressible) fluid is being transmitted through the medium. Absolute permeability is defined through the Darcy Equation, which in the state of a linear horizontal flow of an incompressible fluid can be written in generalized form as follows:

$$Q = -A\frac{K}{\mu}\frac{dP}{dx} \tag{3.8}$$

Where Q is volumetric flow rate, K is absolute permeability, A is cross-sectional area, μ is fluid viscosity and $\frac{dp}{dx}$ is the pressure gradient over the porous medium. The negative sign in the Darcy equation denotes that pressure is decreasing in the flow direction, which gives rise to a negative pressure gradient.

Darcy velocity, u, is defined as the ratio of volumetric injection rate entering the porous media to cross-sectional area of the sample:

$$u = \frac{Q}{A} \tag{3.9}$$

In the petroleum industry, the most commonly used unit for permeability is Darcy (D):

$$1\ Darcy = \frac{1\frac{cm^3}{sec} \cdot 1\ cP}{1\ cm^2 \cdot 1\frac{atm}{cm}} = 0{,}98692\ \cdot\ 10^{-8}\ cm^2 = 0{,}98692\ \cdot\ 10^{-12}\ m^2$$

The experiment being history matched in this thesis was performed by injecting both water and polymer into a radial Bentheimer disc. Fluids were injected into the center of the disc and propagated radially towards a producer at the outer boundary. When propagating through the radial disc, injected fluids moves horizontally between the injection well and outer boundary ($w < r < e$), and passes through the cross-sectional area, $A = 2\pi rh$, where h denotes thickness of the radial disc. Darcy's law for radial one-phase flow may be stated as follows:

$$Q = -\frac{KA}{\mu}\frac{dP}{dr} = -\frac{2\pi hK}{\mu} r\frac{dP}{dr} \tag{3.10}$$

$$Q\int_{r_w}^{r_e}\frac{dr}{r} = -\frac{2\pi hK}{\mu}\int_{p_w}^{p_e} dP \tag{3.11}$$

$$p_e = p_w + \frac{\mu Q}{2\pi hK}\ln\frac{r_w}{r_e} \tag{3.12}$$

Where p_e is the counter pressure from the producer at the outer boundary, p_w is injection well pressure, r_w is injection well radius and r_e is the radius of the outer boundary.

The differential pressure, ΔP, from the injection well to the producer is equal to the difference between p_w and p_e. Therefore, equation (3.12) may be written as:

$$\Delta P = -\frac{\mu Q}{2\pi hK}\ln\frac{r_w}{r_e} \tag{3.13}$$

Figure 3.1 illustrates the radial geometry derived above:

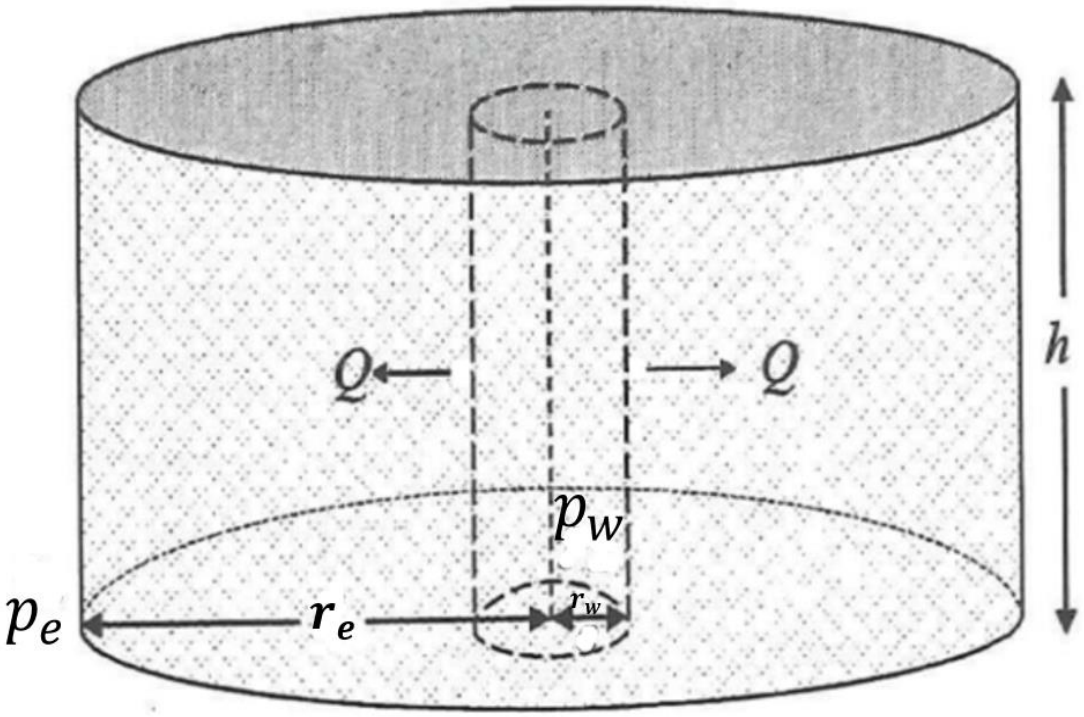

Figure 3.1: Radial flow propagating from injection well to producer in a cylindrical disc (modified from Lien, J.) [22].

3.3.1 Effective and Relative Permeability

When more than one fluid is flowing through porous media, permeability will be dramatically reduced as one fluid hinder the free flow of other fluids. In these situations, there is a need to define an effective permeability for different fluids in the medium. Effective permeability for each of the fluids will then strongly depend upon their relative saturations and wettability preferences of the porous media, and can be defined in accordance with Darcy's law [17]:

$$k_{e,i} = \mu_i \frac{x}{A} \frac{Q_i}{\Delta P_i} \tag{3.14}$$

Where $k_{e,i}$ is effective permeability of fluid i and x is the length of the porous media.

Relative permeability for a particular fluid, coexisting with at least one other fluid in a porous media, is defined as the ratio of effective permeability for that particular fluid and absolute permeability of the porous media:

$$k_{r,i} = \frac{k_{e,i}}{K} \tag{3.15}$$

Where $k_{r,i}$ and $k_{e,i}$ is relative- and effective permeability of fluid i, respectively.

Using the same derivation technique as for one-phase flow, Darcy's law for two-phase flow in radial geometry may be defined as:

$$\Delta P = -\frac{\mu Q}{2\pi h k_{e,i}} \ln \frac{r_w}{r_e} \tag{3.16}$$

Where $k_{e,i}$ is effective permeability instead of absolute permeability used for one-phase flow.

4 POLYMERS

Polymer flooding is the most commonly applied chemical EOR technique in which polymer is added to the injection brine to increase its viscosity [12]. This viscosity increase gives rise to a better mobility ratio between water and oil, which can increase the volumetric sweep efficiency and may improve/accelerate recovery.

The most frequently used polymers in the petroleum industry for chemical EOR purposes is the synthetic polymer, partially hydrolyzed polyacrylamide (HPAM), and the biopolymer Xanthan [23].

In this thesis, experimental data being history matched are exclusively based on polymer flooding using the synthetic polymer HPAM and therefore the only polymer which will be emphasized.

The rheological properties of polymers are not necessarily identical for flow in porous media compared to capillary flow, and a need to discuss both bulk rheology and in-situ rheology is evident. Several contrasting observations have been reported concerning differences in bulk versus in-situ rheology. At low shear rates, some authors have suggested that bulk viscosity is above in-situ viscosity [24], [25], [26], [27] while others have reported the opposite [28].

In relation to whether their viscosity is shear-dependent or not, fluids are categorized into Newtonian and non-Newtonian fluids, whereas polymer solutions is associated with the latter category. The behavior of HPAM in the upper and lower flux regimes are reported to be Newtonian, while at low-to-intermediate and intermediate-to-high flux HPAM may exhibit shear-thinning (pseudoplastic) or shear thickening (dilatant) behavior, respectively [12].

Shear thinning behavior results from shearing, where the flexible coil structure of HPAM is aligned in the flow direction, consequently reducing resistance to flow. In contrast, shear-thickening behavior is caused by molecular stretching and is attributed to the viscoelastic nature of HPAM [29].

To achieve a successful polymer flood, it is essential to review factors affecting the polymer performance (i.e. stability and viscosity of polymer solutions). Several factors are known to affect polymer performance such as degradation, retention, inaccessible pore volume (IPV), molecular weight (MW), polymer concentration and salinity [12]. All factors mentioned will, in turn, be discussed in detail during this chapter.

4.1 HPAM

HPAM is a synthetic, straight-chain polymer with a specified amount of hydrolyzed acrylamide monomers, as illustrated in Figure 4.1.

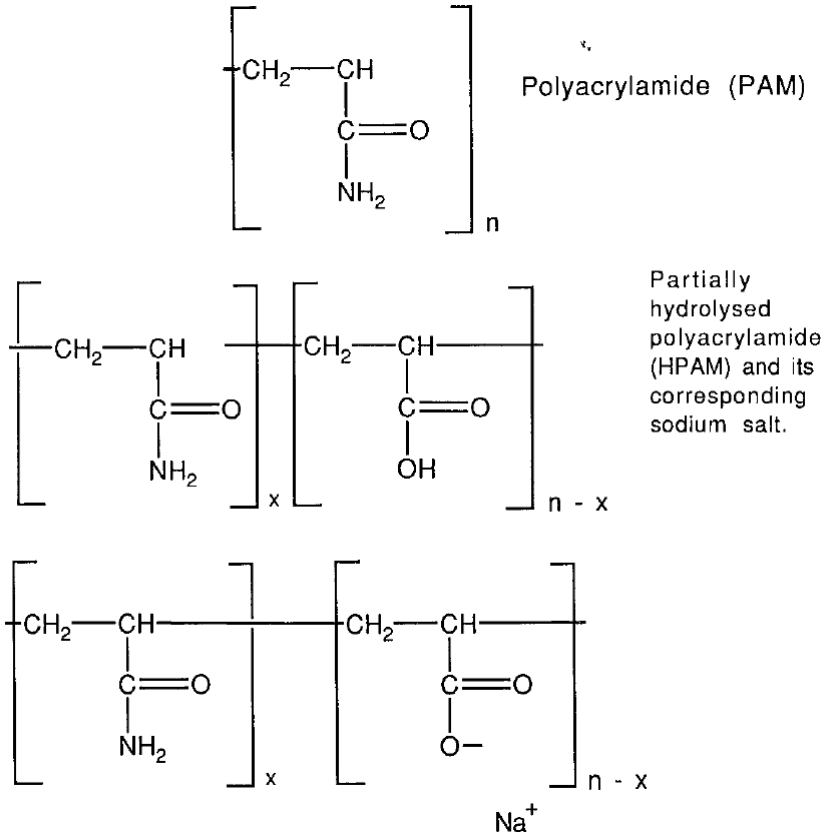

Figure 4.1: The primary chain structure of polyacrylamide (PAM) and partially hydrolyzed polyacrylamide (HPAM) (from Sorbie, K. S.) [12].

The partial hydrolysis of HPAM causes anionic carboxyl groups to be scattered along the backbone chain, thus HPAM molecules are negatively charged [23]. Successful implementation of polymer flood projects requires a carefully selected degree of hydrolysis to optimize properties such as water solubility, viscosity and retention. Typically, the degree of hydrolysis is between 30-35% for HPAM used in polymer flooding. However, hydrolysis will continue at elevated temperatures and selecting a hydrolysis degree close to the upper or lower critical point can therefore be detrimental for polymer performance.

The viscosity increasing feature of HPAM lies in its large molecular weight, accentuated by anionic repulsions [23]. Polymer molecules in solution will be elongated and snag on others elongated as a result of this repulsion. This effect will be enforced with increasing polymer concentration.

The flexible coil structure of HPAM in aqueous solution, frequently known as random coil in polymer chemistry, has significant influence on its solution properties [12]. Because of multiple negative charges distributed along its chain, HPAM is a polyelectrolyte and will therefore interact quite strongly with ions in solution.

Ionic polymers are distinguished from non-ionic polymers by viscosity effects resulting from salt, hardness and pH sensitivities, which are all related to Coulomb forces acting between charged species. A typical flexible polyelectrolyte is generally spherical, but its propensity to change conformation and thus overall size is significant.

Change in molecular size and thus polymer viscosity by reaction with ions, is determined by the ionic strength of the polymer solution. Ionic strength, I_s, is a function of ionic concentration, and is defined as [12]:

$$I_s = \frac{1}{2}\sum m_i z_i^2 \qquad (4.1)$$

Where m_i is molar concentration of the ith ion and z_i is ionic valence, i.e. its charge.

From equation (4.1), it is evident that ionic strength increase with ion valence. For a monovalent ion such as Na^+, the increase in ionic strength will be equal to molarity. However, for a divalent electrolyte such as Ca^{2+}, ionic strength will increase in a non-linear fashion with increasing concentration. Effects of salinity and hardness ions on the flexible HPAM polymer will be discussed further in chapter 4.9.

4.2 Rheology

The principal solution property of interest in polymer rheology is viscosity. The general definition of viscosity is its resistance to shear, where shear stress, τ, between two thin sheets of fluids is given by [12]:

$$\tau = \frac{F}{A} \tag{4.2}$$

Where F is force and A is contact area between the sheets, respectively.

The velocity gradient in the small distance between the sheets is linear for certain types of fluids and has been empirically determined as follows:

$$F \propto \frac{AV}{r} \tag{4.3}$$

Where V is velocity of the upper surface and r is distance between the surfaces of two thin sheets, as illustrated in Figure 4.2.

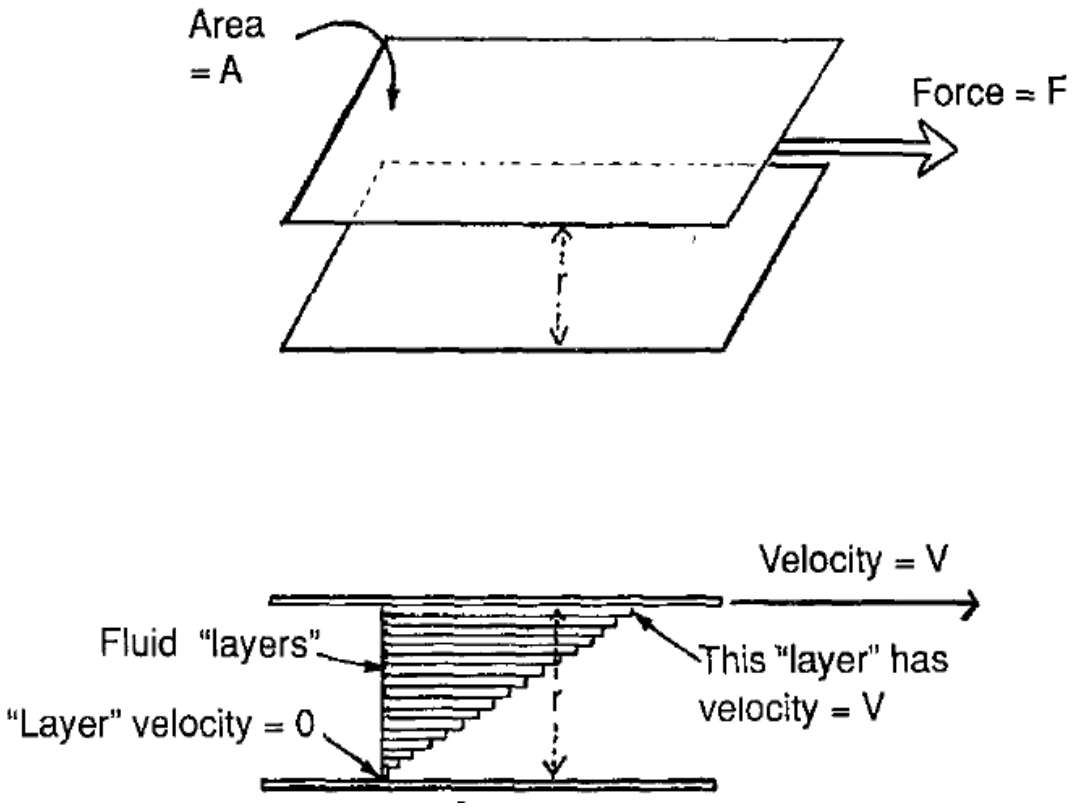

Figure 4.2: Illustration of fluid motion in simple shear flow (from Sorbie, K. S.) [12].

For fluids that exhibit shear independent viscosity behavior, the relationship between shear stress, shear rate, $\dot{\gamma}$, and their independent shear viscosity, μ, can be defined as:

$$\tau = -\mu\left(\frac{dV}{dr}\right) = \mu\dot{\gamma} \tag{4.4}$$

For fluids that exhibit shear dependent viscosity behavior, the relationship between shear stress, shear rate and their shear dependent viscosity, can be defined as:

$$\tau = \eta(\dot{\gamma})\dot{\gamma} \tag{4.5}$$

Where $\eta(\dot{\gamma})$ is a function of shear rate.

Fluids may be characterized based on their shear dependent viscosity behavior. While Newtonian fluids exhibit shear independent behavior, non-Newtonian fluids are shear dependent. Water and oil are characterized as Newtonian fluids, while polymer solutions virtually always show non-Newtonian behavior at sufficiently high polymer concentrations [12]. In Figure 4.3, the relationship between shear stress and shear rate are depicted for different types of fluids.

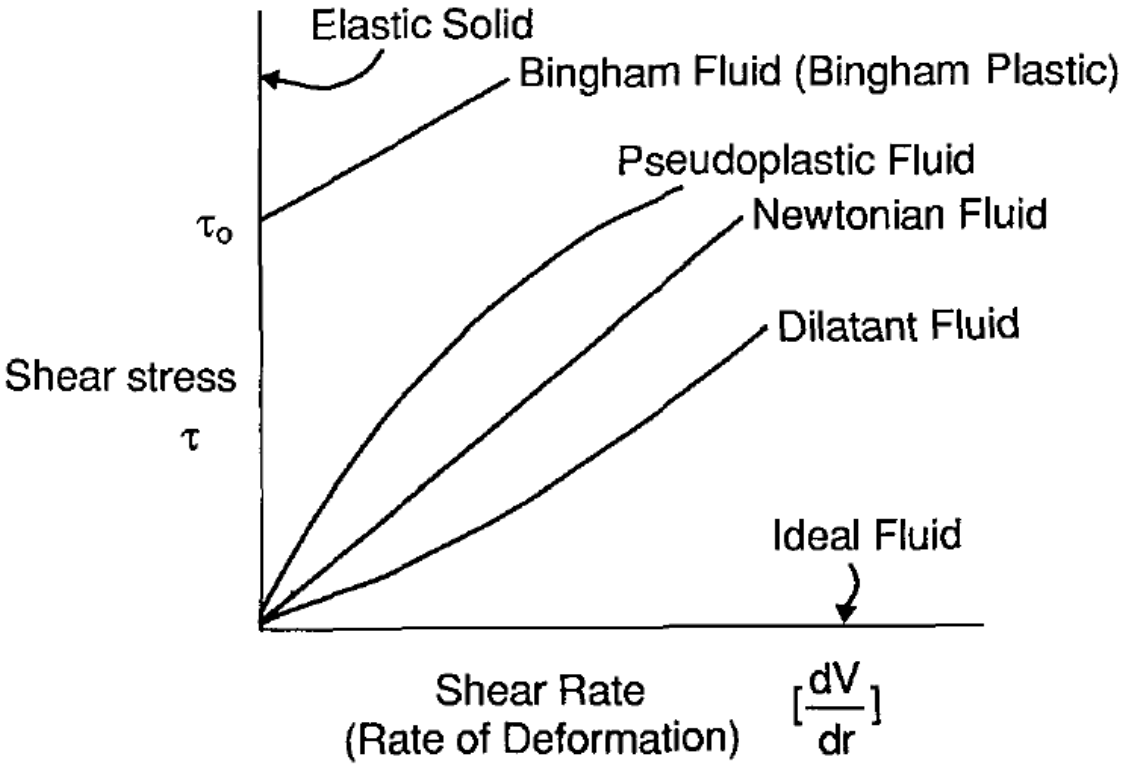

Figure 4.3: Various types of shear stress/shear rate behaviour (from Sorbie, K. S.) [12].

A constant slope corresponds to a Newtonian fluid (viscosity is proportional to slope), while decreasing and increasing slopes (non-Newtonian) corresponds to shear thinning (pseudoplastic) and shear thickening (dilatant) fluids, respectively. In simple shear flow, most polymer solutions are pseudoplastic in nature, while dilatant behavior is rarely experienced in dilute homogeneous polymer solutions [12].

To envisage the rheology of polymers more clearly, it is common to plot viscosity against shear rate. Figure 4.4 shows a typical shear viscosity curve for a HPAM solution at constant concentration, depicting seven distinct regions or points [7].

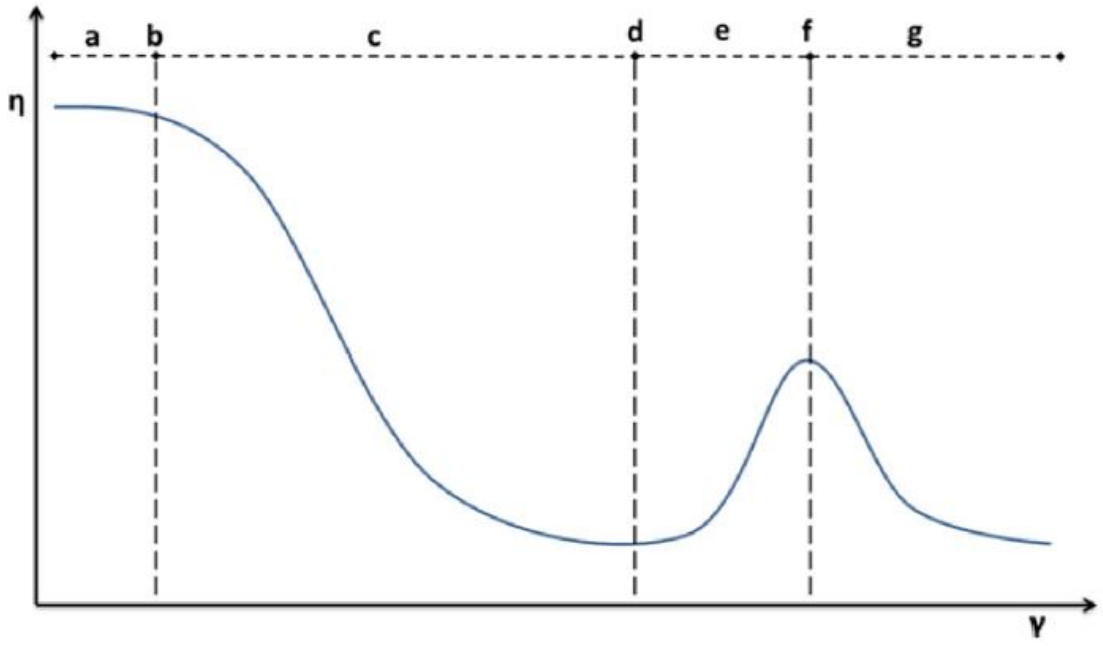

Figure 4.4: Typical shear viscosity curve for a HPAM polymer (from Skauge, T. et al.) [7].

a) Newtonian region: At low shear rates, the hydrodynamic radius of polymer coils and polymer concentration will determine polymer viscosity. The polymer shows a Newtonian behavior, which is due to absence of interactions between polymer coils and thus viscosity will be constant with increasing shear rate.

b) Critical shear rate, $\dot{\gamma}_c$: Defines onset of shear thinning.

c) Shear thinning (pseudoplastic) region: At higher velocity, but still in laminar flow, polymer coils are forced apart and aligned in the flow direction, resulting in a viscosity decrease.

d) Bottom point of shear thinning region: Viscosity reaches its minimum value at higher shear rates where interactions between polymer coils ceases to exist and polymer molecules are at their most aligned conformation.

e) Shear thickening (dilatant) region: Extensional flow becomes dominant if shear rate is further increased, inducing an abrupt increase in viscosity. (Shear thickening will be discussed further in chapter 4.3.2)

f) Maximum shear thickening point: Viscosity of the polymer solution will increase until the strain becomes large enough to fragment molecules by breaking the carbon-carbon chains, thus marking the gap between reversible and irreversible polymer behavior and onset of mechanical degradation.

g) Mechanical degradation: Beyond the maximum shear thickening point fluid stresses become large enough to fragment polymer molecules, resulting in an irreversible viscosity loss [13]. At infinitely high shear rates, viscosity will approach the solvent viscosity [7].

To describe the shear dependent viscosity of non-Newtonian fluids, several empirical models have been suggested. The most frequently encountered analytical model describing the relationship between viscosity and shear rate is the power law model. This model mainly describes the pseudoplastic region and is given by the expression [12]:

$$\eta(\dot{\gamma}) = K\dot{\gamma}^{n-1} \tag{4.6}$$

Where η is shear dependent viscosity, $\dot{\gamma}$ is shear rate, and K and n are constants, where n is known as the power law index. In the pseudoplastic region, $n < 1$, whereas for a Newtonian fluid, $n = 1$, and the constant K will become equal to the constant viscosity, μ. Although not common, the power law model may also describe the dilatant region ($n > 1$).

The power law model describes fluid behavior in the pseudoplastic region at intermediate shear rates quite well, but fails to be satisfactory in upper and lower pseudoplastic shear rate regions.

A better suited model for these pseudoplastic shear regimes is the Carreau equation (Carreau, 1972 [30]; Bird et al., 1987 [31]), defined as [12]:

$$\eta(\dot{\gamma}) = \eta_\infty + (\eta_0 - \eta_\infty)[1 + (\lambda\dot{\gamma})^2]^{(n-1)/2} \tag{4.7}$$

Where η_∞ is infinite shear rate viscosity, η_0 is zero-shear rate viscosity, λ is polymer relaxation time (see chapter 4.3.2) and n is the power law index.

The Carreau model gives an improved fit compared to the power law model, although the former is a four-parameter model instead of the two parameters required of the latter. Figure 4.5 shows a comparison of the two models described above.

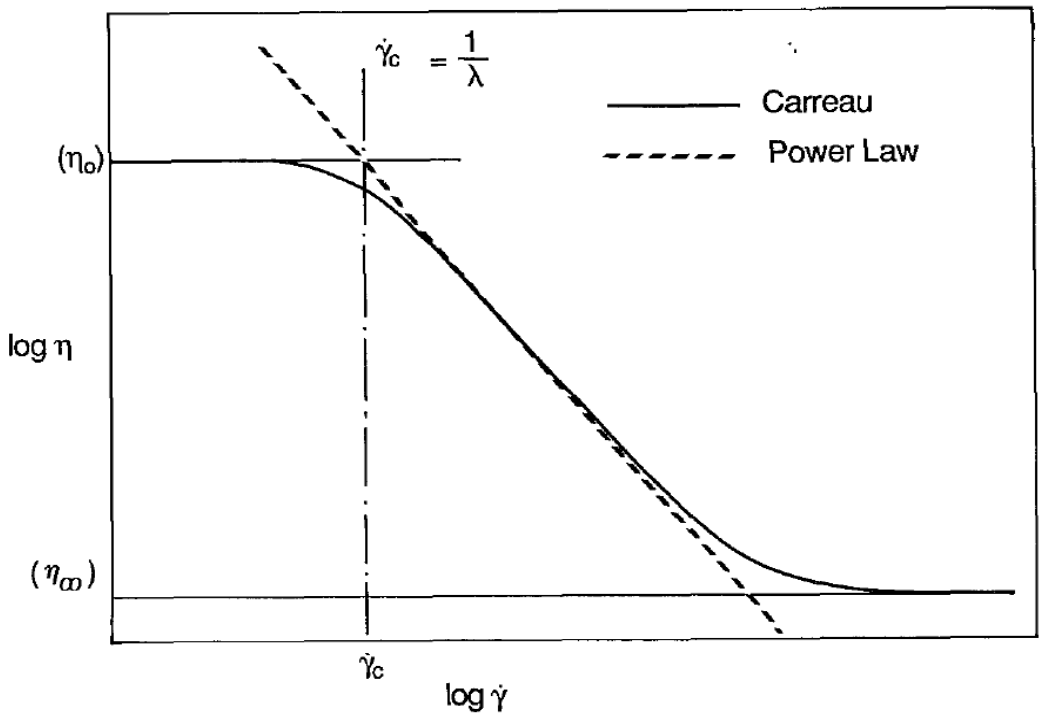

Figure 4.5: Comparison of the Carreau and power law model for the viscosity-shear rate relationship. Critical shear rate, $\dot{\gamma}_c$, defined as in the figure, is related to the Carreau relaxation time (from Sorbie, K. S.) [12].

To describe both shear thinning and shear thickening regimes of viscoelastic polymers, the extended Carreau equation can be utilized, and may be defined as [32]:

$$\eta(\dot{\gamma}) = \eta_\infty + (\eta_0 - \eta_\infty)[1 + (\lambda_1\dot{\gamma})^2]^{\frac{n_1-1}{2}} + \eta_{max}[1 - e^{(-(\lambda_2\dot{\gamma})^{n_2-1})}] \quad (4.8)$$

Where:

$\dot{\gamma}$: Shear rate

$\eta(\dot{\gamma})$: Apparent polymer viscosity as a function of shear rate

η_∞: Apparent polymer viscosity at infinite shear rate

η_0: Apparent viscosity at zero shear rate

λ_1 and λ_2: Time constants related to the polymer molecule relaxation time

n_1 and n_2: Power law indexes

4.3 In-situ Rheology

As mentioned at the beginning of this chapter, rheological properties of polymers are not necessarily identical for flow in porous media compared to capillary flow. It is therefore necessary to define in-situ rheology, which refers to rheology of non-Newtonian polymeric solutions as they flow though porous media [12]. In-situ rheology will affect both injectivity and sweep efficiency, and is therefore of great importance when considering a polymer flood project.

Like bulk rheological behavior, molecular structure plays an essential role in determining in-situ rheology. In addition, microscopic structure and geometry of porous media will affect in-situ rheology. While flow through a rheometer is well-defined, flow through porous media will be more complex and the flow path will be much more tortuous.

To define macroscopic, in-situ apparent viscosity, η_{app}, for a non-Newtonian fluid, the Darcy equation (equation (3.8)) may be rearranged as follows [12]:

$$\eta_{app} = \frac{KA\Delta P}{QL} \tag{4.9}$$

Where the pressure drop, ΔP, will generally not be a linear function of flow rate, Q.

It is important to consider that the value of absolute permeability, K, in equation (4.9), may be reduced because of polymer retention (chapter 4.5) in porous media, thereby overestimating the value of η_{app}. It is therefore crucial to be certain of whether the observed pressure drop is a consequence of only the viscous effect of the fluid, or if pore blocking and permeability reduction is partly responsible. Phenomenon's which may lead to pore blocking and permeability reductions will be discussed in subsequent sections of this chapter.

As previously mentioned, the experiment being history matched in this thesis consists of alternating water and polymer floods. This sequential order of floods is performed to exclude the overestimation of apparent viscosities by determining the absolute permeability of the porous media both before and after polymer flooding. Thus, permeability reduction caused by polymer retention mechanisms will be accounted for in the permeability rather than the apparent viscosity values. (Polymer retention mechanisms will be discussion in chapter 4.5).

While pseudoplastic polymers only show Newtonian and shear thinning behavior, viscoelastic polymers additionally exhibit shear thickening behavior at high flow rates [12]. This has been shown schematically by Heemskerk et al. (1984) [33] as depicted in Figure 4.6.

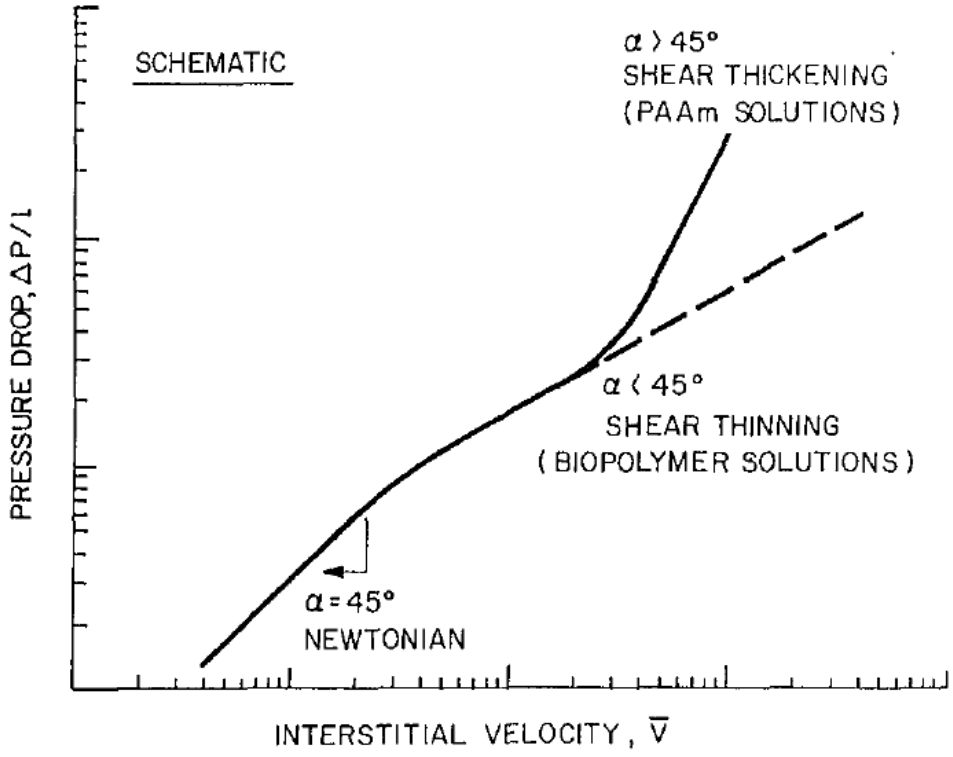

Figure 4.6: Schematic diagram of the in-situ rheological behaviour of polymer solutions (from Heemskerk, J. et al.) [33].

To predict the flow behavior of non-Newtonian polymers in porous media, the microheterogeneity must be considered. Shear rates in porous media are known to vary. Because of the rate-dependent nature of non-Newtonian polymers, in-situ viscosity will vary accordingly. A common approach to this discrepancy between bulk and in -situ behavior is to operate with apparent viscosity values, i.e. averaged values [12]. Equation (4.10) shows a frequently used model for two-phase flow that relates shear rate, flux and rock properties of the porous media (modified from Sorbie, K. S.) [17].

$$\dot{\gamma}_{pm} = \alpha' \frac{4u}{\sqrt{8k_{e,i}\phi}} \tag{4.10}$$

Where $\dot{\gamma}_{pm}$ is porous medium effective shear rate, α' is a shape parameter of the pore structure, which is determined experimentally for porous media flow, u is the Darcy velocity defined in equation (3.9), $k_{e,i}$ is effective permeability and ϕ is porosity.

Equation (4.10) will be used when comparing bulk and in-situ rheology of 2000ppm HPAM in chapter 9.1.8.

4.3.1 Apparent Slip Effect and Inaccessible Pore Volume (IPV)

A phenomenon that increase polymer velocity in flow through porous media is the apparent slip effect. The mechanism responsible for the apparent slip effect is thought to be molecular surface exclusion, caused by entropic exclusion of polymer molecules on pore walls in porous media [12]. This entropic exclusion results in a depleted polymer layer at pore walls, as illustrated Figure 4.7.

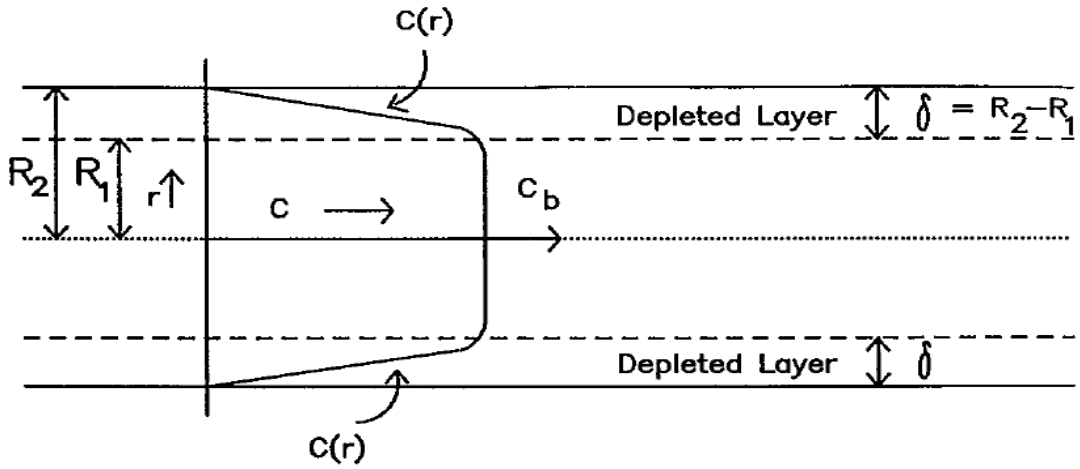

Figure 4.7: Illustration of depleted layers of polymer on a pore wall as a result of the apparent slip effect (from Sorbie, K. S.) [12].

The apparent slip effect will reduce in-situ viscosity and thus accelerate the flow of polymer through porous media. The significance of the apparent slip effect is greatest when the dimensions of typical pore sizes and polymer macromolecules approach each other.

Based on core flooding experiments, (Chauveteau and Zaitoun, 1981 [24]; Chauveteau, 1982, 1986 [25], [26]; Chauveteau et al. 1984 [27]) in-situ viscosity in the low shear rate regime was reported to be below bulk fluid viscosity. The explanation to this observed phenomenon was attributed to the apparent slip effect.

In contrast, Canella et al. (1988) [28] observed that in-situ viscosity in the low shear rate regime was above bulk fluid viscosity. An explanation to these contrasting results may lie in the polymer concentrations investigated. While Chauveteau presented results for polymer concentrations in the dilute regime, Canella et al. investigated solutions in the semi-dilute regime.

Even though Canella et al. investigated the biopolymer Xanthan in their experiments, consistent results have been reported for HPAM in both adsorbing and non-adsorbing porous media [12].

Like apparent slip effects, the phenomenon of inaccessible pore volume (IPV) accelerates the flow of polymer through porous media. The most common explanation for IPV states that polymer molecules are unable to propagate through certain parts of the porous media because of their size. Consequently, a fraction of the pore volume is inaccessible to polymer and accelerated polymer flow results.

IPV is known to depend on porosity, absolute permeability, pore size distribution and polymer molecular weight. The value of IPV is generally in the range of zero to 30%, whereas the latter has only been observed in extreme cases [23].

Szabo (1975) [34] reported that at residual oil saturation, higher polymer retention is computed during polymer flow than after brine flush. This phenomenon was partly attributed to the IPV effect.

4.3.2 Viscoelasticity

Elastic materials will return to their original configuration if they are deformed through a small enough displacement [12]. Flexible chain structures such as HPAM will show some degree of elasticity due to its coil structure, and can therefore be classified as an elastic material.

While propagating through porous media, polymers will encounter a sequence of pores, whereas the polymer molecule gyration radius (molecular radius in its most relaxed state) may be smaller than the pore throats. When polymers propagate through these pore throats, polymer molecules are forced to elongate, thus entering the elongational flow regime. Polymer molecules will now experience both stretching and shearing.

When passing through a sequence of pore bodies and pore throats, polymer molecules will contract and expand sequentially. If polymer molecules have sufficient time to readjust to the flowing conditions when propagating alternatingly through pore throats and pore bodies, elastic effects will not be seen. However, if the polymer relaxation time (time it takes for a polymer molecule to fully expand after being elongated) is greater than the transit time, the elasticity of a fluid would have an effect. In these situations, the polymer molecule is incapable of reaching its fully relaxed state and a resistance to flow is observed. This flow resistance induced by the viscoelastic character of polymer molecules is referred to as shear thickening. In the shear thickening regime, polymer resistance (apparent viscosity) will therefore increase with increasing flux [29].

The time-dependent elastic phenomena are of crucial importance for viscoelastic polymer flow in porous media and may be represented by a parameter called the Deborah number, D_e [12]:

$$D_e = \frac{\theta_f}{\theta_p} \tag{4.11}$$

Where θ_f is the relaxation time of a polymer fluid and θ_p is the duration time of a process, i.e. the transit time, where the latter is dependent upon geometries present within the porous medium.

While small values of the Deborah number will result in fluid-like behavior, i.e. Newtonian or shear thinning, large values will induce solid-like behavior, i.e. Newtonian or shear thickening. The degree of viscoelasticity for a polymer is known to depend on factors such as salinity and concentration.

4.4 Degradation

When utilizing polymers in oil recovery processes it is desirable and often a necessity that polymer properties are not degraded, at least not within the timeframe of the flood. Polymer degradation refers to any process that will break down the molecular structure of the macromolecule, thereby reducing the average molecular weight. This phenomenon may affect the polymers' performance by reducing its viscosity. Polymer solution viscosity is generally the principal property of interest being affected by degradation although, permeability reduction induced by degradation may also be of importance. There exist three main degradation pathways in oil recovery applications: Chemical, biological and mechanical degradation [12].

4.4.1 Chemical and Biological Degradation

The term chemical degradation denotes any of several possible processes such as thermal oxidation, free radical substitution, hydrolysis and biological degradation. The temperature above which a polymer will thermally crack is an inherent property of any polymer solution. This temperature is normally quite high, and laboratory results indicate that HPAM may be stabilized up to about 121°C at optimal conditions. Since the original temperature of oil reservoirs seldom approach this limit the remaining degradation reactions are of higher practical concern for polymer flooding [23].

The most serious source of chemical degradation is usually considered to be free radical substitution, i.e. oxidation reactions. To remediate these degradation sources, reducing agents such as oxygen scavengers and antioxidants are often added. These chemicals are also advantageous because of their ability to prevent phenomenon's such as gelation and agglomeration which are known to cause wellbore plugging and reduced injectivity [12].

In polymer floods, even slow reactions at low temperatures are potentially serious because of the average residence time in a reservoir, which is typically a few years. Dependence of reaction rates on other variables such as pH and hardness is also very significant. As previously mentioned, hydrolysis may continue at elevated temperatures. A possible effect of continued hydrolysis for HPAM may be to destroy the carefully selected hydrolysis degree present in the initial product, thus increasing the sensitivity to salinity and hardness.

Biological degradation may occur with HPAM, but is rarely observed. If a HPAM solution is known to be susceptible to biological degradation, biocides may be used as a preventative. Formaldehyde has been applied frequently for this purpose.

4.4.2 Mechanical Degradation

Mechanical degradation is a short-term effect and refers to the breakdown of a macromolecule, induced by high mechanical stresses. Since high-MW polymers are especially susceptible to mechanical degradation, the average MW of the polymer will decrease and an irreversible viscosity reduction may ensue [12].

The degree of mechanical degradation experienced by the polymer correlates with the applied pressure gradient [13]. The high velocity flows which causes the polymer molecules to be mechanically degraded may be present in surface equipment, injection well and/or the sand face itself [23]. The elastic properties of HPAM renders it highly susceptible to mechanical degradation, where dominant factors are molecular weight, salinity and hardness [35], [36], [37].

The flow velocity falls off quickly with distance from the injector during a polymer flood (radial geometry) and little mechanical degradation occurs within the reservoir itself [23]. Polymer solutions will therefore be exposed to mechanical degradation mainly in the vicinity of the well-bore region.

The overall effect of mechanical degradation is to reduce the differential pressure from the injection well to the producer because of reduced apparent viscosities that results. This reduced pressure drop is referred to as an entrance pressure drop and its value correlates well with the degree of mechanical degradation.

Based on laboratory experiments, mechanical degradation has been reported to be more significant in linear core floods compared to floods performed in radial geometry [7]. The dominating difference between linear and radial geometry is the steady state pressure obtained in linear core plugs compared to the non-linear pressure response in radial models (transient and semi-steady state).

It has been suggested that since polymers experience a high pressure drop for a short duration of time, polymer molecules may be able to readjust themselves in radial models, resulting in a reversible degradation mechanism. However, in linear core plugs, the duration of high pressure drops experienced by polymer molecules are significantly greater. Polymer molecules may not be able to recover, thus resulting in an irreversible degradation process [7].

To investigate whether a HPAM molecule has been mechanically degraded during polymer flooding, both injected and effluent bulk viscosities are measured. The viscosity loss caused by

mechanical degradation will be irreversible. Therefore, if viscosity of the effluent is significantly reduced compared to injected viscosity, a polymer may have been subjected to mechanical degradation.

To alleviate the problem associated with mechanical degradation in the near well bore region, partial preshearing of the polymer solution may be a viable option. Figure 4.8 shows a plot of viscosity versus shear rate for both unsheared and presheared HPAM solutions.

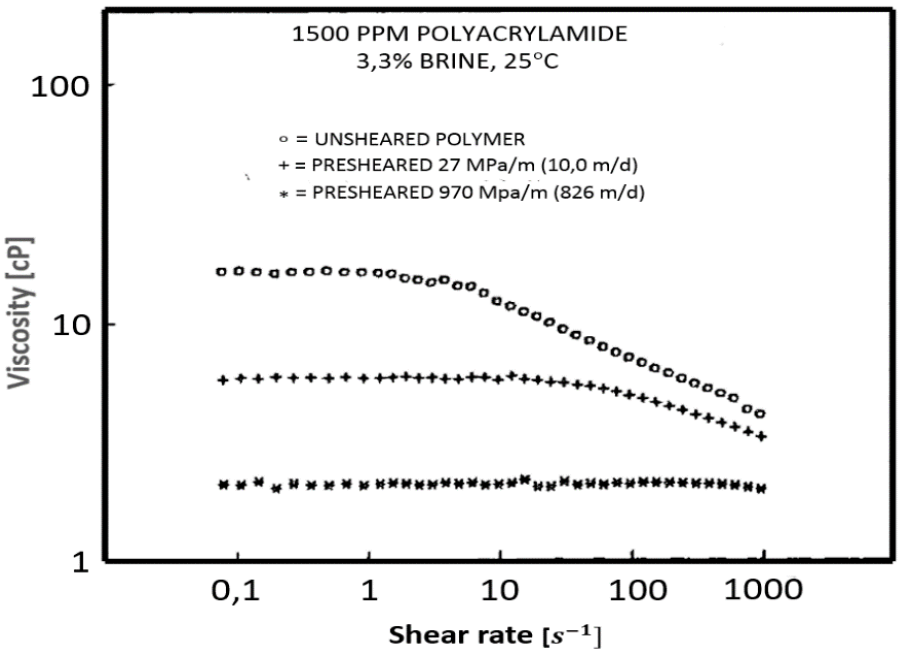

Figure 4.8: Effects of severe shearing and resulting mechanical degradation in a Berea core on viscosity of a HPAM sample (modified from Seright, R. et al.) [38].

4.5 Retention

Polymer molecules will interact with the porous media during a polymer flood. This interaction may cause polymers to be retained, which will reduce polymer solution viscosity. In addition, polymer retention may also cause the permeability of the porous media to be lowered. However, the overall effect of polymer retention is typically to reduce oil recovery. In general, polymer retention will increase with decreasing rock permeability [39].

Retention, Γ_m, in flow through porous media can be stated as follows [12]:

$$\Gamma_m = \Gamma \cdot 2{,}7194 \cdot \rho_r \qquad (4.12)$$

Where Γ is retention level (in mass of polymer per unit mass of solid) and ρ_r is bulk formation density including rock grains and pore space. Equation (4.12) gives retention in pound per acre foot and will be used when calculating adsorptions of both 800 and 2000ppm in STARS simulations (chapter 8.5).

As illustrated in Figure 4.9, three principal mechanisms are responsible for polymer retention during flow through porous media. These mechanisms include adsorption on rock surfaces, mechanical entrapment in small pores and flow induced hydrodynamic retention [40].

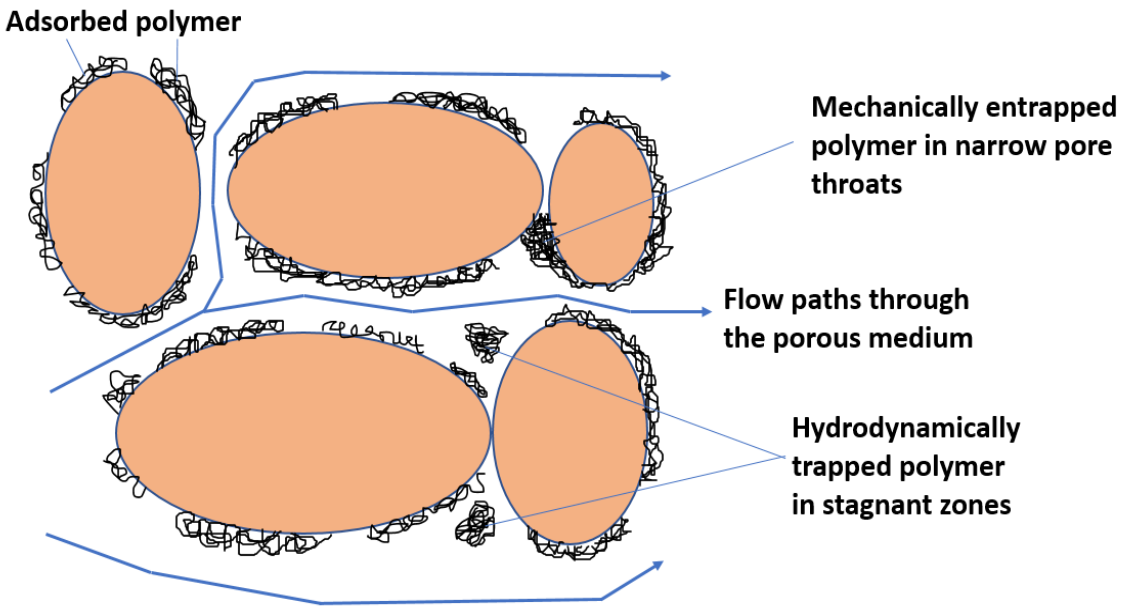

Figure 4.9: Schematic diagram of polymer retention mechanisms in porous media (modified from Sorbie, K. S.) [12].

The level of retention during polymer flooding can be determined by investigating the difference between injected and effluent polymer concentration after a sufficient number of

pore volumes has been injected. A lower effluent than injected concentration indicates that retention has occurred during polymer flooding.

It has been reported by Zhang and Seright (2014) [5] that if a dilute HPAM solution is injected into porous media to satisfy retention, the subsequent injection of a higher concentration solution will not result in additional polymer loss. Since polymer retention is a huge expenditure in polymer flood projects, the economic feasibility of some projects may be positively affected by the implementation of the method suggested by Zhang and Seright.

Polymer retention in porous media flooded with HPAM solutions has been observed to be lower in cores containing residual oil than in absence of residual oil [34], [41].

4.5.1 Polymer Adsorption

Polymer adsorption occurs both in bulk solutions and in flow through porous media, and refers to the interaction between polymer molecules and the solid surface [12]. Due to physical adsorption, this interaction causes polymer molecules to be bound to the surface of the solid. The polymer molecules will effectively occupy surface adsorption sites where the level of adsorption is proportional to surface area.

During polymer adsorption, flux of adsorbing polymer layers adjacent to pore walls will effectively be zero. Therefore, flow of polymer solutions through porous media may be reduced because of adsorption.

The level of polymer adsorption in porous media is strongly dependent upon the inherent properties of species involved in the adsorption mechanism. It is dependent upon polymer type and its specific molecular properties in solution (flexible or rigid structure, molecular weight, molecular size, charge density, degree of hydrolysis in the case of HPAM), solvent conditions (salinity, hardness, temperature, pH) and the adsorbing surface (silica, sandstone, clay, etc.).

Because EOR polymers such as HPAM generally have high molecular weights and extended chains, it is statistically very unlikely that a polymer molecule will detach from all points at the same time. Polymer adsorption is therefore assumed to be approximately irreversible [5].

Because of the associated high costs related to polymer adsorption, it is considered one of the key factors when determining the economic viability of a polymer flood project [12], [5].

4.5.2 Mechanical Entrapment

The mechanism of mechanical entrapment occurs exclusively in flow through porous media, and retention resulting from this mechanism is due to polymer molecules becoming trapped in narrow flow channels. The complex pore structure of porous media can be envisaged as a large interconnected network with a multitude of possible routes connecting the inlet and outlet of the core. A given fraction of the network will consist of pore throats and as the polymer solution propagates through the porous media, some molecules will become trapped in the narrow pores. This entrapment will block the smaller pores and flow will be reduced. Mechanical entrapment is most likely to occur in low permeability materials where the pore sizes are smaller and appears to increase in the presence of residual oil compared to situations where the porous media is fully water-saturated [34].

Mechanical entrapment may be the result of both straining and concentration blocking [42], as illustrated in Figure 4.10.

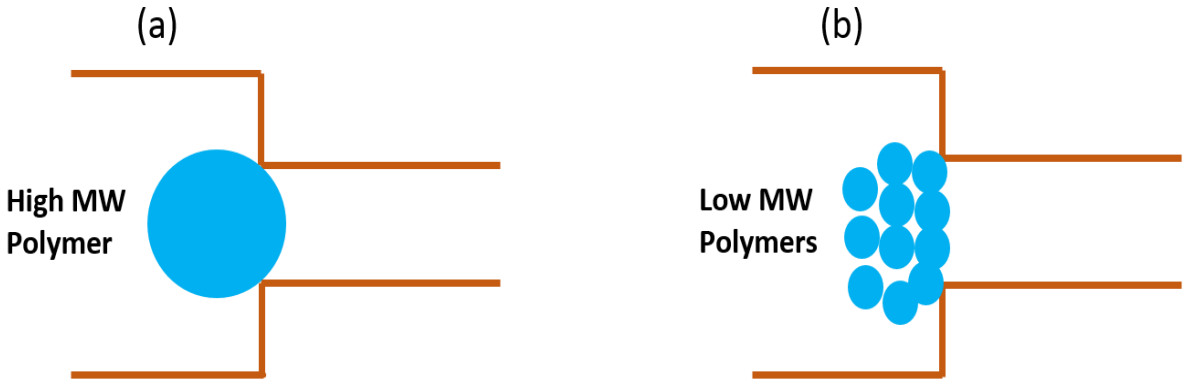

Figure 4.10: Straining (a) of high MW polymers and concentration blocking (b) of low MW polymers relative to pore throats in flow through porous media.

Straining may occur when large molecular weight polymers relative to pore throat size propagates through porous media and become mechanically trapped in pore throats. However, concentration blocking may occur for low molecular weight polymers relative to pore size after injection or after mechanical degradation of high molecular weight polymers.

Mechanical entrapment during polymer flooding may lead to several anticipated consequences. Firstly, the effluent polymer concentration will be reduced below the input concentration. At least until a sufficient number of pore volumes has been injected. Secondly, the distribution of entrapped polymer should show a longitudinally exponential decrease from the inlet to the outlet of the core. Thirdly, if the number of entrapment sites exceeds a critical value, the core will be completely blocked, thus rendering it impermeable [12].

4.5.3 Hydrodynamic Retention

Hydrodynamic retention of polymer is considered the least well defined and understood retention mechanism, and occurs like mechanical entrapment exclusively in flow through porous media [12].

The phenomenon of hydrodynamic retention refers to the observed increase of polymer retention with flow rate and was shown by Maerker (1973) [43]. By measuring effluent concentration during a polymer flood, Maerker found greater polymer retention with increasing flow rate for a polyacrylamide polymer, thus concluding that the loss of polymer molecules through interaction with the porous medium was greater at higher flow rates. However, it was reported by Zhang et al. (2015) [44] that hydrodynamic retention increases abruptly with increased flow rate in the low-flow region, in contrast to the more gradual increase in the high-flow region. They also concluded that almost all hydrodynamic retention is reversible and had limited effect on polymer flow behavior in porous media.

The physical mechanism of hydrodynamic retention is thought to result from hydrodynamic drag forces temporarily trapping polymer molecules in stagnant flow regions [12].

4.6 Mobility Reduction

Polymer solutions are known to resist flow in porous media because of increased apparent viscosity values and their ability to reduce permeability, where the latter is caused by retention mechanisms. To describe mobility reduction caused by polymer flooding in terms of resistance to flow and permeability reductions, the following factors may be defined:

Resistance factor (R_F) is an indication of the total mobility lowering contribution of a polymer, and is defined as the ratio of water mobility (λ_w) to polymer solution mobility (λ_p) at similar conditions [23], [45]. When combined with equation (2.2), resistance factor can be stated as follows:

$$R_F = \frac{\lambda_w}{\lambda_p} = \frac{k_{e,w}\,\mu_p}{k_{e,p}\,\mu_w} \tag{4.13}$$

Where $k_{e,w}$ and $k_{e,p}$ is effective permeability of water and polymer, respectively, and μ_w and μ_p is viscosity of water and polymer, respectively.

To isolate the flow resistance caused by permeability reductions alone, permeability reduction factor (R_k) is defined as the ratio between water permeability (k_w) and polymer permeability (k_p) [12]:

$$R_k = \frac{k_w}{k_p} = \frac{\mu_w}{\mu_p}\,R_F \tag{4.14}$$

Residual resistance factor (R_{RF}) indicates the permanence of the permeability reduction effect caused by the polymer solution, and is defined as the ratio of water mobility before (λ_w) and after (λ_{wa}) polymer injection:

$$R_{RF} = \frac{\lambda_w}{\lambda_{wa}} = \frac{k_w}{k_{wa}} \approx \frac{k_w}{k_p} \tag{4.15}$$

Where k_w and k_{wa} is water permeability before and after polymer injection, respectively.

4.7 Molecular Weight (MW)

As mentioned in chapter 4.1, the viscosity increasing feature of HPAM lies in its large molecular weight. Molecular weight is reported in Dalton (Da), which is equivalent to grams per mole [12]. Figure 4.11 illustrates the effect of increased molecular weight of several HPAM polymers on solution viscosity, while Table 4.1 list MW of polymers from the figure.

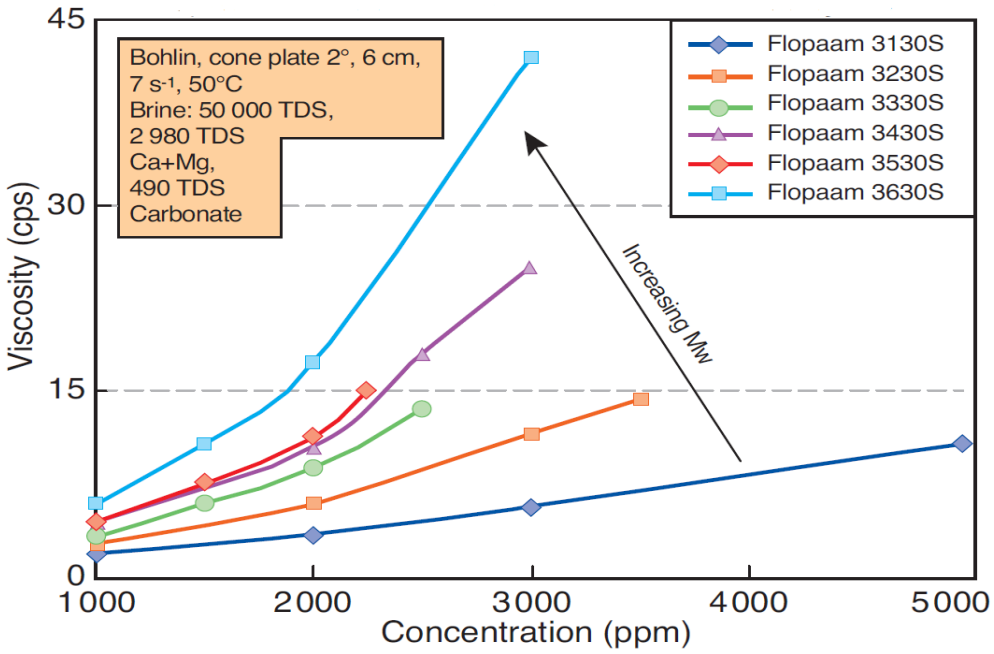

Figure 4.11: Viscosity as a function of concentration for different molecular weight HPAMs (from Thomas, A., Gaillard, N. and Favero, C.) [15].

Table 4.1: Molecular weights of Flopaam polymers from Figure 4.11 [6], [46], [47].

Polymer Type	Molecular Weight (Da)
Flopaam 3130S	2
Flopaam 3230S	7
Flopaam 3330S	8
Flopaam 3430S	12
Flopaam 3530S	16
Flopaam 3630S	20

Because polymers are not monodisperse and thus will have a molecular weight distribution, molecular weights reported from Table 4.1 are average values [12]. The large molecular weight HPAM polymer investigated in this thesis is Flopaam 3630S.

Figure 4.11 shows that an increase in MW is not necessarily proportional to the increase in polymer viscosity at constant concentration. For example, when increasing the MW from 12 to 16 Da (Flopaam 3430S versus 3530S) at a concentration of 2000ppm, the corresponding viscosity increase is negligible. Therefore, a direct functional relationship between MW and viscosity is difficult to establish.

Use of high MW polymers may improve the economic aspect of a polymer flood project. A drawback of using high MW polymers is unwanted effects on flow through porous media associated with retention mechanisms such as adsorption and mechanical entrapment.

High MW flexible coil polymer solutions such as HPAM are reported to be highly shear degradable [36] and mechanical degradation is seen to increase with increasing MW [48]. Consequently, high MW polyacrylamides may lose a significant fraction of their viscofying power when subjected to mechanical degradation. Thus, choosing a lower MW polymer may be a superior option for field applications where shearing conditions are not well controlled [48]. The preshearing approach discussed in chapter 4.4.2 may therefore be circumvented when choosing lower MW polymers for polymer flood projects.

It has been reported by Heemskerk et al. [33] that onset of shear thickening shift towards higher values with decreasing MW when injecting HPAM into consolidated and unconsolidated sandstones.

High MW polymers tend to have a wide MW distribution, whereas the larger MW species will generally propagate faster through the porous media. Because the larger MW species contacts flow channels in the medium first, they will be adsorbed more often. This may result in a dramatic decrease in the polymer solution viscosity [12]. It is therefore crucial to consider the polydispersity nature of high MW polymers when conducting a polymer flood.

In flow through porous media, it is the highest MW species that are believed to be responsible for the shear thinning behaviour of HPAM. As mentioned, these ultra-high MW species are especially susceptible to mechanical degradation and may therefore be degraded in the injection well where flux is at its maximum value in radial models. If severe mechanical degradation does occur, HPAM rheology behaviour is considered Newtonian or at least near-Newtonian at low flux [6], [7].

4.8 Polymer Concentration

Polymer molecules may interact in solution and the degree of interaction is known to be strongly influenced by concentration. The viscosity increasing feature of large MW species in HPAM will be accentuated with increasing polymer concentration [23].

Three concentration regimes have been proposed (de Gennes 1979 [49]; Ying and Chu 1987 [50]) as dilute ($c < c^*$), semi-dilute ($c^* < c < c^{**}$) and concentrated ($c^{**} < c$), where c^* and c^{**} is the critical overlap concentration from dilute to semi-dilute and semi-dilute to concentrated, respectively.

In dilute solutions, polymer molecules have freedom to move independently of each other, which excludes the possibility for aggregation and entanglement. In semi-dilute solutions, the hydrodynamic radii of individual polymer molecules overlap, thereby enabling the possibility for aggregation and entanglement. At concentrations exceeding the semi-dilute regime (concentrated regime) solutions will form a network structure and is termed a viscoelastic solid [7], [12], [5]. The three concentration regimes are illustrated in Figure 4.12.

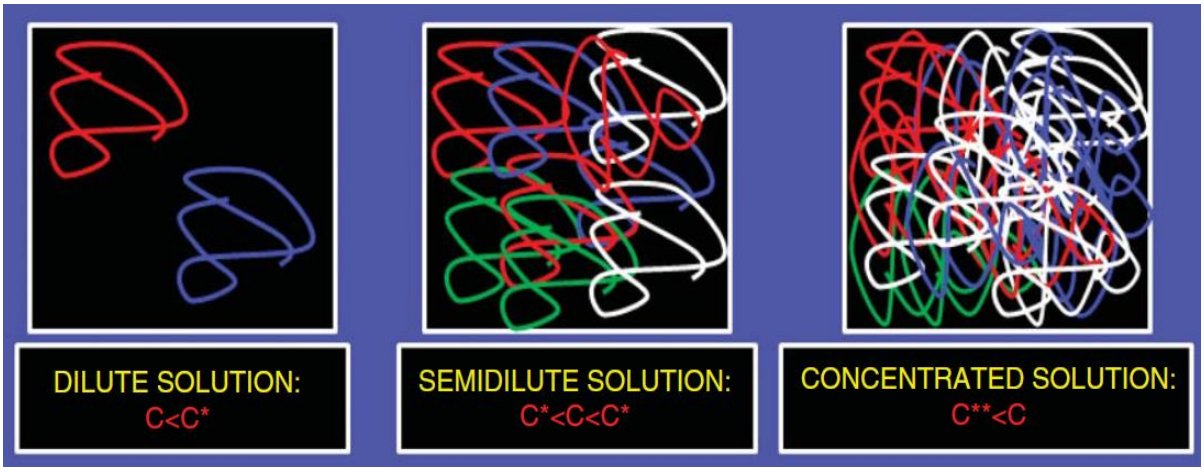

Figure 4.12: Polymer-molecule interaction at different concentrations (from Zhang, G. and Seright, R.) [5].

Maerker (1975) [36] investigated the relation between HPAM polymer concentration and mechanical degradation in porous media. He concluded that viscosity reduction induced by mechanical degradation was completely independent of polymer concentration, at least for the narrow concentration range of 300-600ppm.

Effects of HPAM concentration on retention in porous media has been investigated in a comprehensive study by Zhang and Seright (2014) [5]. Consistent results indicated that different retention behavior exist in dilute, semi-dilute and concentrated regions. In both dilute

and concentrated regions, polymer retention was practically independent of concentration. In the semi-dilute region however, polymer retention was concentration dependent. Figure 4.13 illustrates the region-dependent retention behavior observed in different concentration regimes.

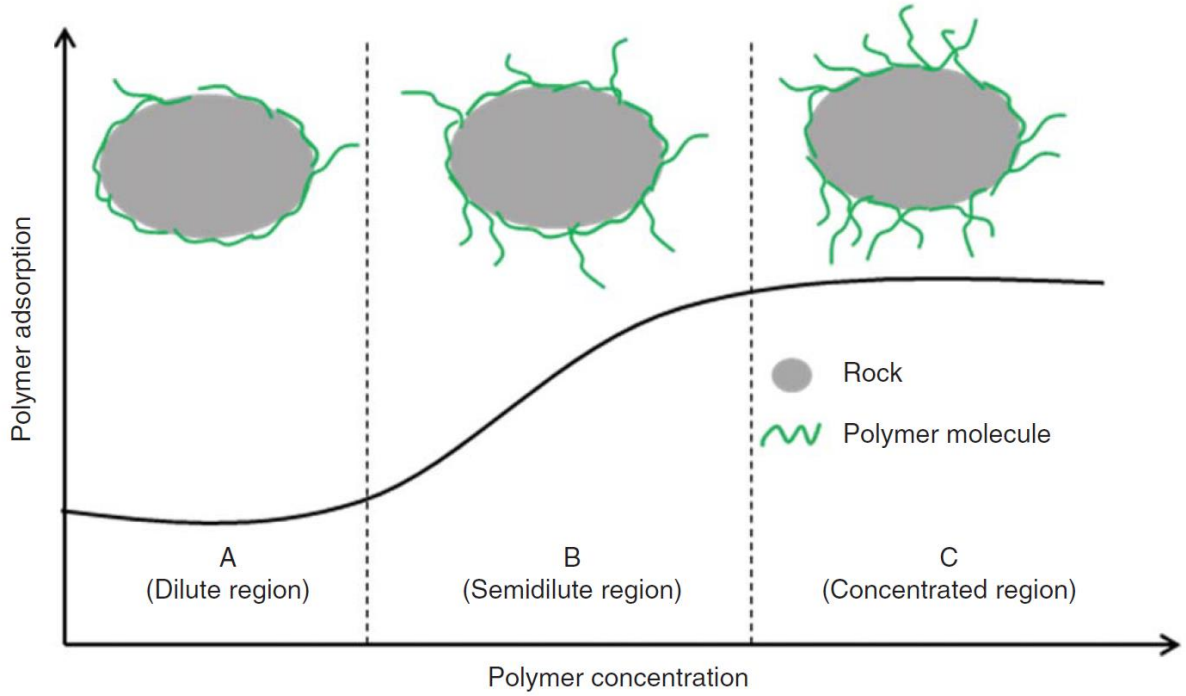

Figure 4.13: Proposed polymer adsorption mechanism on the rock surface (from Zhang, G. and Seright, R.) [5].

Since polymer concentrations of 800 and 2000ppm HPAM investigated in this thesis are in the semi-dilute regime it is expected that polymer retention will be concentration dependent [7].

The concentration of HPAM also influences the onset of shear thickening. In both unconsolidated and consolidated sandstone the onset of shear thickening has been reported to shift towards higher values with decreasing polymer concentration [6], [33]. Effects of concentration on the onset of shear thickening in the presence of residual oil will be investigated in chapter 9.1.9.

4.9 Salinity and Hardness

As mentioned in chapter 4.1, because HPAM is a polyelectrolyte it will interact with ions in solution. The influence of increasing salt concentration in a HPAM solution will be to effectively contract polymer molecules, resulting in a viscosity reduction as shown in Figure 4.14 [12].

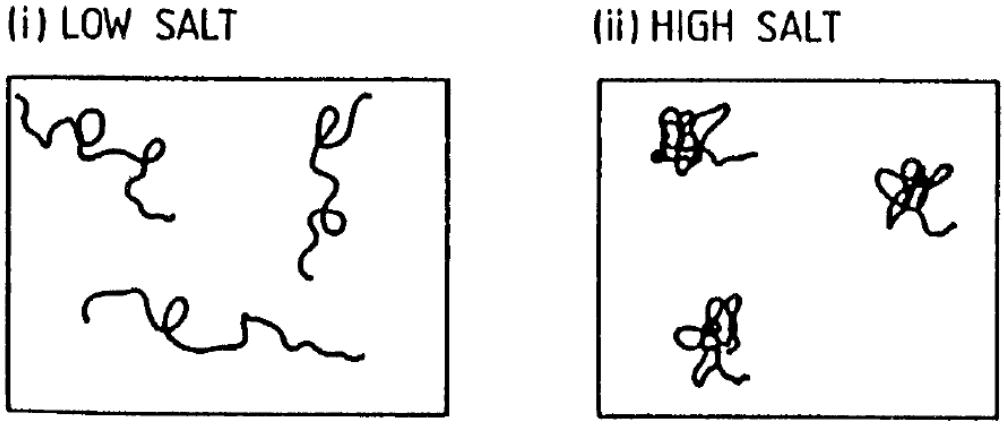

Figure 4.14: Schematic of the effect of increasing the salt concentration on the conformation of flexible coil polyelectrolytes such as HPAM (from Sorbie, K. S.) [12].

Salinity has also been observed to influence adsorption. Smith (1970) [51] has shown that there exists a positive relationship between salinity and adsorption level for HPAM. Szabo (1975) [34] observed the same increase in adsorption with increased salinity while studying retention of HPAM in unconsolidated silica sands and Berea cores. However, the increase in adsorption with salinities exceeding 2% was negligible. It was concluded that at salinities above 2% NaCl solution ionic strength does not significantly change the hydrodynamic volume of the polymer.

From equation (4.1), divalent hardness ions such as Ca^{2+} and Mg^{2+}has a higher valence and consequently a greater ionic strength than does monovalent salinity ions such as $Na^{+}$and K^{+}. The effect of hardness ions compared to salinity ions have been reported to be more significant due to their higher charge and polarizability. This causes divalent ions to bind more tightly to polymers [12].

For HPAM, sensitivity to mechanical degradation has been reported to increase with brine salinity [48].

The brine used in the history matched experiment in this thesis was of relatively low salinity with a low content of divalent hardness ions (total dissolved solids equal to 4659ppm).

5 INJECTIVITY

Injectivity, I, is a critical parameter for implementation of polymer flood projects [7] and may be defined as the ratio of volumetric injection rate, Q, to the pressure drop associated with polymer propagation between an injection well and a producer, ΔP [10].

$$I = \frac{Q}{\Delta P} \tag{5.1}$$

If significant injectivity decline ensues from polymer flooding, a remediation measure may be to increase volumetric injection rate. Since this parameter is constrained by the fracturing pressure of the formation it is often not possible to significantly increase Q without inducing fractures in the formation. Thus, problems of well injectivity may be difficult to avoid if fracturing is not a viable option. The need to reduce injection rate may be detrimental to the economic feasibility of a polymer flood project because of resulting delays in oil production.

If fracturing is considered a viable option, injectivity may be improved by increasing volumetric injection rate above fracture rate. Remediating the problem associated with injectivity loss by fracture growth may in some cases be a satisfactory approach. Kyunghaeng et al. (2011) [52] reported that fracture growth does not have a significant impact on oil recovery and reservoir sweep in homogenous reservoirs. However, in layered reservoirs, influence on oil recovery and water cut has been reported to be significant. When injecting into a layered reservoir it has been shown that fracture growth in one layer may leave other layers almost entirely unswept.

Differential pressure will generally increase with propagation distance because of friction along the pore walls of porous media. Increasing the propagation length of polymer solutions through porous media will therefore effectively reduce injectivity [7]. It may therefore be an option to drill additional wells to increase injectivity. However, drilling additional wells is expensive and may be detrimental for the economic feasibility of a polymer flood project.

In radial models, differential pressure decreases drastically with distance from the injection well, as depicted in Figure 5.1.

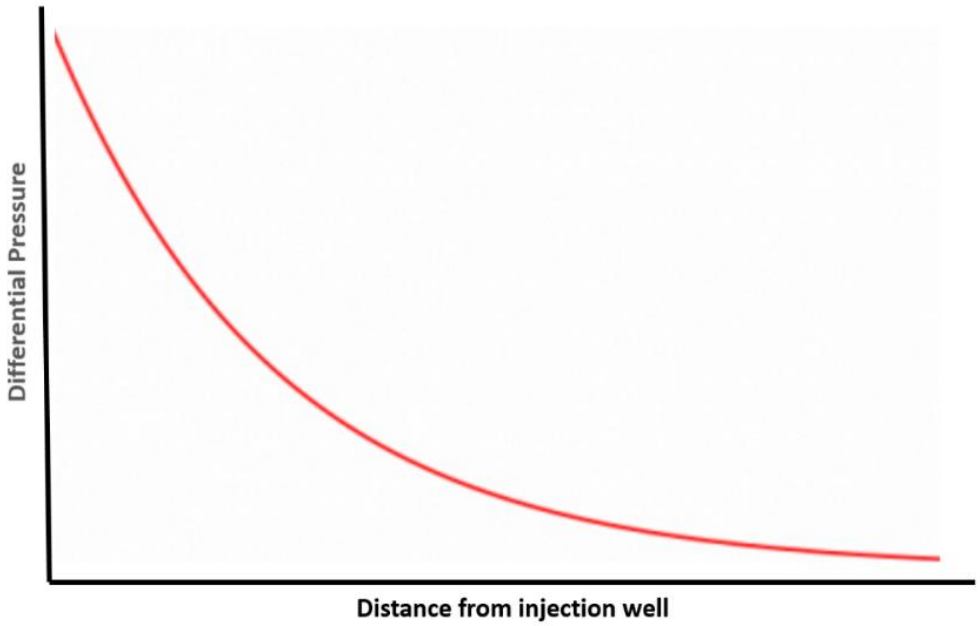

Figure 5.1: Differential pressure as a function of distance from injection well in radial models.

Because of the dramatic differential pressure decrease with distance from the injection well in radial models, well injectivity will be of most practical concern in polymer flooding. This is because differential pressure will be much higher in the near well bore region compared to the rest of the reservoir and according to equation (5.1), high differential pressures will have detrimental effects on injectivity.

In-situ rheological properties of HPAM are crucial for injectivity [7]. The viscoelastic nature of HPAM results in both shear thinning and shear thickening behavior in flow through porous media. Based on equation (5.1), without considering the shear dependent viscosity behavior of HPAM, injectivity will reach its highest value at maximum volumetric injection rates. Since HPAM may exhibit shear thickening behavior in the high flow rate regime, optimal injectivity is not necessarily found at these rates.

In the low flow rate region, HPAM may exhibit shear thinning behavior. Therefore, both low volumetric injection rate and possibly high absolute apparent viscosity values will contribute to potentially very low injectivity values. In addition, at low volumetric injection rates the oil production will be delayed and the economic feasibility of the polymer flood project may be affected.

In radial geometry, polymer flux will decrease from the injection well towards the producer when injecting at constant volumetric rate. The shear thickening behavior of HPAM that occurs

in the high flux regime is therefore well known to cause injectivity problems near the well region where velocities are highest.

Mechanical degradation will improve injectivity due to reduced polymer viscosities resulting in lower differential pressures [13]. However, the occurrence of mechanical degradation is not sought after and represents a major challenge in polymer flooding because of its detrimental effect on mobility ratio. As mentioned in chapter 2.5, volumetric sweep in reservoirs will be largely determined by the mobility ratio between water and oil. Reduced viscosity values resulting from mechanical degradation will result in a less favorable mobility ratio and thus decrease volumetric sweep efficiency.

As mentioned in chapter 4.4.2, Seright (1983) observed an abrupt pressure drop at the inlet sandface at sufficiently high volumetric injection rates. This entrance pressure drop was not observed until some mechanical degradation was detected and the degree of mechanical degradation correlated well with the observed pressure drop. To alleviate problems associated with mechanical degradation, partial preshearing of polymer solutions may be a viable option.

Retention during polymer flooding may reduce the permeability of the porous media. Retention induced permeability reduction was defined in chapter 4.6 as the permeability reduction factor. This permeability decrease will induce larger differential pressures and thus decreases injectivity. Retention is therefore of great concern when assessing polymer injectivity. To remediate the problem of reduced injectivity resulting from a permeability reduction, preflushing the porous media may be a satisfactory option if polymer retention is assumed to be reversible [23].

Plugging of HPAM in injection wells are well known to cause injectivity impairment, and can ensue is several ways. Firstly, gels may form if the polymer solution is insufficiently dispersed before injection. Secondly, if completely dissolved HPAM are crosslinked by multivalent ions present in the injection brine, gel formation may ensue. This may occur in high-saline injection brines or injection brines containing a large number of hardness (multivalent) ions. HPAM may also form gels by flocculating in the polymer solution or by reacting with rock minerals in porous media [13].

Both increased polymer molecular weight and concentration will generally induce larger viscosity values and injectivity will be reduced when increasing these parameters [14], [23] [13]. The effects of concentration on HPAM injectivity in the presence of residual oil will be investigated in chapter 9.1.12.

Since injectivity of polymer relative to brine is of main concern in polymer flooding, relative injectivity may be derived from equation (5.1). Because injectivities of both polymer and brine are investigated at identical volumetric injection rates, the following definition of relative injectivity may be utilized:

$$I = \frac{\frac{Q}{\Delta P_p}}{\frac{Q}{\Delta P_b}} = \frac{\Delta P_b}{\Delta P_p} = \frac{\eta_b k_{e,p}}{\eta_p k_{e,b}} \tag{5.2}$$

Where ΔP_p is pressure drop during polymer flooding and ΔP_w is pressure drop during water flooding.

As mentioned in chapter 4.6, resistance factor (R_F) is defined as the ratio between water and polymer mobility. Thus, injectivity is equal to the inverse of resistance factor, according to equation (5.2).

Equation (5.2) enables injectivity to be compared in terms of one-phase versus two-phase flow. When the flow is one-phase, effective permeabilities are equal to absolute permeability. This equation will be used when effects of residual oil of polymer injectivity is investigated. This is because the two values of injectivity compared are obtained from two different experiments where a major difference is one versus two-phase flow. Therefore, brine injectivity must be considered as to not underestimate the polymer injectivity in presence of residual oil. This point will become clearer and discussed further in the results and discussion part of this thesis.

6 PREVIOUS WORK AT UNI CIPR

Extensive ongoing research on polymer flooding is being conducted at Centre for Integrated Petroleum Research at the University of Bergen (Uni CIPR) and a multitude of papers has been published in recent years. This chapter will review some of these papers and their findings.

6.1 Radial and Linear Polymer Flow – Influence on Injectivity (2016)

Skauge et al. investigated the differences between linear and radial flow of polymer and its consequent effects on injectivity. Consistent with previous literature, linear core floods showed degradation of polymer at high flow rates and significant shear thickening, thus inducing high injection pressures. However, polymer flow in radial geometry exhibits significantly reduced differential pressures compared to linear core floods. Also, onset of shear thickening occurred at significantly higher velocities in radial compared to linear flow conditions.

While linear core floods show predominately shear thickening behaviour, radial polymer flow demonstrated both shear thinning and shear thickening behaviour. Occurrence of shear thinning in absence of mechanical degradation is not consistent with previous literature based on linear core floods [3].

They attributed differences between linear and radial flow results to deviating pressure conditions. While linear core floods are performed at steady state conditions, radial injections pass through both transient and steady state pressure regimes.

In this thesis, the part of the paper concerning radial flow of 2000ppm HPAM polymer is used to compare its behaviour in presence of residual oil. Both rheology behaviour and injectivity will be assessed.

6.2 2-D Visualisation of Unstable Waterflood and Polymer Flood for Displacement of Heavy Oil

Oil displacement at adverse mobility ratios by injection of brine and polymer were investigated by Skauge et al. to improve description of viscous instabilities, mechanisms for finger growth, water channelling at adverse mobility ratio and oil mobilization by polymers [53].

Experiments were performed in radial models when studying waterflooding and polymer injection with high viscous oils. The utilization of an X-ray imaging system enabled visualization of oil displacement and the underlying flow mechanisms and oil recovery could be investigated quantitatively.

They observed that capillary forces smeared displacing fronts and prevented viscous fingering, even at high adverse viscosity ratio at water wet conditions. Wettability alterations (aging the rock material) mitigated the capillary forces and thus viscous fingering became more pronounced. While water flooding achieved microscopic recovery of up 30% after five pore volumes injected, polymer flooding impressively increased recovery an additional 30%, thus resulting in final recoveries in excess of 60%.

Effects of water floods on front instabilities was to create multiple thin sharp fractal-like fingers. Generally, the finger structure varied with mobility ratio and produced sharper fingers at increasing oil viscosities.

A quick increase in fractional flow of oil was observed after tertiary polymer flooding was initiated. This occurrence was attributed to crossflow of mobilized oil into established water channels (fingers) and displacement of mobilized oil into these water channels.

6.3 Effect of porous media properties on the onset of polymer extensional viscosity

The onset of polymer extensional viscosity were investigated exclusively in terms of rock properties by Nematollah et al. [29].

In this study, numerical simulation using a modified form of the Carreau model was utilized. They observed that that the degree of porous media tortuosity influenced the onset of extensional viscosity. Results indicated that as the tortuosity of a rock sample increased, onset of extensional viscosity decreased. Based on these finding, a linear correlation was proposed between stretch rate and Darcy velocity, whereas the linearity coefficient was related to the tortuosity of the rock sample. Using this correlation, the Deborah number at the onset of extensional viscosity was equal for all rock samples investigated.

The effect of microscopic properties of pore geometry on the onset of extensional viscosity was also studied using simplified 2D contraction-expansion channels. Investigated properties encompass aspect ratio and pore throat length.

The effect of increasing aspect ratio was to reduce Darcy velocity for onset of extensional viscosity. This occurrence was attributed to the larger stretch rates experienced by polymer molecules when increasing aspect ratio.

The effect of increasing pore throat length was to increase Darcy velocity where onset of extensional viscosity commenced. This observation was due to the increase in relaxation time of polymers when flow channels were increased, thus decreasing the Deborah number.

6.4 Influence of Polymer Structural Conformation and Phase Behavior on In-Situ Viscosity

In-situ viscosity of HPAM was investigated in terms of different conformational states and phase behavior by Skauge et al [35].

In-situ viscosity was determined as a function of molecular weight, concentration and salinity. An improved description and prediction of in-situ viscosity based on classification of polymer behavior was the main objective of the study.

HPAM polymers utilized in the study consisted of both high and low molecular weights and was dissolved in different brines. All concentrations regimes were investigated which encompass: dilute, semi-dilute and concentrated regimes.

It was reported that salinity was the dominating factor affecting in-situ viscosity in both the dilute and semi-dilute concentrations regimes. However, in the concentrated regime and upper semi-dilute regime, the dominating factor for in-situ viscosity was molecular weight.

They observed that bulk and in-situ rheology differs significantly. While both shear thinning and shear thickening was observed in bulk, in-situ rheology also exhibits Newtonian behavior.

Occurrence of shear thickening was reported as independent of polymer molecular weight and brine salinity. Conclusions drawn from this observation was that shear thickening may be an inherent rock property related to tortuosity, permeability and pore size distribution.

Onset of shear thickening was constant for both molecular weights investigated and was also independent on brine salinity, phase and polymer concentration.

Polymers dissolved in brines at sea water salinity was more prone to mechanical degradation than polymers in low saline brine. In both brines, low molecular weight HPAM did not show any signs of mechanical degradation, while this was not the case for high MW species. Thus, high molecular weight polymers are more susceptible to shear degradation. Also, sensitivity to shear degradation was seen to increase with increasing brine salinities.

7 SIMULATION MODELS

Three water floods and two polymer floods serves as the basis for history matches performed in this thesis and will collectively be referred to as the X4 experiment. In this experiment, a radial Bentheimer disc saturated with residual oil was flooded sequentially with alternating water and polymer injections in the following order:

1. Initial Water Flood (IWF)
2. 800ppm HPAM Flood (PF800)
3. Secondary Water Flood (SWF)
4. 2000ppm HPAM Flood (PF2000)
5. Tertiary Water Flood (TWF)

Relevant fluid and petrophysical properties from the X4 experiment are shown in Table 7.1.

Table 7.1: X4 experiment: Fluid and petrophysical properties.

X4 Experiment	IWF	PF800	SWF	PF2000	TWF
Disc Height [cm]	2,205	2,205	2,205	2,205	2,205
Disc Radius [cm]	15	15	15	15	15
Injection Well Radius (R_w) [cm]	0,3	0,3	0,3	0,3	0,3
Area [cm^2]	175,5	175,5	175,5	175,5	175,5
Pore Volume [mL]	352,2	352,2	352,2	352,2	352,2
Porosity [$fraction$]	0,228	0,228	0,228	0,228	0,228
Residual Oil Saturation [$fraction$]	0,22	0,22	0,22	0,22	0,22
Brine Viscosity [cP]	0,96	0,96	0,96	0,96	0,96
Oil Viscosity [cP]	250	250	250	250	250
Polymer Concentration [ppm]	-	800	-	2000	-
Injection Rate Interval [mL/min]	0 - 6	0,01 – 2,0	0 - 10	0,002 – 1,6	0 – 10
Temperature [$°C$]	22	22	22	22	22

The brine used for the X4 experiment was of relatively low salinity with a low content of divalent (hardness) ions. Table 7.2 shows brine composition by ions.

Table 7.2: X4 experiment: Brine composition by ions.

Ion	Concentration [ppm]
Na	1741
K	28
Ca	26
Mg	17
HCO_3	0
SO_4	160
Cl	2687
TDS (Total Dissolved Solids)	4659
Hardness	43

Two polymer concentrations of 800 and 2000ppm was investigated in the X4 experiment. The HPAM polymer used in the experimental conditions of X4 are assumed to be in the semi-dilute regime in the entire concentration range of 800-2000ppm [7].

During the X4 experiment, water and polymer solutions were injected sequentially into an injection well located at the centre of the radial disc and injected fluids propagated radially towards the circumferential outer boundary. Since no oil production was observed during the X4 experiment, the residual oil saturation is assumed to be immobile.

The purpose of history matching water floods in the X4 experiment was to estimate the permeability of the porous media both before and after polymer flooding. In contrast, polymers floods were history matched to assess the rheology of 800 and 2000ppm HPAM in presence of residual oil.

As mentioned in chapter 4.5, polymer molecules will interact with porous media during a polymer flood. This interaction may result in a permeability reduction due to retention mechanisms. If retention is irreversible, permeability reductions will be permanent and is termed residual resistance factor (defined in equation (4.15)). As mentioned in chapter 4.3, apparent viscosity may be overestimated if there is uncertainty about whether the observed differential pressure during polymer flooding is due to polymer rheology or residual resistance

factor. Since permeability reduction could be accounted for by adjusting residual resistance factor before simulating polymer floods, the true rheology of both 800 and 2000ppm was obtained.

Only one pressure port was utilized in the X4 experiment and was located in the injection well. To calculate the pressure drop from the injection well to the outer boundary, the counter pressure from the outer boundary had to be determined. This was achieved by measuring the pressure in the negative propagation direction at a time where no fluids were injected. All pressure readings during water and polymer floods was corrected for this counter pressure, thereby determining the differential pressure.

The radial Bentheimer disc utilized in the X4 experiment is illustrated in Figure 7.1 (not to scale), where pressure in the injection well (P_I) and pressure at the outer disc boundary (P_O) are denoted with a green and red dot, respectively. The size of the injection well is exaggerated in Figure 7.1 and does not represent its relative size.

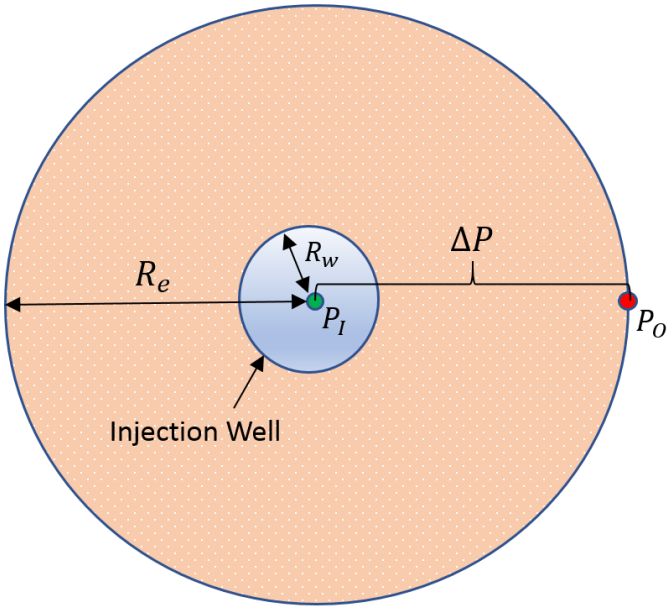

Figure 7.1: Schematic of the radial Bentheimer disc utilized in the X4 experiment (injection well size is exaggerated in this figure).

Bulk viscometric viscosities were also obtained during the X4 experiment. This was performed to establish the possibility of mechanical degradation of polymer during propagation through the porous media. The effluent and injected viscosities was sampled for both 800 and 2000ppm HPAM flooding parts of the experiment. As mentioned in 4.4.2, if significant mechanical degradation has occurred, a drastic viscosity reduction of effluent compared to injected viscosity will be observed.

Bulk viscometric viscosities for the 800ppm HPAM flood are shown numerically in Table 7.3 and graphically in Figure 7.2.

Table 7.3: X4 experiment: Bulk viscometric measurements of 800ppm HPAM, shown numerically (reference viscosities are marked yellow).

	Injected	**Effluent at Q=0,5 mL/min**	**Effluent at Q=2,0 mL/min**	**Injected, second batch**	**Effluent at Q=1,0 mL/min**
Shear rate [1/s]	Viscosity [cP]	Viscosity [cP]	Viscosity [cP]	Viscosity [cP]	Viscosity [cP]
1	32,6	30,3	29,6	35,8	34,9
1,259	30,9	29,5	28,8	34,7	32,6
1,585	28,9	27,6	27,0	32,1	30,1
1,995	27,1	25,6	25,2	29,3	27,9
2,512	25,4	24,2	23,7	26,9	26,1
3,162	23,6	22,4	22,0	25,3	24,2
3,981	21,9	20,8	20,4	22,9	22,3
5,012	20,3	19,3	19,0	21,4	20,6
6,310	18,8	18,0	17,7	19,4	18,9
7,944	17,4	16,6	16,3	17,8	17,4
10,00	**16,0**	**15,3**	**15,1**	**16,4**	**16,0**
12,59	14,8	14,1	13,9	15,0	14,7
15,85	13,6	13,0	12,8	13,8	13,5
19,95	12,5	12,0	11,8	12,7	12,4
25,12	11,6	11,1	10,9	11,7	11,5
31,62	10,7	10,2	10,1	10,8	10,6
39,81	10,0	9,5	9,4	10,1	9,9
50,12	9,4	8,9	8,7	9,5	9,3
63,10	8,8	8,6	8,4	8,9	8,8
79,44	8,3	8,2	8,0	8,4	8,2
100,0	7,7	7,7	7,6	7,8	7,7

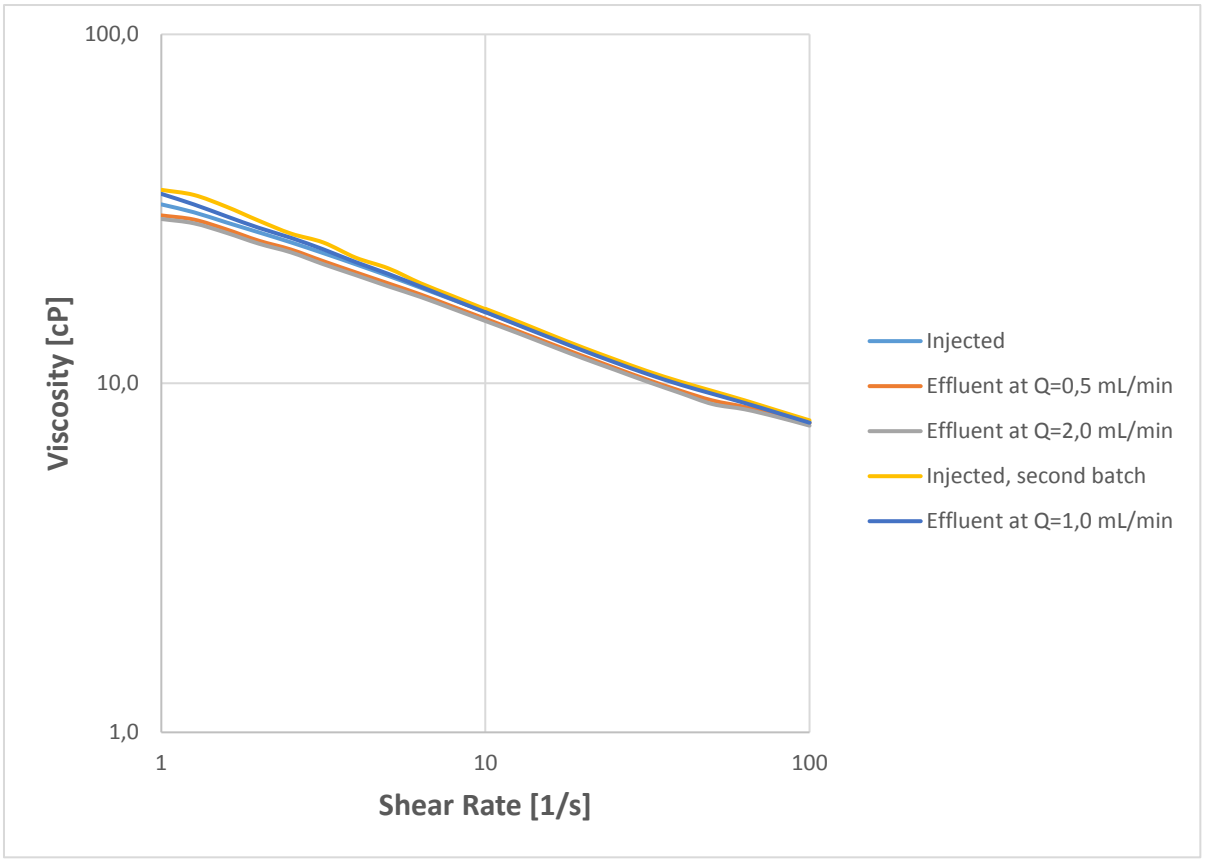

Figure 7.2: X4 experiment: Bulk viscometric measurements of 800ppm HPAM, shown graphically.

In bulk viscometric measurements of 800ppm HPAM, viscosity was measured both before and after propagation through porous media. Viscosity marked injected are viscosity values obtained prior to polymer injection and effluent is viscosity after propagating through porous media at a specified volumetric injection rate. Both injected and effluent polymer samples were sheared in a viscometer at shear rates between 1 and 100 s^{-1}.

The viscosity deviation between injected and effluent viscosity at the reference shear rate of $10s^{-1}$ is below 6%, thus excluding the possibility of mechanical degradation.

Bulk viscometric viscosities for the 2000ppm HPAM flood is shown numerically in Table 7.4 and graphically in Figure 7.3.

Table 7.4: X4 experiment: Bulk viscometric measurements of 2000ppm HPAM, shown numerically (reference viscosities are marked yellow).

	Injected, sampled downstream filter at 1,0 mL/min	**Injected, sampled downstream filter at 10,0 mL/min**	**Effluent at Q=1,0 mL/min**
Shear rate [1/s]	Viscosity [cP]	Viscosity [cP]	Viscosity [cP]
1	322,8	249,7	218,3
1,259	281,4	219,2	192,9
1,585	245,0	191,9	170,2
1,995	213,6	168,9	149,6
2,512	186,0	148,1	131,6
3,162	161,7	129,5	115,6
3,981	141,2	113,7	101,8
5,012	123,4	99,6	89,5
6,310	108,4	87,7	79,1
7,944	95,5	77,5	70,1
10,00	**85,8**	**69,7**	**63,0**
12,59	75,5	61,8	56,0
15,85	66,6	55,0	49,9
19,95	58,9	49,0	44,6
25,12	52,1	43,6	39,8
31,62	46,2	38,9	35,7
39,81	41,1	34,8	32,0
50,12	36,6	31,2	28,8
63,10	32,8	28,1	26,0
79,44	29,4	25,3	23,5
100,0	26,4	22,9	21,3

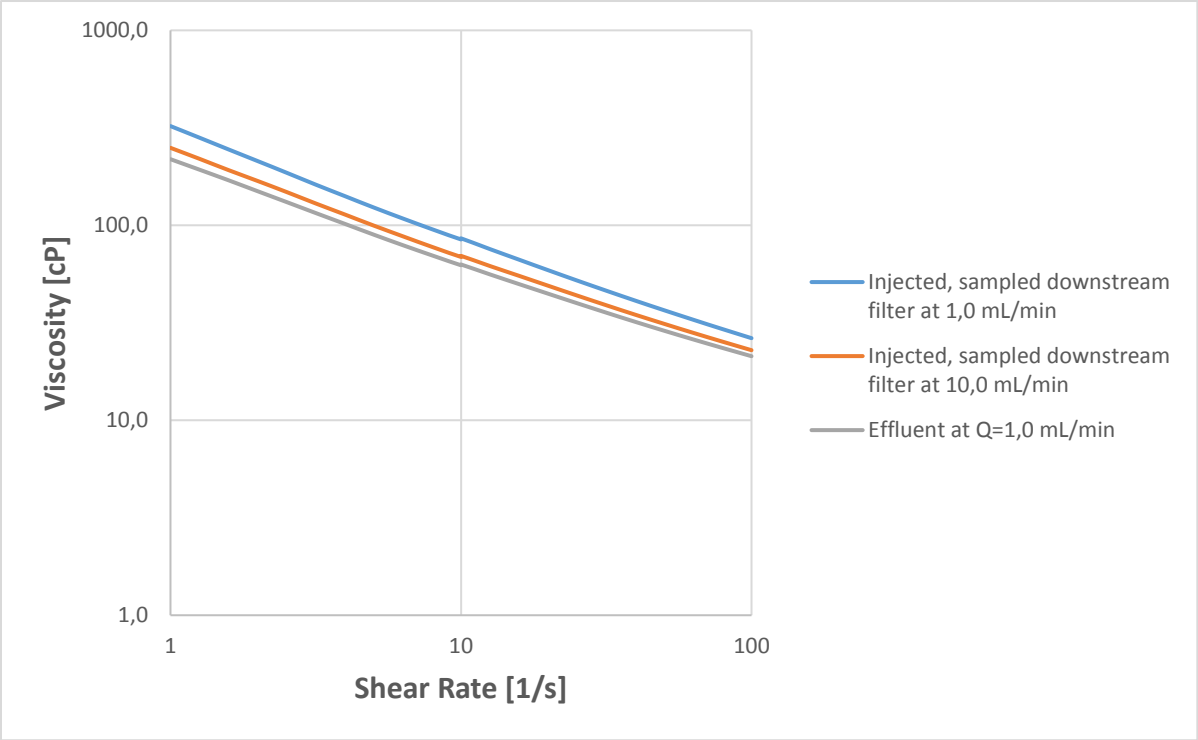

Figure 7.3: X4 experiment: Bulk viscometric measurements of 2000ppm HPAM, shown graphically.

As mentioned in chapter 5, if a polymer solution is insufficiently dispersed before injection, gel formation may ensue and plugging of HPAM in the injection well may result. The 2000ppm HPAM solution was therefore passed through a filter before injection to avoid injectivity impairment because of injection well plugging. The filter size was in the order of four to six times the average pore throat size in the Bentheimer radial disc. This filter size was selected to efficiently remove microgels from the solution while minimizing polymer shearing.

The viscosity deviation between injected and effluent viscosity at the reference shear rate of $10s^{-1}$ was 27%. This is a clear indication of mechanical degradation and will have a major impact on both HPAM rheology and injectivity as discussed in chapter 9.

Results from the X4 experiment are shown in sequential order (Figure 7.4 through Figure 7.***8***), where differential pressures are plotted against injection rates for all five consecutive floods.

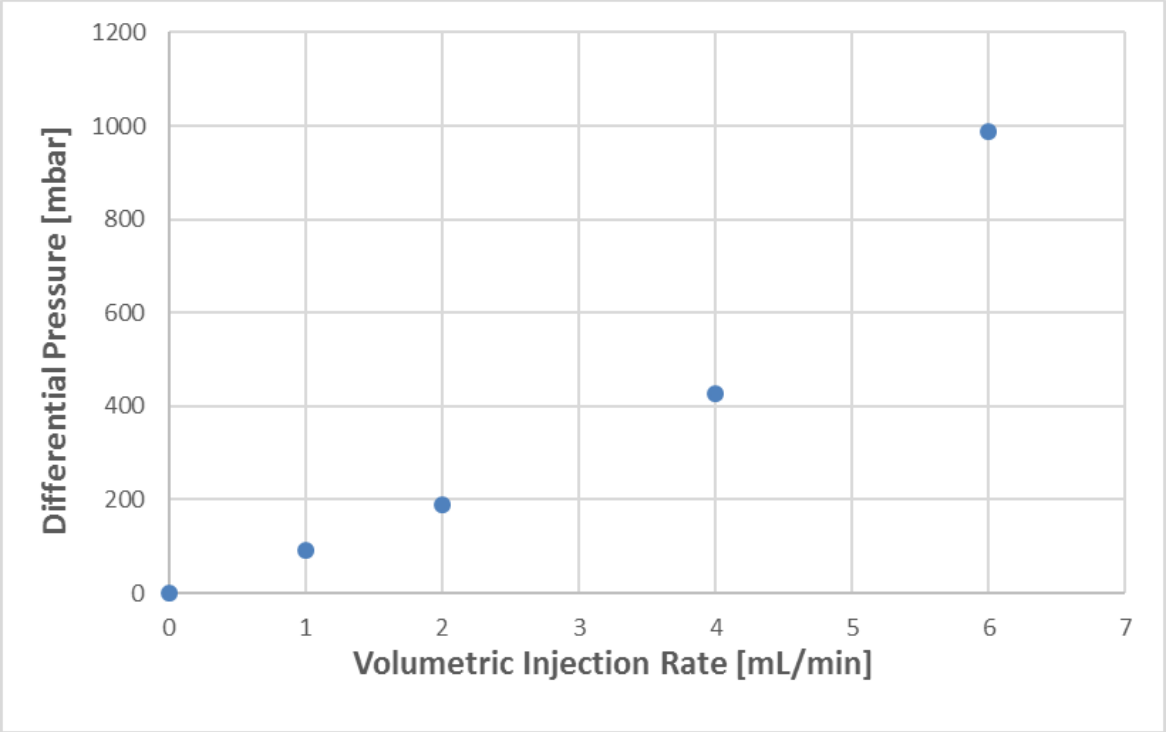

Figure 7.4: X4 experiment: Initial Water Flood (IWF): Differential pressure as a function of volumetric injection rate.

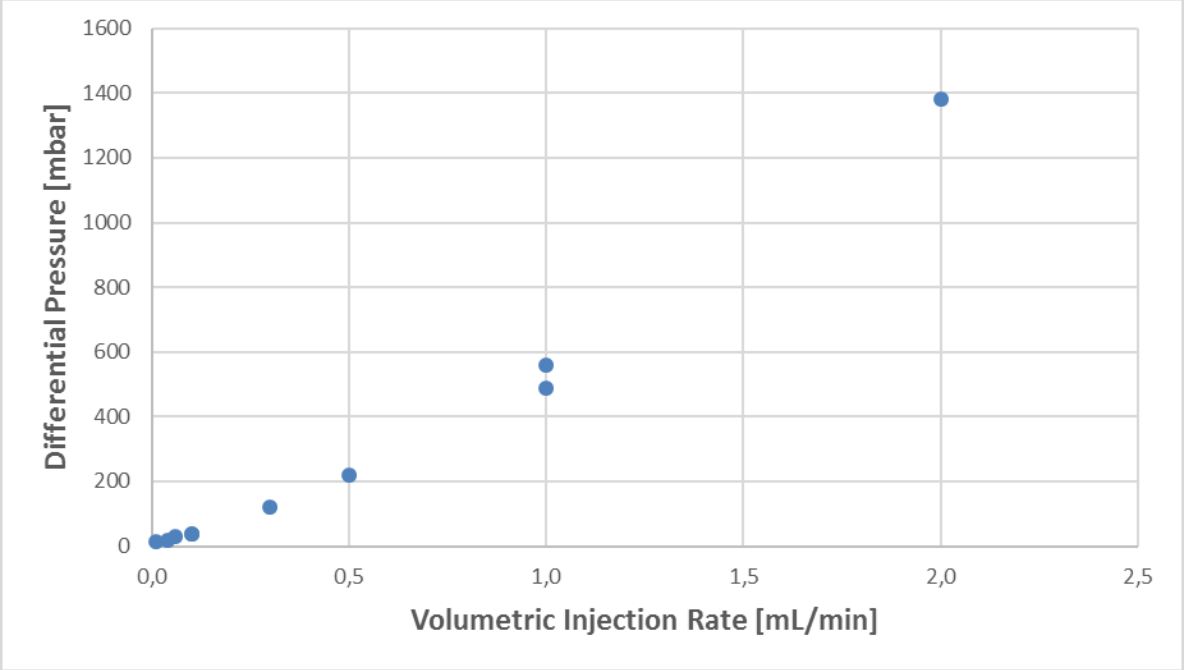

Figure 7.5: X4 experiment: 800ppm HPAM Flood (PF800): Differential pressure as a function of volumetric injection rate.

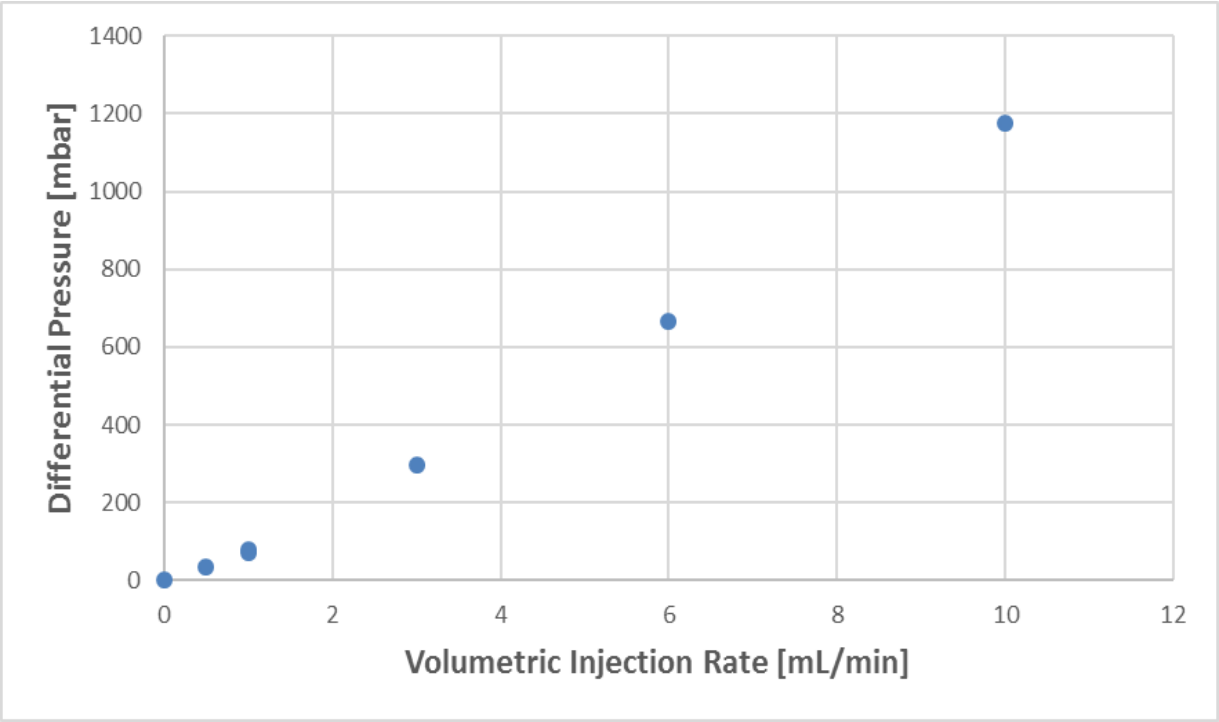

Figure 7.6: X4 Experiment: Secondary Water Flood (SWF): Differential pressure as a function of volumetric injection rate.

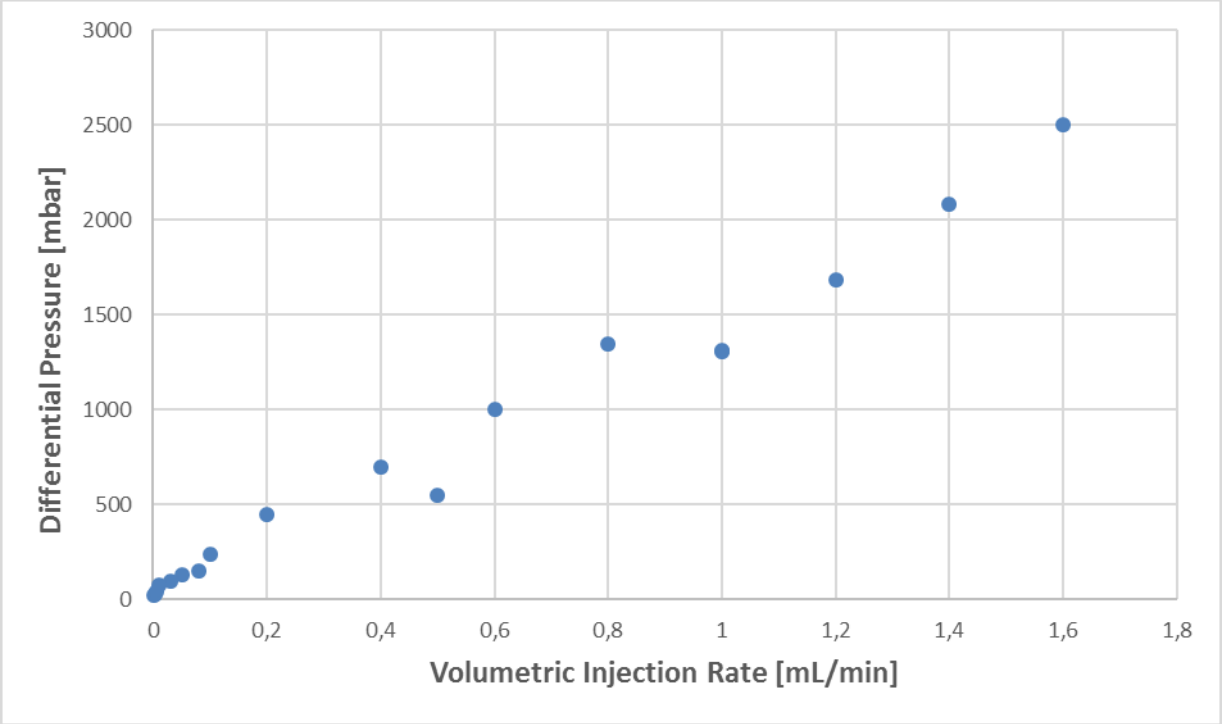

Figure 7.7: X4 Experiment: 2000ppm HPAM Flood (PF2000): Differential pressure as a function of volumetric injection rate.

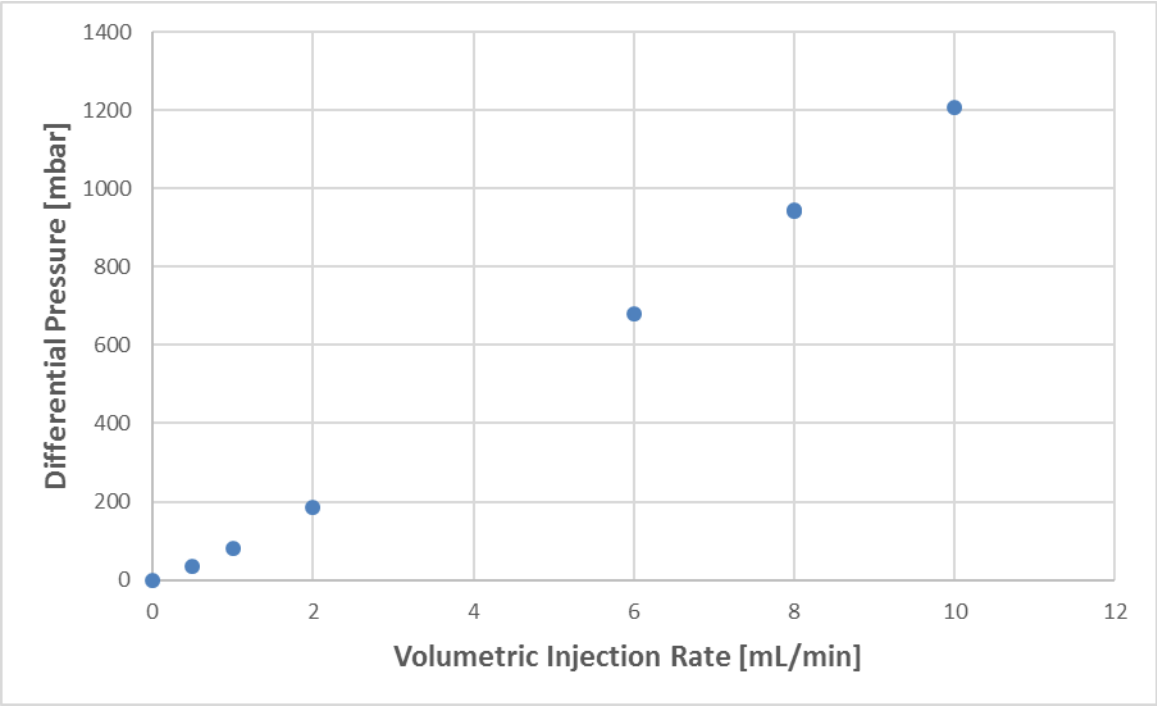

Figure 7.8: X4 Experiment: Tertiary Water Flood (TWF): Differential pressure as a function of volumetric injection rate.

The differential pressure as a function of volumetric injection rate for all five floods will be history matched in two different simulator tools (chapter 7.1) and results obtained from each of these tools will be compared in chapter 9.

7.1 Reservoir Simulators

Two conventional simulators used to history match the X4 experiment are presented in this section and consist of STARS by Computer Modelling Group (CMG) and MATLAB Reservoir Simulation Toolbox (MRST). The MRST tool was used in combination with an Ensemble Kalman Filter (EnKF) module extension. While STARS was used for manual simulations, MRST performed simulations automatically. The advantage of combining two different simulators to perform the same investigation is that they enforce the credibility of the history match result if the results are consistent.

7.1.1 STARS

STARS by CMG is an advanced process reservoir simulator developed to simulate a variation of chemical processes using a wide range of grid and porosity models on both field and laboratory scale [54]. The two-phase polymer flooding option available in this simulation tool was utilized for the history matches of both water and polymer floods.

As mentioned, STARS is a manual simulation tool and reported differential pressure values in experimental data corresponding to volumetric injection rates were simulated individually. To run simulations in STARS a data file describing all parameters involved in the simulation process had to be created. The STARS data file used for simulations of both water and polymer floods is located in the appendix part of this thesis together with a description of the most important parameters used. After each simulation run, results were available for inspection using the Results 3D feature.

The tuning parameter in the water floods was absolute permeability (relative permeability was chosen to be an arbitrarily assigned value in the initial water flood and kept constant during the remainder of the simulations in the X4 history match). In the polymer flood simulations, the tuning parameter was viscosity table.

A review of parameters used in STARS simulations that affects topics investigated in this thesis will be presented in the sensitivity analysis (chapter 8). The reader is referred to the STARS user guide to review basic reservoir modelling keyword not presented in the appendix section of this thesis [54].

7.1.2 MRST

Simulations in MRST was obtained automatically using the EnKF module to history match experimental values of differential pressure. MRST and EnKF was developed at SINTEF and University of Bergen, respectively.

EnKF uses a Monte Carlo approach to estimate parameters based on a specified amount of iterations and ensemble members within each iteration. The iteration approach performed by EnKF during simulations is beyond the scope of this thesis and the reader is therefore referred to Evensen (2003) [55] for a comprehensive description.

Four iterations and 100 ensemble members was utilized when running MRST simulations for both water and polymer floods in this thesis. The EnKF iteration module will commence the first iteration by choosing 100 random values within a specified best guess interval for each parameter. These parameter intervals will continuously improve for each iteration, based on results from precursory iterations. After four successive iterations, a probability distribution will display the different parameter intervals according to their history match results.

7.1.2.1 Water Floods

The tuning parameter in the water floods was effective permeability. MRST use Darcy's law for two-phase flow in radial geometry (equation (3.16)) to calculate differential pressure using permeability as ensemble members. The probability distribution obtained from the initial water flood is shown in Figure 7.9.

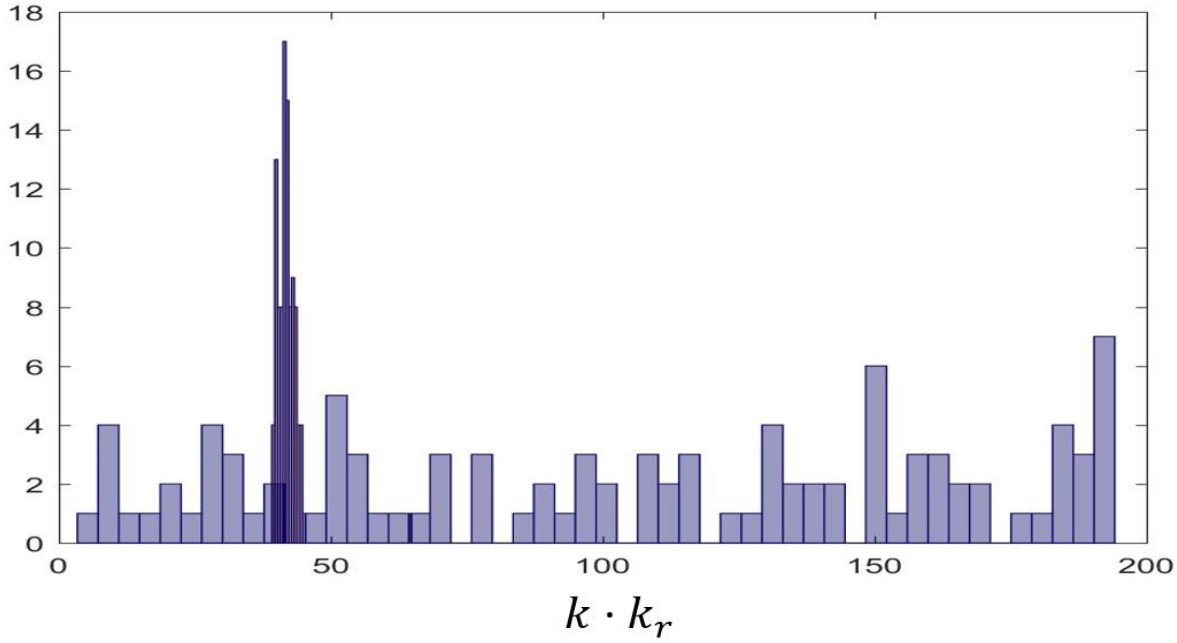

Figure 7.9: Effective permeability distribution from the initial water flood using MRST.

The light blue bars in Figure 7.9 correspond to randomly selected ensemble members from the initial best guess interval, while the purple bars show the narrowed interval after four successive iterations. The highest purple bar represents the parameter which provided the best history match during the simulation run. Using this effective permeability value, the history match obtained from the initial water flood in MRST is shown in Figure 7.10.

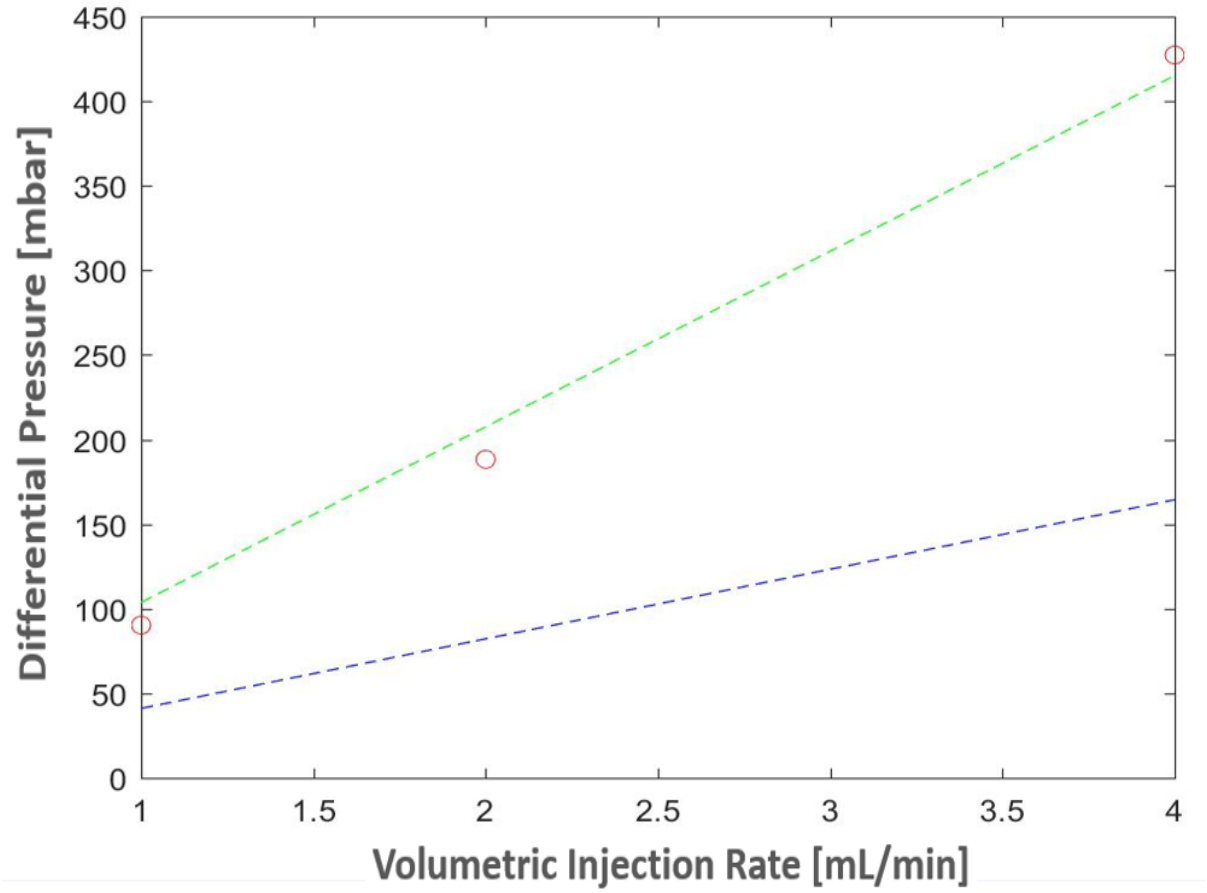

Figure 7.10: History match of the Initial Water Flood using MRST.

History match results shows differential pressure as a function of volumetric injection rate for both the match obtained from a random initial ensemble members (blue curve) and the match obtained from the final ensemble member (green curve).

7.1.2.2 Polymer Floods

The tuning parameter in the polymer floods is apparent viscosity as a function of Darcy velocity. MRST use a combination of Darcy's law for two-phase flow in radial geometry combined with the extended Carreau equation (equation (4.8)) where the ensemble members consist of the six different Carreau parameters.

The extended Carreau equation will be repeated here for emphasis:

$$\eta(\dot{\gamma}) = \eta_\infty + (\eta_0 - \eta_\infty)[1 + (\lambda_1\dot{\gamma})^2]^{\frac{n_1-1}{2}} + \eta_{max}[1 - e^{(-(\lambda_2\dot{\gamma})^{n_2-1})}] \quad (4.8)$$

Where:

$\dot{\gamma}$: Shear rate

$\eta(\dot{\gamma})$: Apparent polymer viscosity as a function of Shear rate

η_∞: Apparent polymer viscosity at infinite shear rate

η_0: Apparent viscosity at zero shear rate

λ_1 and λ_2: Time constants related to the polymer molecule relaxation time

n_1 and n_2: Power law index

The probability distribution of Carreau parameters obtained in the 800ppm HPAM Flood in shown in Figure 7.11.

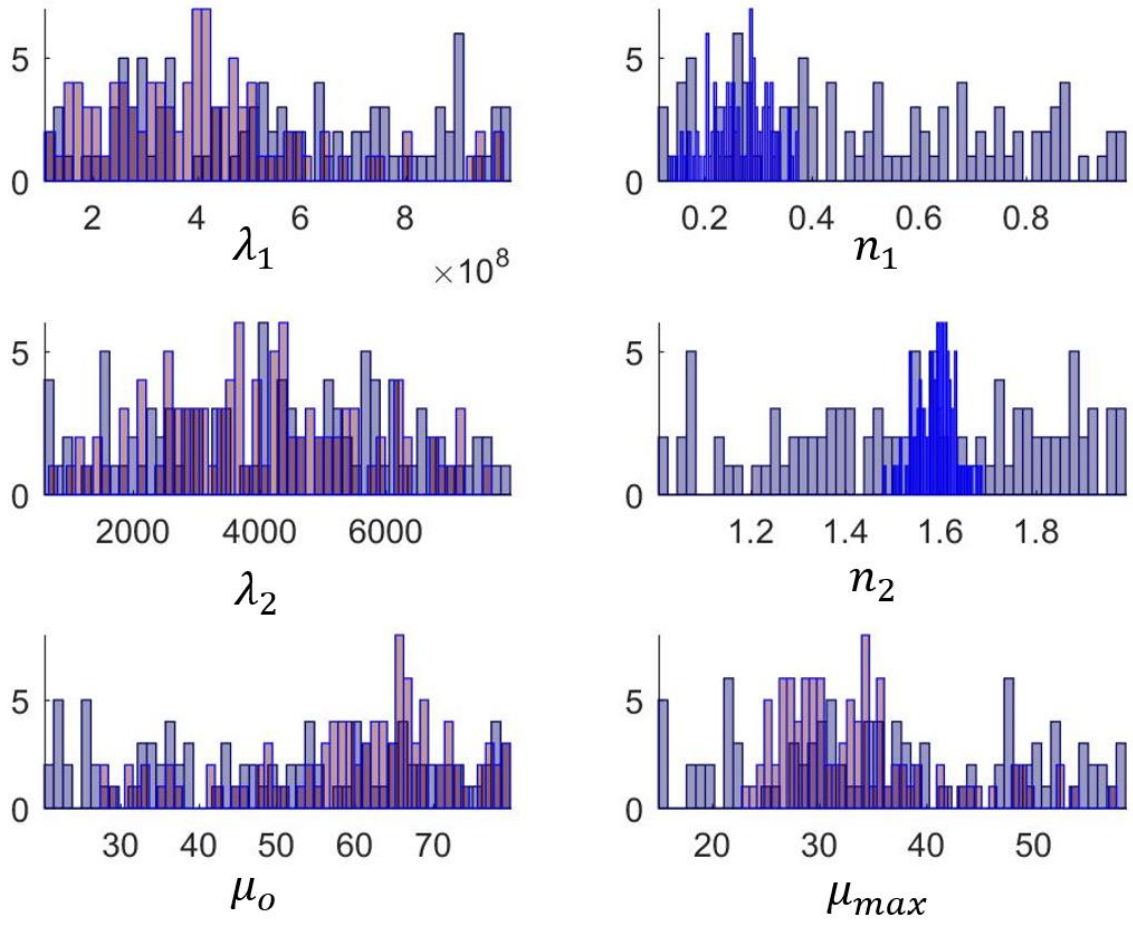

Figure 7.11: Probability distribution from 800ppm HPAM Flood using MRST.

The light blue bars in Figure 7.11 correspond to randomly selected ensemble members from the initial best guess intervals, while purple and dark blue bars shows the narrowed intervals after four successive iterations. Generally, the first power law index, n_1, is constrained within the range $0 < n_1 < 1$ while the second power law index, n_2, is recommended to reside within the range $1 < n_2 < 2$ to avoid numerical errors. The remaining Carreau parameters exhibits a high degree of freedom and their distributions intervals are highly dispersed compared to the power law indexes. Therefore, there will be a limitation to how narrow the intervals may be for these four parameters if satisfactory history matches are to be obtained.

Using the six values corresponding to the highest purple and dark blue bars in the distribution results, a final history match is obtained. The history match obtained for the 800ppm HPAM flood is shown in Figure 7.12.

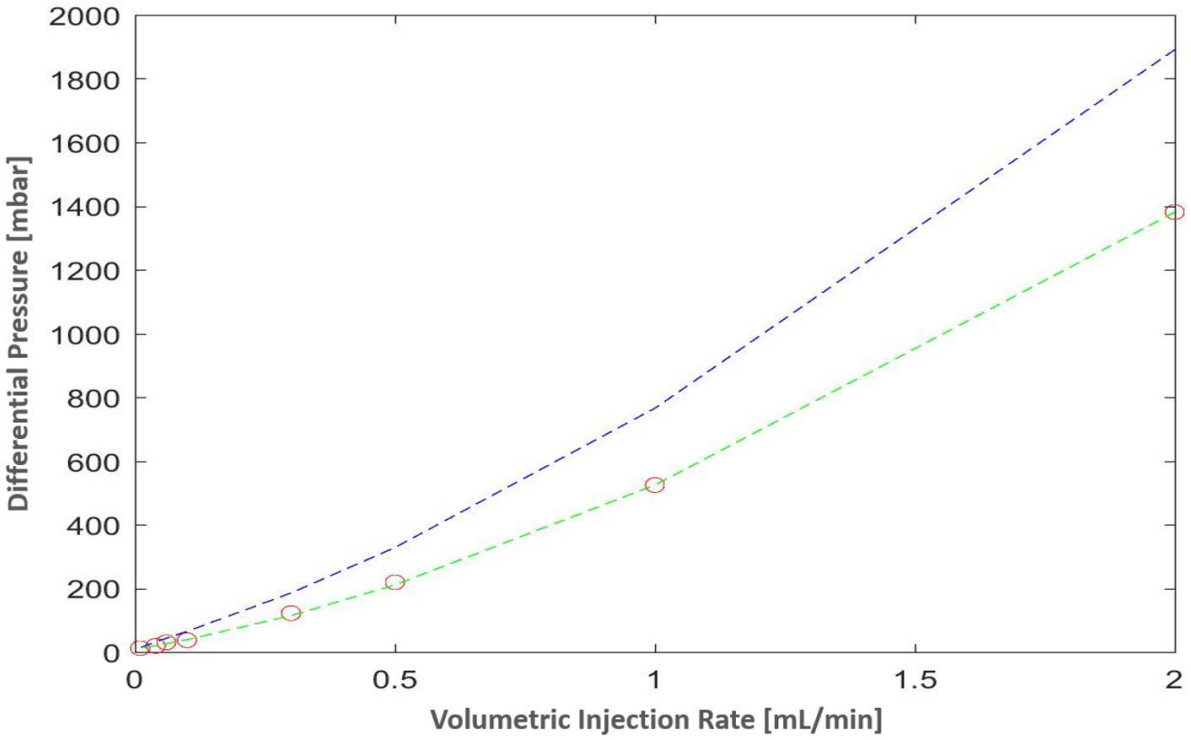

Figure 7.12: History match of 800ppm HPAM Flood using MRST.

As mentioned, the green curve corresponds to the history match obtained after four successive iterations, while the blue curve represents the best match obtained with the initial ensemble members.

8 SENSITIVITY ANALYSIS

To investigate effects of different parameters on history matches performed in STARS, a comprehensive sensitivity study was conducted. Sensitivity analysis is commonly used as a basis of determining compatibility of simulator tools to specific simulation processes. The 800ppm HPAM flood (PF800) part of the X4 experiment serves as the base file for the sensitivity analysis. The parameters investigated encompass:

- Grid Block Length
- Maximum Timestep
- Molecular Weight
- Polymer Concentration
- Polymer Adsorption
- Polymer Adsorption Reversibility
- Inaccessible Pore Volume (IPV)
- Residual Resistance Factor
- Endpoint Relative Permeability
- Polymer Viscosity

Differential pressures reported in the X4 experiment is based on measured stabilized pressures. It is therefore essential that deviations from base case stabilised pressures are within an acceptable error range when changing sensitivity analysis parameters. Since only stabilized differential pressures are of concern, variations in pressure build up will not affect history match results. Differential pressure will be plotted against time to investigate whether parameters assessed affects stabilized differential pressure and to what extent. Sensitivity parameters will be altered individually to investigate isolated effect on differential pressure.

8.1 Grid Block Length

STARS simulation tool calculates a distinct output value for each grid block defined in the simulation model. Flow direction is directed horizontally from the injection well towards the outer boundary, where grid blocks are concentric rings as depicted in Figure 8.1.

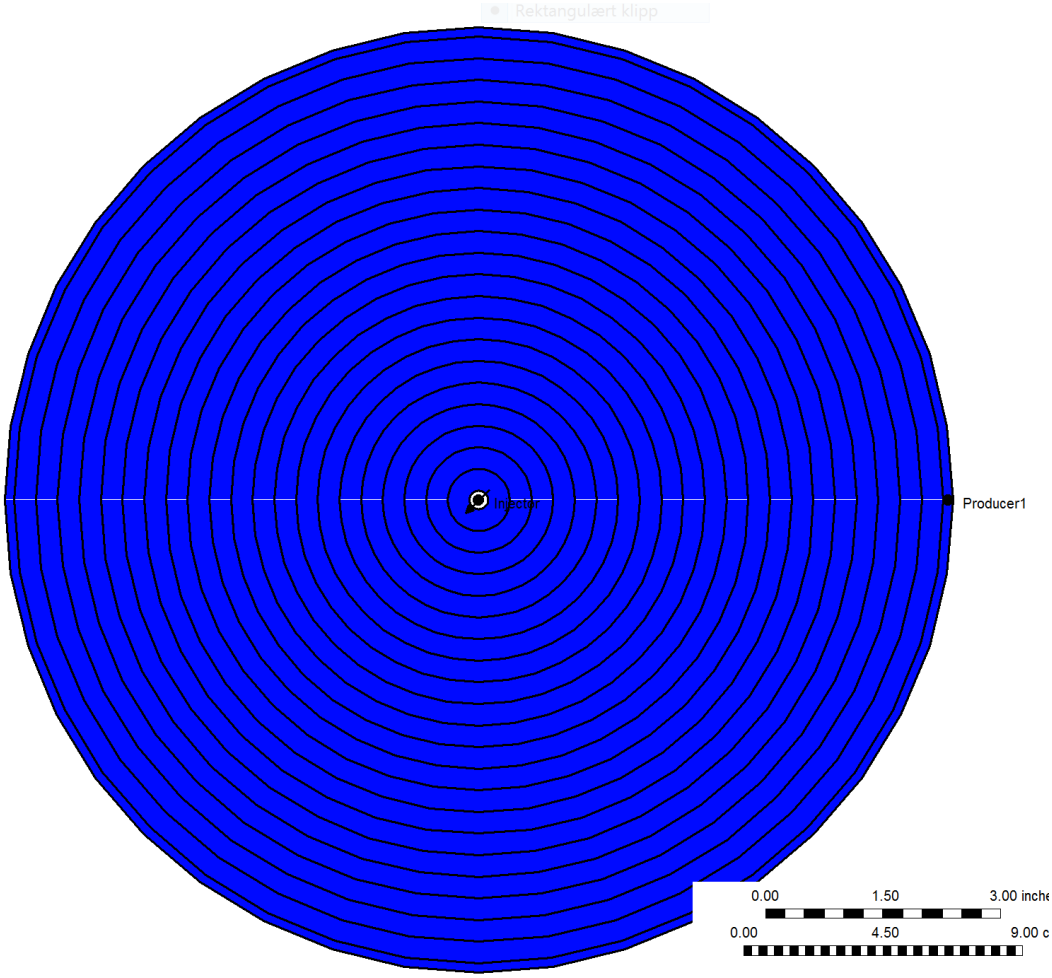

Figure 8.1: STARS grid model consisting of concentric grid blocks.

To obtain reliable output values from STARS, grid block lengths in the propagation direction must be small enough to avoid numerical dispersion. As mentioned in chapter 5, differential pressure decreases drastically with both distance and flux from the injection well in radial models. If too few grid blocks are defined in the simulation model, there will exist a large interval of different pressure drops within each grid block. Since STARS only calculate one value for each grid block, a multitude of differential pressures within each grid block interval is reduced to one individual value. Differential pressures obtained in STARS will therefore converge towards the analytical solution as the number of grid blocks are increasing, i.e. grid block length becomes smaller and the numerical error decreases. This is shown graphically in Figure 8.2 and Figure 8.***3*** for two different grid block lengths.

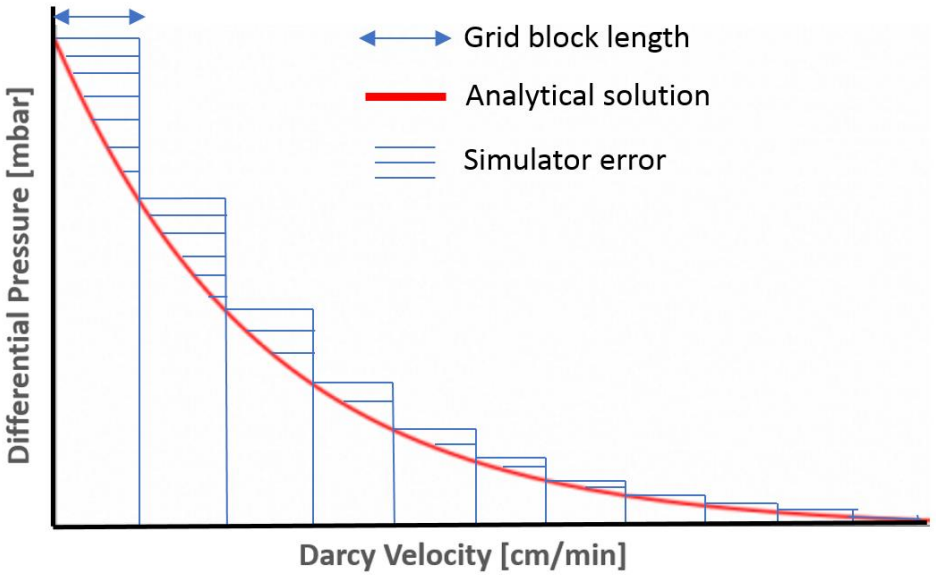

Figure 8.2: Deviation from analytical solution when choosing a small grid block length.

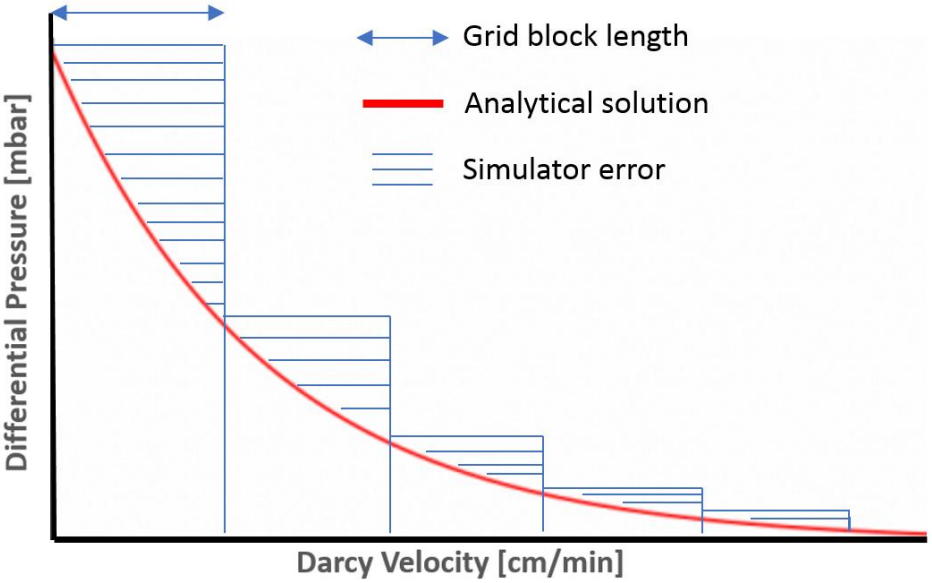

Figure 8.3: Deviation from analytical solution when choosing a large grid block length.

As seen from Figure 8.2 and Figure 8.***3***, the simulation error is increasing with increasing grid block length and will overestimate differential pressure. It is therefore important that the chosen grid block length is small enough to minimize the simulation error. An acceptable margin of error is normally within a few per cent.

Four different grid block lengths were investigated: 0,2 cm, 0,1 cm (base case), 0,05 cm and 0,01 cm. Effect of different grid block lengths will be assessed based on their influence on stabilized differential pressure. Due to a STARS limitation, the first grid block after the injection well had to be at least 20% of the injection well radius. Therefore, the first grid block was assigned a value of 0,1 cm for all grid block lengths investigated. Figure 8.4 shows a plot of differential pressure versus time for the four different grid block lengths.

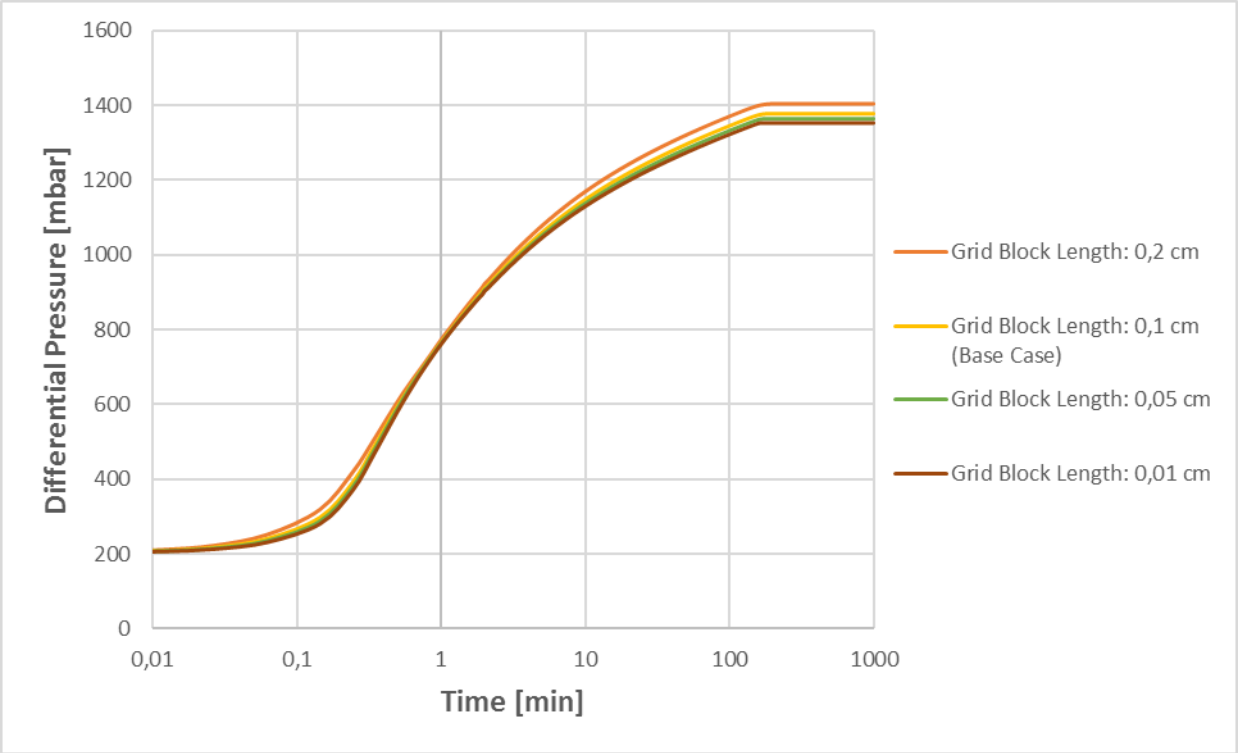

Figure 8.4: Effect of grid block length on differential pressure.

It is evident from Figure 8.4 that numerical deviation of stabilized differential pressure is decreasing as grid block length is decreasing, whereas the highest numerical effect is observed for the largest value of grid block length.

The differential pressure deviation of 2% between the lowest grid block length and base case is well within an acceptable margin of error.

8.2 Maximum Timestep

The number of successive iterations in STARS will be determined by the timestep sizes utilized in the simulation run. The first timestep used in the simulation run is specified by the DTWELL option in the data file. The maximum timestep (DTMAX) selected may be equal or higher than DTWELL. STARS will attempt to approach the specified maximum timestep by converging at successively higher timesteps. If convergence is successful at all intermediate timesteps including DTMAX, the remainder of simulation runs will commence at the timestep specified by DTMAX. However, if convergence is unsuccessful before reaching DTMAX, STARS will finish the simulation using the highest of intermediate timesteps where convergence was successful. Three different DTMAX values were investigated: 0,2 min, 0,1 min and 0,01 min. Their effect on differential pressure is shown in Figure 8.5.

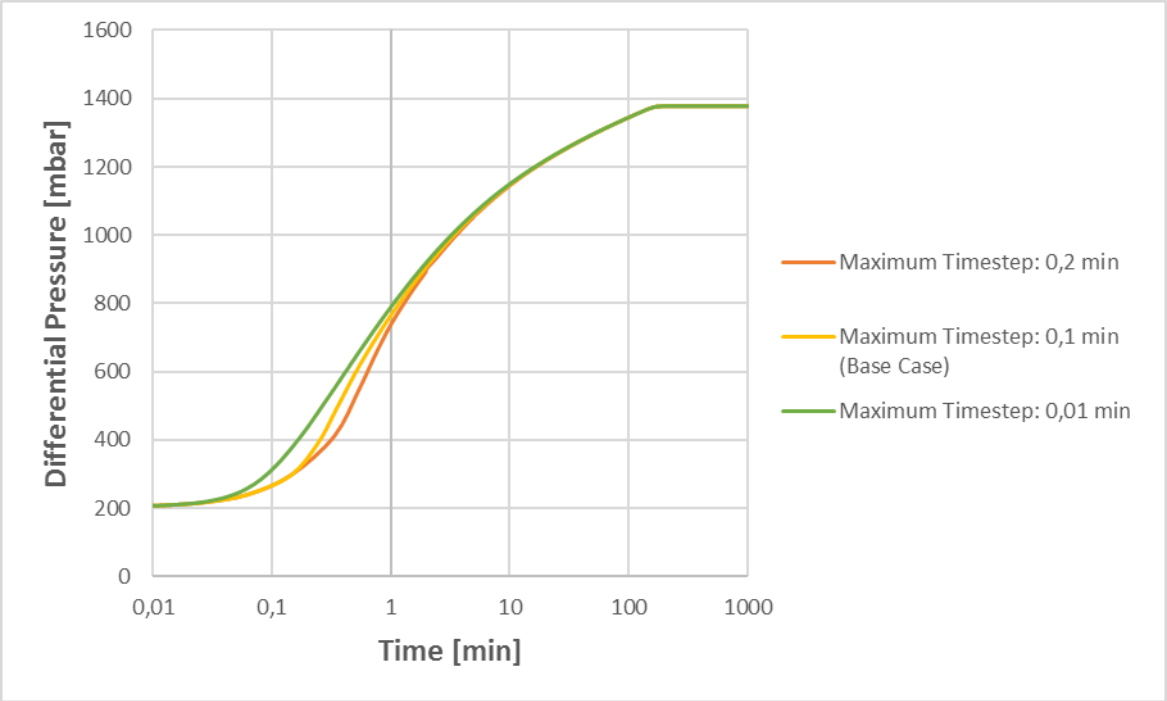

Figure 8.5: Effect of maximum timestep on differential pressure.

During the first minute of the simulation, an observable deviation in pressure build up between the three maximum timestep values was detected. However, after the first minute, differential pressure curves aligned and remained identical throughout the simulation run. As mentioned, STARS will not implement the specified maximum timestep if convergence is unsuccessful at intermediate timesteps. Therefore, DTMAX will have zero influence on stabilized differential pressures. This inherent property of the STARS simulation tool prevents erroneous results caused by too high DTMAX values.

8.3 Molecular Weight

The HPAM polymer investigated in this thesis has a high molecular weight of $20 \cdot 10^6$ Dalton (g/mol). If this molecular weight would have been used during STARS simulations, there would have been problems with too low mole fractions (mole fraction of polymer should not be below 10^{-7}) and consequently too low adsorption values. The solution to this problem, according to a CMG software engineer, was to scale the molecular weight of HPAM down to 8000 g/mol. This could be done because the main influence of molecular weight is on polymer viscosity, which is the tuning parameter during history matches of polymer floods and is therefore predetermined. Even though both mole fraction and adsorption depends on molecular weight, these will not be changed because it is the isolated effect of molecular weight that is of concern. Isolated effects of both mole fraction and adsorption on differential pressure will be investigated during subsequent sections of this chapter.

To investigate the influence of molecular weight on stabilized differential pressure, it is crucial to assess whether the real molecular weight of the HPAM polymer used does not result in a discrepancy. If there exist a discrepancy between stabilized differential pressures at different molecular weights, the downscaling approach cannot be utilized. Three different molecular weights were investigated: 8000 g/mol (base case), 10^6 g/mol and $20 \cdot 10^6$ g/mol (actual molecular weight of HPAM used in the X4 experiment) as shown in Figure 8.6.

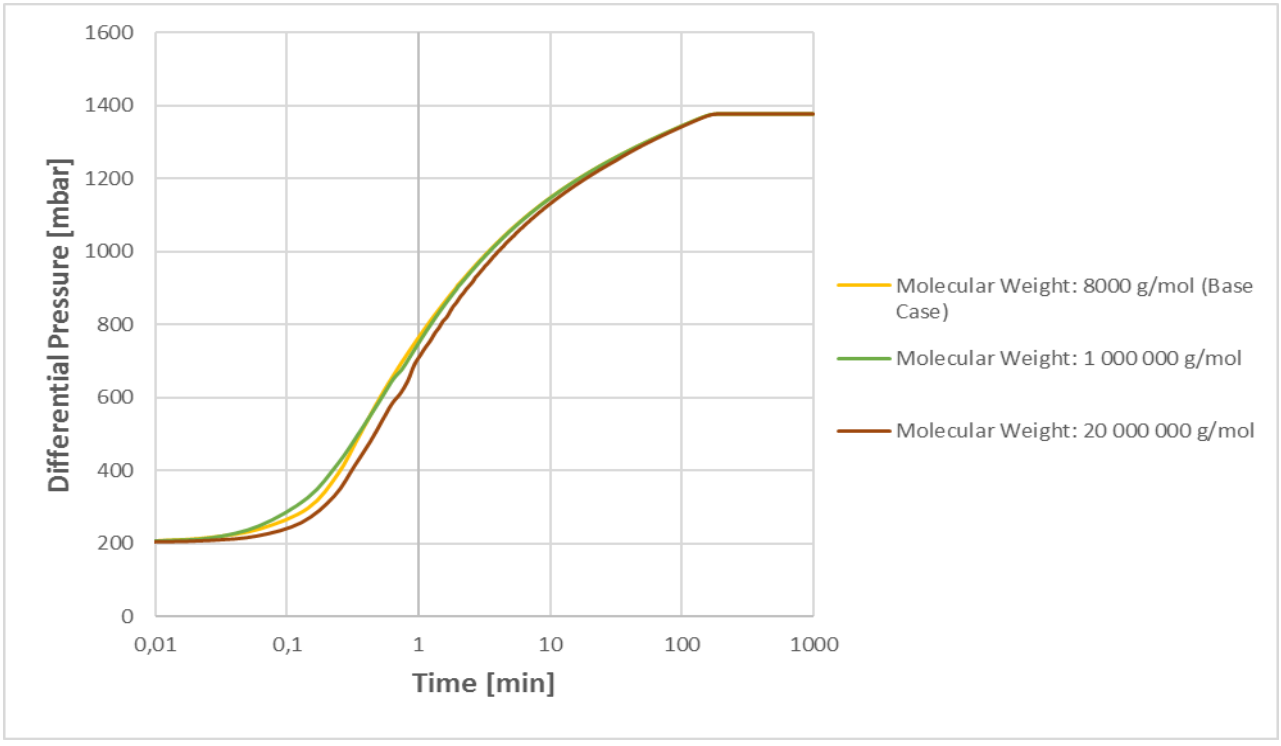

Figure 8.6: Effect of molecular weight on differential pressure.

An observable deviation in differential pressure occurs within the 10 first minutes of the simulation. From 10 minutes and onwards the differential pressure curves are identical and attains the same differential pressure. Deviations in differential pressure during the first 10 minutes can be attributed to a material balance error in STARS. Material balance is a concept of mass conservation and since molecular weight was changed, but mole fraction and adsorption did not change accordingly, material balance will not be in equilibrium. Because both mole fractions and adsorption values specified in base case are based on a molecular weight of 8000 g/mol, the material balance error increase with increasing deviation from base case molecular weight.

Since altering molecular weight did not affect stabilized pressure, the downscaling approach is safe to implement.

8.4 Polymer Concentration

Polymer rheology is strongly dependent upon concentration, where an increase in polymer concentration will increase the viscofying ability of the polymer. Since the viscosity table in the sensitivity analysis of polymer concentration is constant, the only parameter in the simulation that might be affected is rate of adsorption.

Effect of polymer concentration is accounted for by changing mole fraction of polymer in the STARS data file. Four polymer concentrations and corresponding mole fractions were chosen: 100ppm, 800ppm (base case), 2000ppm and 5000ppm, corresponding to mole fractions of $(2{,}25 \cdot 10^{-7})$, $(1{,}8 \cdot 10^{-6})$, $(4{,}5 \cdot 10^{-6})$ and $(1{,}125 \cdot 10^{-5})$,respectively. While the two intermediate polymer concentrations of 800 and 2000ppm are in the semi-dilute regime, 100ppm and 5000ppm are in the dilute and concentrated regime, respectively [7]. Figure 8.7 shows pressure responses for the different polymer concentrations investigated.

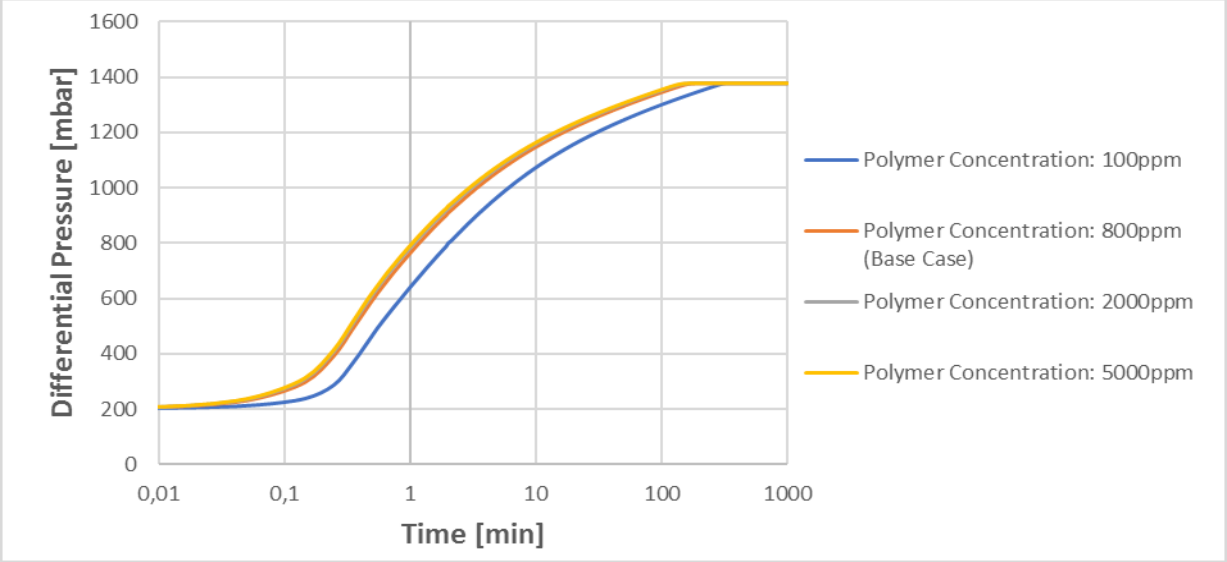

Figure 8.7: Effect of polymer concentration on differential pressure.

Pressure build up for 100ppm HPAM deviates significantly from the three other HPAM concentrations. As mentioned in chapter 4.5.1, flow velocity of polymer solutions may be reduced due to adsorption. Since adsorption is specified on a per mole basis, it will affect low concentration solutions more than solutions of higher concentration. The 100ppm HPAM solution proves this statement and is deaccelerated when propagating through porous media and consequently, stabilized differential pressure is attained later than the three other polymer solutions of higher concentration. However, stabilized differential pressure is identical for all four HPAM concentrations. Therefore, polymer concentration will not affect simulations performed in this thesis.

8.5 Polymer Adsorption

In addition to reducing flow velocities of polymer solutions through porous media, adsorption may also induce a permeability reduction. However, permeability is predetermined when running simulations in STARS and adsorption induced permeability reductions should not be able to affect stabilized differential pressure.

Polymer adsorption is defined in STARS using the keywords ADSTABLE and ADMAXT. ADSTABLE is defined as concentration dependent polymer adsorption. The specified adsorption curve was linear and ABSTABLE therefore consisted of only two points: zero adsorption at zero polymer concentration and a maximum adsorption at a specified polymer concentration. The keyword ADMAXT specifies maximum adsorption of polymer onto porous media. Therefore, ADMAXT will be the variation parameter when investigating polymer adsorption. Slope of polymer adsorption as a function of concentration will remain constant.

The maximum polymer adsorption value (ADMAXT) used in STARS simulations was calculated using equation (4.12), where polymer retention was defined as:

$$\Gamma_m = \Gamma \cdot 2{,}7194 \cdot \rho_r \qquad (8.1)$$

Where Γ is retention level (in mass of polymer per unit mass of solid) and ρ_r is bulk formation density including rock grains and pore space.

Although equation (4.12) defines total retention and not just polymer adsorption, literature suggest that retention is dominated by polymer adsorption [30, 37, 49] which justifies use of equation (4.12) to calculate an approximate value of adsorption.

To investigate influence of adsorption on differential pressure, three values of adsorption relative to the base case ($1{,}65 \cdot 10^{-8}\ \frac{mole}{cm^3}$), were chosen: 10% of base case, base case, and 1000% of base case. Influence of adsorption on differential pressure is shown in Figure 8.8.

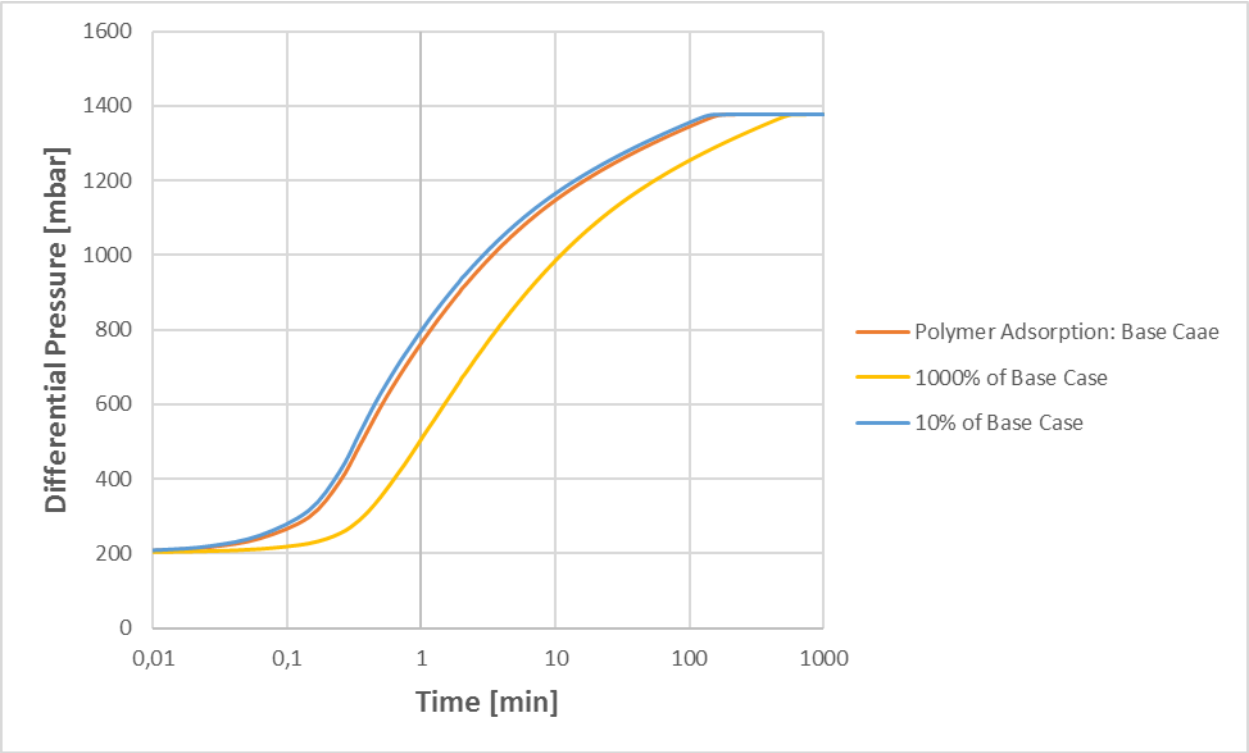

Figure 8.8: Effect of polymer adsorption on differential pressure.

Since an adsorbed polymer layer will reduce flux of polymer in flow through porous media, differential pressure will stabilize slower when polymer adsorption increase. This is observable in Figure 8.8 where stabilization of differential pressure is delayed when polymer adsorption is increased one order of magnitude compared to base case. The opposite is observed when polymer absorption is reduced to 10% of its original value. However, the difference is not nearly as large when adsorption is decreased. This indicates that the level of adsorption in base case was already at such a low level that a further adsorption reduction had a negligible effect.

Even though adsorption affected numerical dispersion, it did not affect stabilized differential pressures. Since polymer adsorption does not influence the predetermined permeability, it will not influence stabilized differential pressure and the value of adsorption will therefore not affect history matches performed in STARS.

8.6 Polymer Adsorption Reversibility

In addition to specifying amount of adsorption, it is also possible in STARS to define polymer adsorption reversibility through the keyword ADRT. While an ADRT value of zero defines polymer adsorption as completely reversible, completely irreversible adsorption is defined by an ADRT value equal to ADMAXT. To assess the sensitivity of polymer adsorption reversibility, three different reversibility values were chosen: Completely reversible adsorption (ADRT=0), partially reversible adsorption (ADRT=ADMAXT/2) and completely irreversible adsorption (ADRT=ADMAXT). Their influence on differential pressure is shown in Figure 8.9.

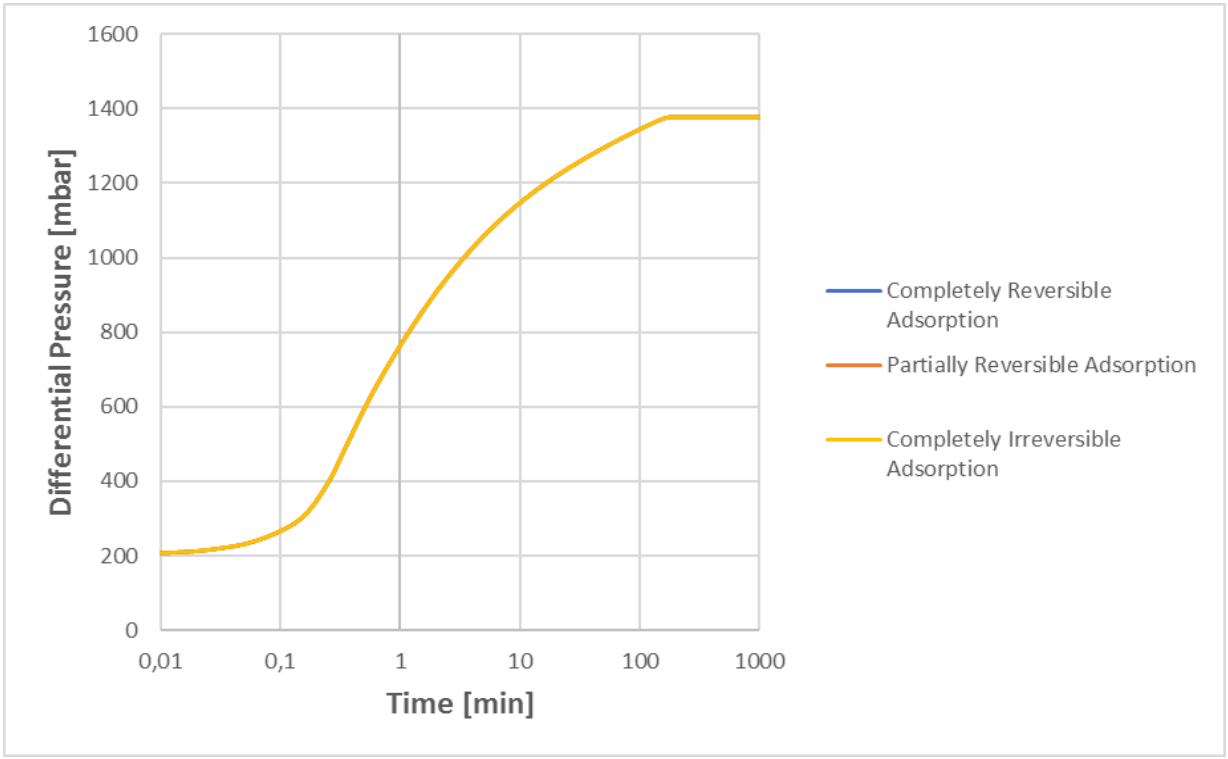

Figure 8.9: Effect of polymer adsorption reversibility on differential pressure.

Since simulations conducted in the sensitivity analysis of polymer adsorption only consist of a single polymer flood, the effect of polymer adsorption reversibility is zero. The concept of polymer adsorption reversibility applies to whether a subsequent water flood reduce the adsorbed polymer layer or not. Since polymer floods in this simulation is not followed by a water flood, adsorbed amount of polymer will be constant, as is evident from identical pressure responses seen in Figure 8.9.

8.7 Inaccessible Pore Volume (IPV)

As mentioned in chapter 4.3.1, the range of IPV extends from zero to one, whereas IPV equal to zero indicates total accessible pore volume, and a value of unity corresponds to completely inaccessible pore volume. IPV can be specified in STARS by using the keyword PORFT, which determines the fraction of accessible pore volume in the simulation model. PORFT equal to one is the equivalent of IPV equal to zero and a value of for example 0,8 indicates that a fraction of 0,2 of the pore volume is inaccessible.

To investigate the influence of IPV on stabilized differential pressure, three different IPV values were chosen: 0% (base case), 10% and 30%, as shown in Figure 8.10.

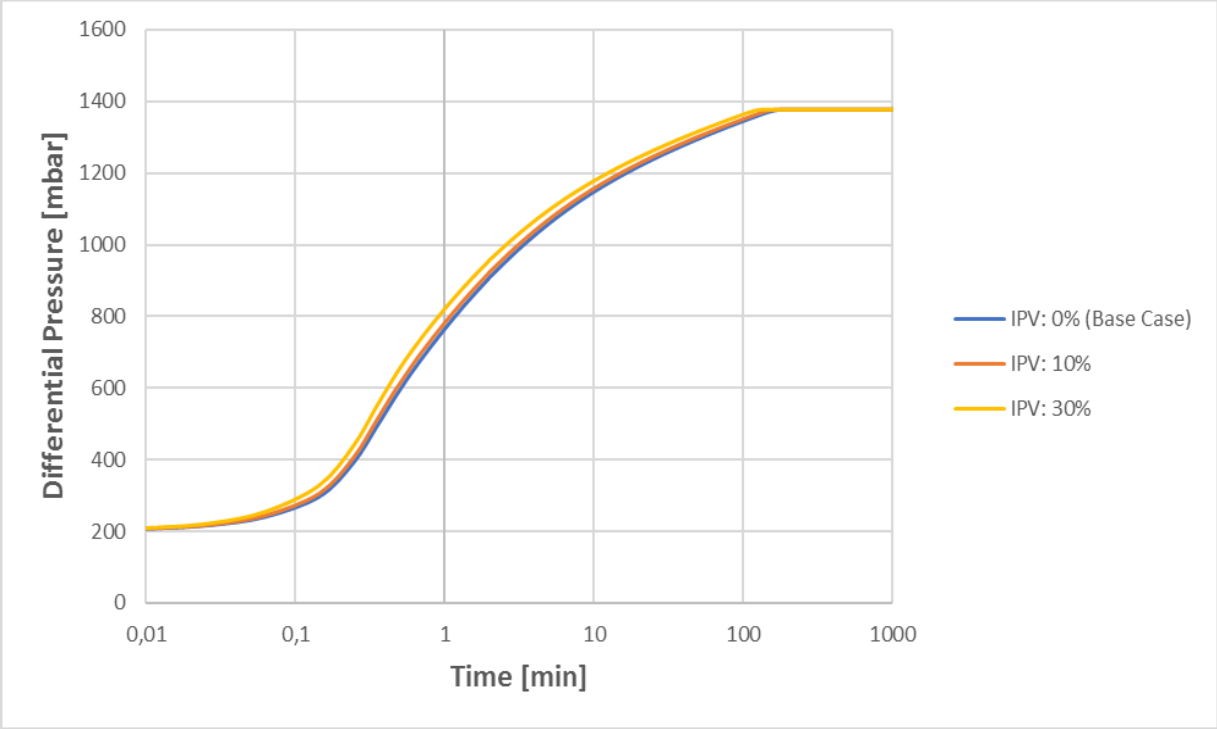

Figure 8.10: Effect of IPV on differential pressure.

The variation in differential pressure build up for different IPV values are small, but observable. As mentioned in chapter 4.3.1, the phenomenon of inaccessible pore volume (IPV) accelerates flow of polymer through porous media. This effect is illustrated in Figure 8.10 where an increasing amount of IPV accelerates the polymer solution through porous media and thus will attain a stabilized differential pressure at an earlier time compared to lower values of IPV. However, since the value of stabilized differential pressure is identical for all values of IPV, the latter will not affect simulation results.

8.8 Residual Resistance Factor

As mentioned in chapter 4.6, residual resistance factor (R_{RF}) indicates the permanence of a permeability reduction caused by polymer retention. This permeability reduction is accounted for in STARS by changing the keyword RRFT. However, in MRST this option is not available and therefore, to compare history match results from STARS and MRST, absolute permeability of porous media was changed instead. In the secondary water flood for example, a new absolute permeability value was obtained rather than estimating a value of R_{RF}. The relationship between absolute permeability before (K_w) and after (K_{wa}) polymer flooding can be defined according to residual resistance factor:

$$k_w = k_{wa} R_{RF} \tag{8.2}$$

Sensitivity analysis of R_{RF} consist of investigating if different combinations of R_{RF} and absolute permeability values results in identical differential pressures. If differential pressures are consistent, permeability can safely be altered instead of R_{RF}. Three values of R_{RF} were chosen, 1,0 (base case), 1,2 and 1,5, corresponding to absolute permeability values of 870md, 1044md and 1305md. Figure 8.11 shows a plot of differential pressure versus changes made in R_{RF} and absolute permeability for the three cases.

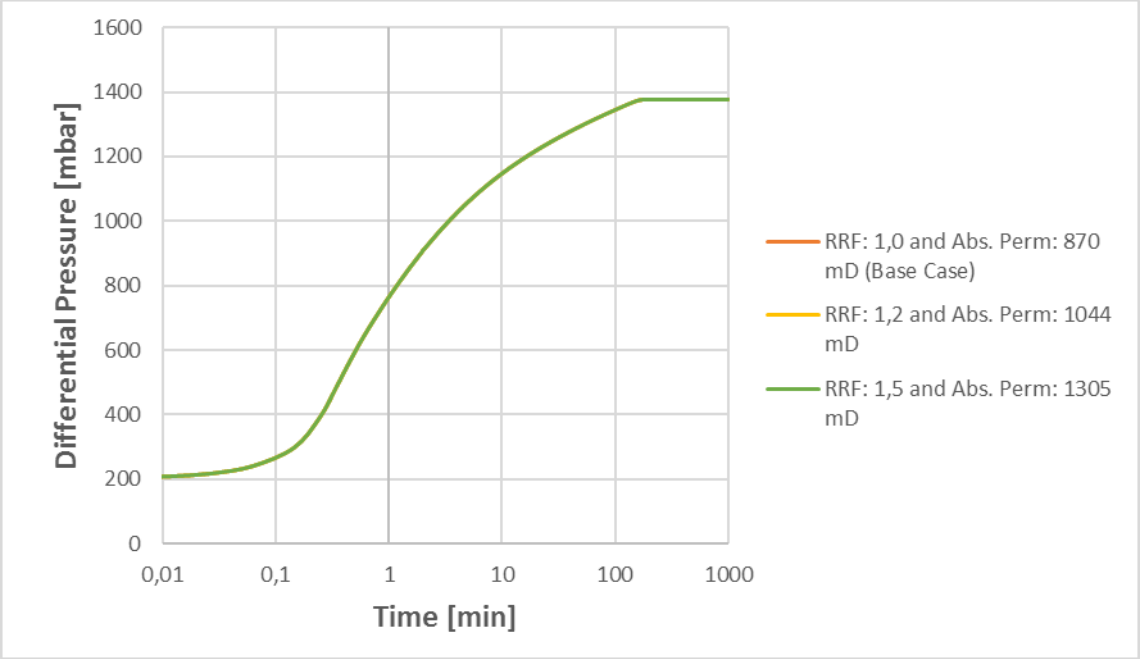

Figure 8.11: Combined effect of RRF and absolute permeability on differential pressure.

As shown in Figure 8.11, the differential pressure obtained is indifferent between changing R_{RF} or absolute permeability of the porous media. Therefore, absolute permeability can safely be altered instead of R_{RF}.

8.9 Endpoint Relative Permeability

In the X4 experiment, no oil production was detected and residual oil saturation was assumed to be immobile throughout simulations performed in STARS. Therefore, saturation of both oil and water/polymer will remain constant throughout simulations.

Endpoint relative permeability of water was arbitrarily assigned a value of 0,05. Based on this value, absolute permeability of the porous media was determined. Since STARS required a minimum of two relative permeability values, both endpoint permeability of oil and water was specified. The only value of relative permeability that will affect simulations is endpoint permeability of water at constant saturation throughout the X4 experiment. Since oil was immobile, endpoint relative permeability of oil was chosen as zero.

Endpoint relative permeability values of water investigated were: 0,1, 0,05 (base case) and 0,01. Effect of endpoint relative permeability on differential pressure is shown in Figure 8.12.

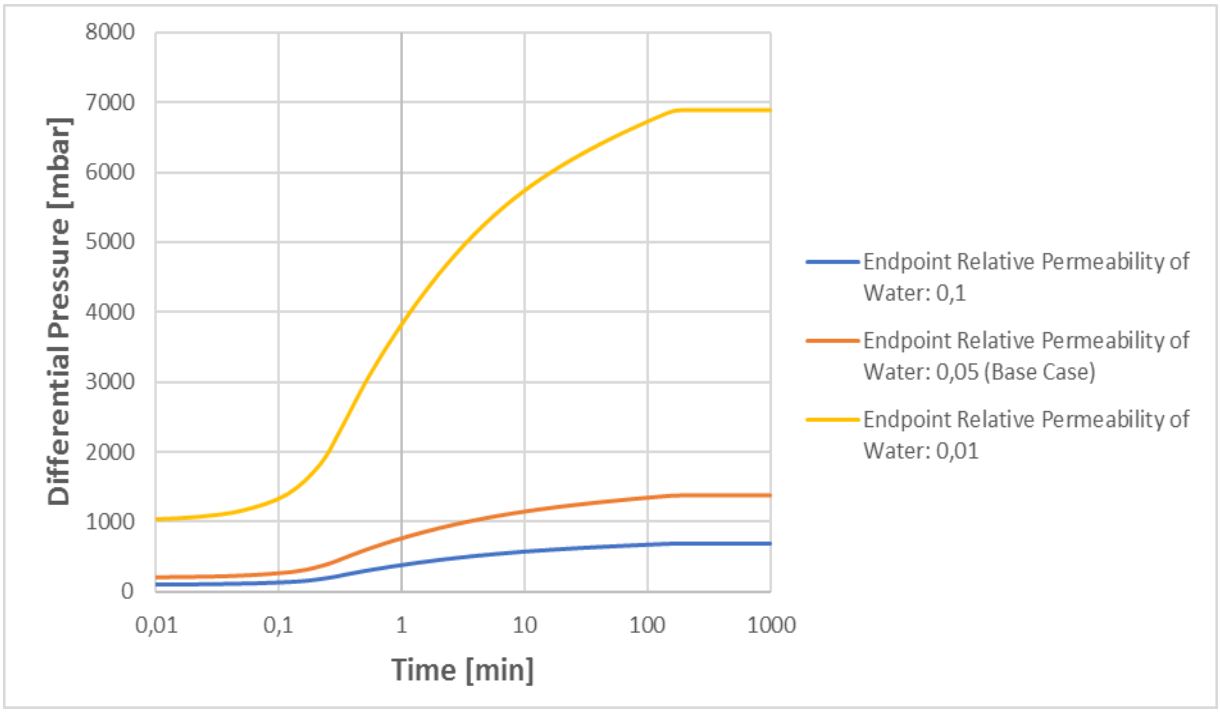

Figure 8.12: Effect of endpoint relative permeability on differential pressure.

Not surprisingly, since effective permeability of water is defined as the product of relative and absolute permeability (equation (3.15)), stabilized differential pressure will be influenced significantly as a result of different endpoint relative permeability values as depicted in Figure 8.12. Endpoint relative permeability of water will be held constant in all simulations and will be equal to 0,05.

8.10 Polymer Viscosity

Viscosity is the main physical property of interest while studying polymer in this thesis and should be the governing factor affecting differential pressure. Viscosity as a function of Darcy velocity was the tuning parameter during history matches of polymer floods. The main objective in this thesis is to assess the rheology of two polymer solutions in order to compare this behaviour in absence and presence of residual oil, and its consequent effect on injectivity.

Polymer viscosity is defined by the keyword SHEARTAB in STARS, which is a table consisting of Darcy velocities and corresponding viscosity values. To investigate the influence of viscosity on stabilized differential pressure, three different viscosity tables, relative to base case, were chosen: 50% of base case, base case and 150% of base case, as shown in Figure 8.13.

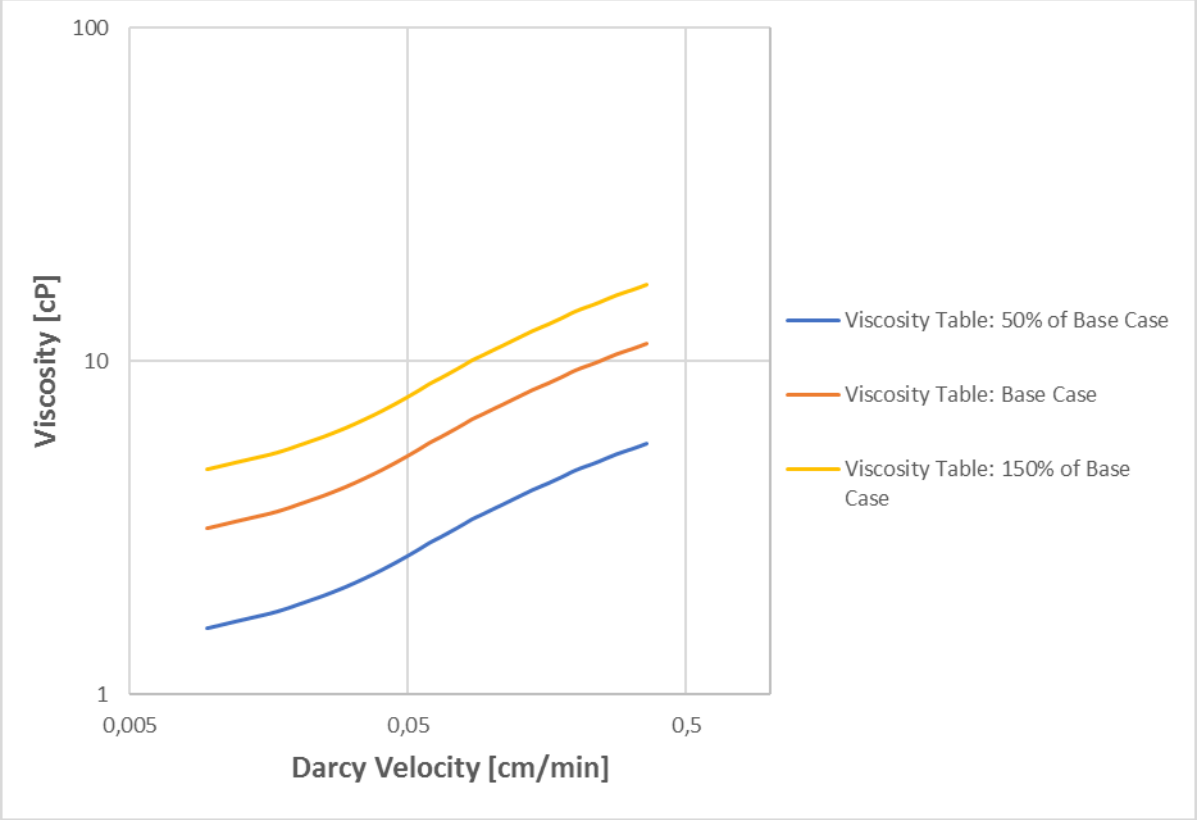

Figure 8.13: Viscosity tables chosen for sensitivity analysis.

Viscosity tables shown in Figure 8.13 resulted in the three differential pressure profiles shown in Figure 8.14.

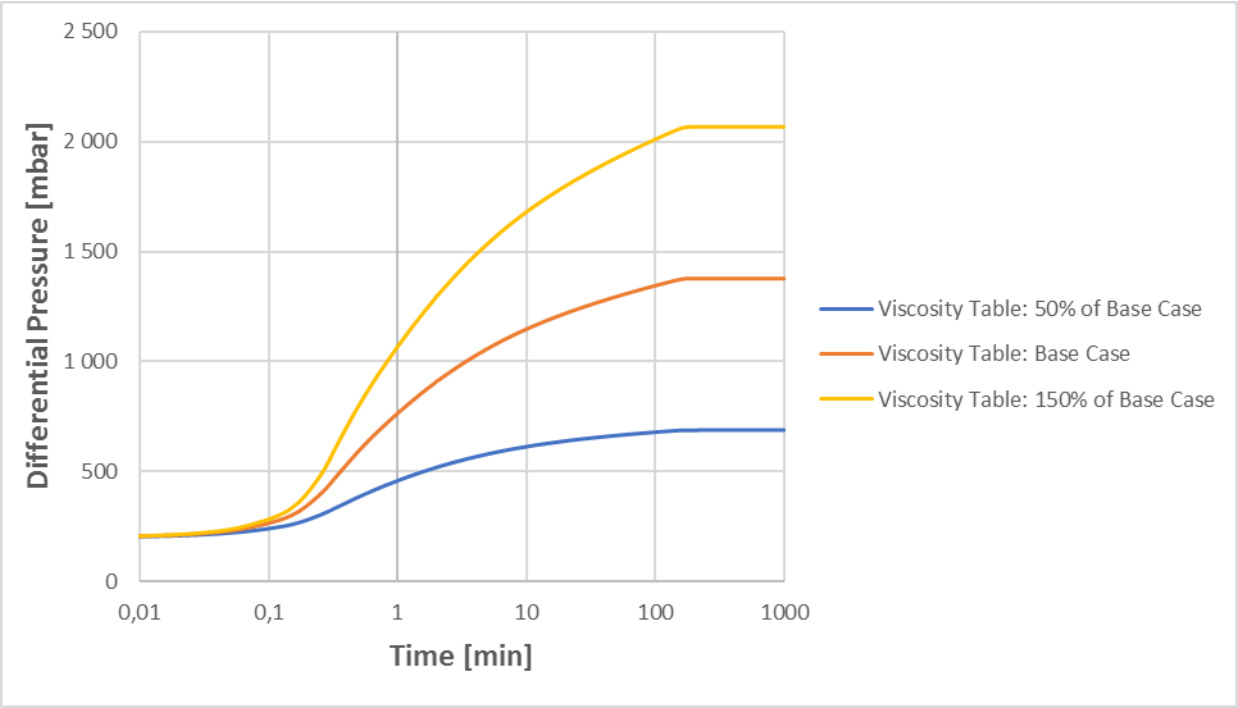

Figure 8.14: Effect of viscosity table on differential pressure.

Observable from Figure 8.14, differential pressure is proportional to absolute values of viscosity tables and consequently, STARS is extremely sensitive to changes in viscosity. If this had not been the case, use of viscosity curves as the tuning parameter to history match differential pressures would have been pointless.

8.11 Summary of Sensitivity Analysis

In this sensitivity analysis, various parameters utilized in history matches in the X4 experiment was investigated, and their influence on stabilized differential pressure was assessed.

It was found that the STARS simulator tool was sensitive of the grid block lengths defined, where the degree of sensitivity seemed to increase with increasing grid block lengths. The grid block length used for history matches in the X4 experiment deviated by 2% from the lowest grid block length investigated This deviation is considered to be within an accepted error margin.

Maximum timestep had no effect on stabilized differential pressure. In addition, it was revealed that STARS has an inherent property that prohibits the use of a specified maximum timestep if convergence is unsuccessful at intermediate timesteps.

It was assumed that molecular weight did not have an isolated effect in STARS, and was downscaled to satisfy mole fractions and adsorption criteria. Fortunately, sensitivity analysis confirmed this assumption and the downscaling approach could be safely implemented.

Neither polymer adsorption, adsorption reversibility, IPV nor polymer concentration affected stabilized differential pressures and therefore, STARS will not be affected by these parameters during history matches.

Residual resistance factor was not changed during successive simulations. Instead, absolute permeability was changed accordingly to compare results in a simpler manner with MRST. The sensitivity analysis confirmed the assumption that absolute permeability could be changed instead of R_{RF}.

Endpoint relative permeability of water was also assessed in terms of a sensitivity parameter and had a significant impact on stabilized differential pressure. However, this parameter will remain constant throughout simulations performed in STARS.

Sensitivity analysis of relevant STARS parameters revealed that only viscosity and permeability affected stabilized differential pressure. Since permeability was obtained from precursory water floods and predetermined in history matching of polymer floods, the only parameter affecting simulations was viscosity and thus reliable determination of rheology could be attained.

9 RESULTS AND DISCUSSION

In this thesis, the X4 experiment was history matched using both STARS and MRST. Discussions will commence by comparing history match results obtained by both simulator tools in chapter 9.1.1 through 9.1.5, followed by a summary of history match results in chapter 9.1.6.

History match deviations will be assessed in percentage terms which will represent deviations in a clearer manner. Results from all water floods will be discussed in the same sections as STARS versus MRST comparisons, whereas discussion of polymer rheology obtained from history matching polymer floods in the X4 experiment will be assigned their own subsequent sections.

Theoretically, permanent permeability reductions caused by polymer retention is related to residual resistance factor. As mentioned in chapter 8.8, since MRST did not have an option for R_{RF}, absolute permeability was changed instead. Therefore, absolute permeability reductions during successive water flood will be emphasized although, it is actually R_{RF} that increases.

Since both endpoint relative permeability and absolute permeability will influence mobility of water/polymer, there exist an infinite amount of combinations giving the same history match. Therefore, it was a necessity to keep one of these values fixed. An educated guess was made in the initial water flood and endpoint relative permeability of water/polymer was assumed to be 0,05. This value of relative permeability will be kept constant throughout all successive floods.

To investigate rheology and injectivity behavior, history match results from either STARS or MRST are selected and their corresponding rheology curves are used in the remainder of the discussions when rheology and injectivity are investigated. Selection of simulator tool based on history match results will be revealed in chapter 9.1.6 after they have been compared.

An investigation of 800 and 2000ppm HPAM rheological behavior in presence of residual oil will be assessed in chapters 9.1.7 and 9.1.8, respectively. Effect of concentration on HPAM rheology in presence of residual oil will then follow in chapter 9.1.9.

Injectivity of both 800 and 2000ppm HPAM will be investigated and compared to corresponding brine injectivities in chapters 9.1.10 and 9.1.11, followed by an assessment of the effect of concentration on injectivity in chapter 9.1.12.

To investigate the effect of residual oil on HPAM rheology and injectivity, the history match results obtained from X4 was compared to another experiment without the presence of residual oil. This experiment will be referred to as X1 and will be further described in chapter 9.2.

The final sections of this chapter are devoted to investigating the effects of residual oil on polymer rheology, retention and injectivity (chapter 9.3 through 9.5).

9.1 X4 Experiment

9.1.1 History Match of Initial Water Flood

As mentioned in chapter 7, the purpose of performing water floods in the X4 experiment was to estimate absolute permeability of the porous media, both before and after polymer flooding. Determined uniform permeability from a precursory water flood would be applicable in the history match of a subsequent polymer flood, thereby reducing the number of tuning parameters to only the viscosity table.

As mentioned in chapter 4.2, Newtonian fluids exhibit shear independent viscosity behavior. The porous media was assumed to be reasonably homogeneous and since the porous media was flooded with a Newtonian fluid, it was expected that the relationship between differential pressure and volumetric injection rate would be linear. In the experimental data, a clear deviation from linear behavior was observed at an injection rate of 6 mL/min. However, it was reported a displacement of residual oil that propagated from the injection well and a small distance into the porous media, consequently inducing the disproportionate differential pressure response. The outlier at a volumetric injection rate of 6 mL/min was therefore omitted from the simulation. History match results from STARS and MRST are shown in Figure 9.1.

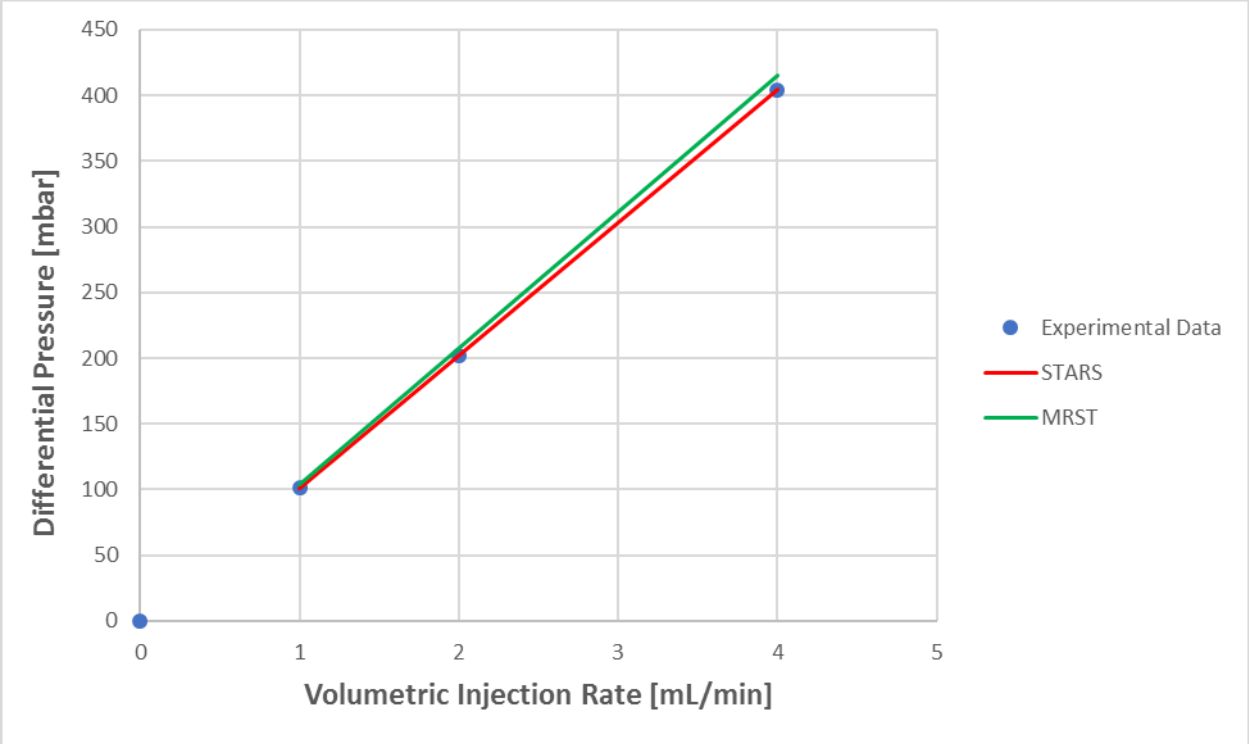

Figure 9.1: X4 experiment: History match of initial water flood.

A satisfactory history match is observed in both STARS and MRST when the obvious outlier is omitted from the simulations. Absolute permeability of the porous media was estimated at 870 and 840mD in STARS and MRST, respectively. This permeability deviation between STARS and MRST amounts to about 3,5%.

Only minor history match deviations of differential pressure between STARS and MRST are observed although, they seem to become more pronounced at higher volumetric injection rates. However, this numerical observation and is more readily assessed when differential pressure deviations between history match results obtained in STARS and MRST are compared in percentage terms (Figure 9.2).

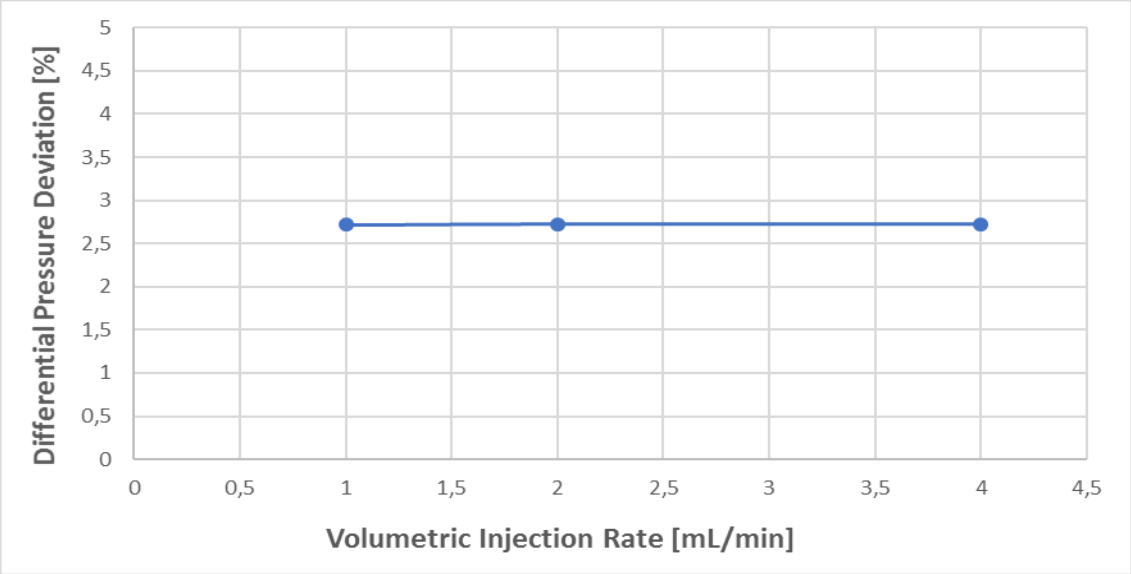

Figure 9.2: Percentage history match deviation of initial water flood between STARS and MRST.

The percentage differential pressure deviation between MRST and STARS at different volumetric injection rates are nearly identical and amounts to about 2,7%. Based on this relatively minor deviation, confidence in the obtained history match is enforced by two simulator tools providing approximately the same results.

The history match obtained in both STARS and MRST shows a linear relationship between differential pressure and volumetric injection rate. While MRST uses a least squares approximation to obtain the history match, STARS is performed manually without the use of a least mean square method and is subject to the potential source of error related to the numerical observation mentioned above. It is therefore a suggestion that the history match performed by MRST obtains the most reliable result because the error between experimental data and history match are minimized.

9.1.2 History Match of 800ppm HPAM Flood

As mentioned chapter 4.2, non-Newtonian fluids exhibit shear dependent viscosity behavior. It is therefore not expected that the relationship between differential pressure and volumetric injection rate is linear for 800ppm HPAM. Permeability values of 870 and 840 mD obtained from the initial water flood was specified in the simulation of the 800ppm HPAM flood in STARS and MRST, respectively. A satisfactory history match was obtained in both STARS and MRST as shown in Figure 9.3 and Figure 9.*4*, where Figure 9.4 depicts the history match for the lowest injection rates not readily observable from Figure 9.3:

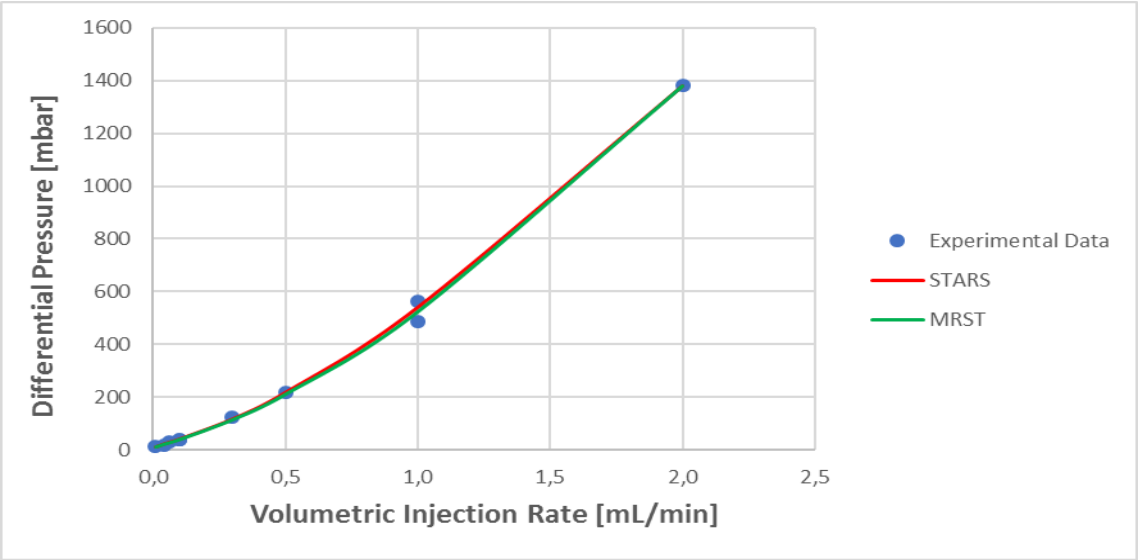

Figure 9.3: X4 experiment: History match of 800ppm HPAM flood.

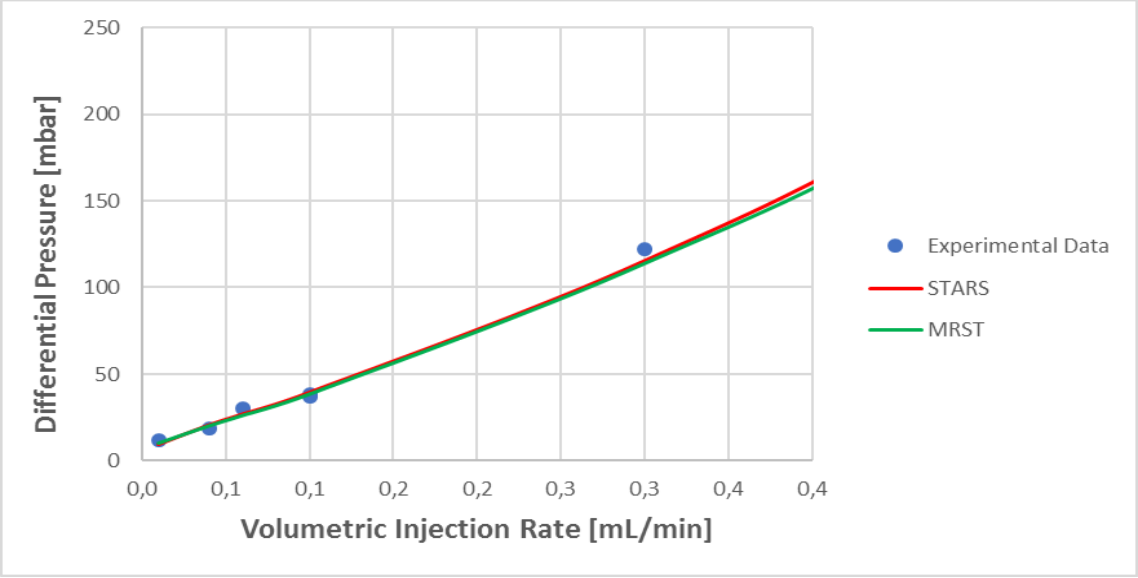

Figure 9.4: X4 experiment: History match of 800ppm HPAM flood (lower region).

The history match obtained in both STARS and MRST are excellent and deviations between them seems to be negligible. Figure 9.5 shows the percentage differential pressure deviations between the two simulator tools.

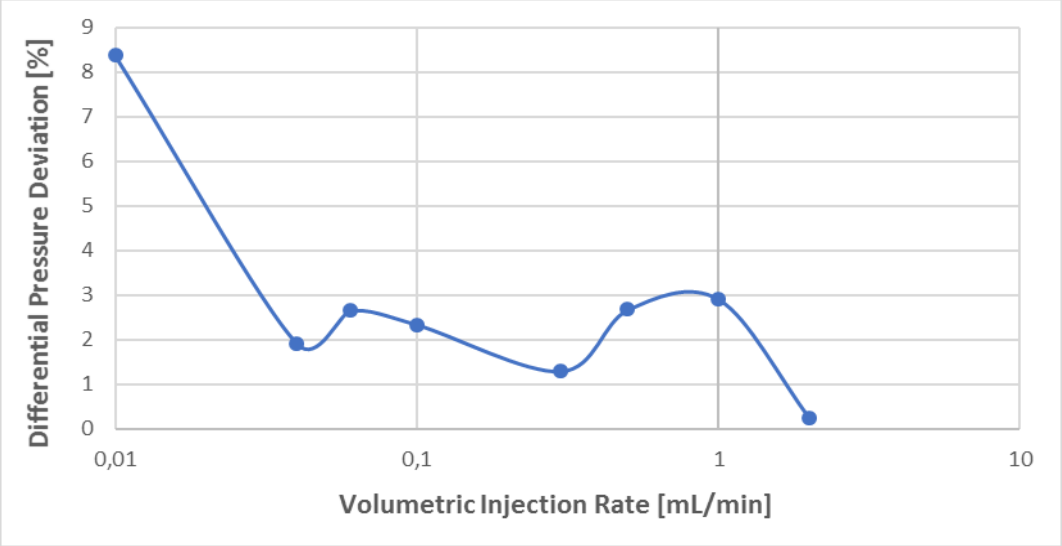

Figure 9.5: Percentage history match deviation of 800ppm HPAM flood between STARS and MRST.

Differential pressure deviations between STARS and MRST are generally insignificant. However, at the lowest injection rate of 0,01 mL/min, differential pressure deviation between STARS and MRST was in excess of 8%. This abnormally high deviation was due to difficulties in STARS at low rates when the slope of the specified rheology curve was too steep. Obtained rheology curves of 800ppm HPAM using both STARS and MRST are shown in Figure 9.6.

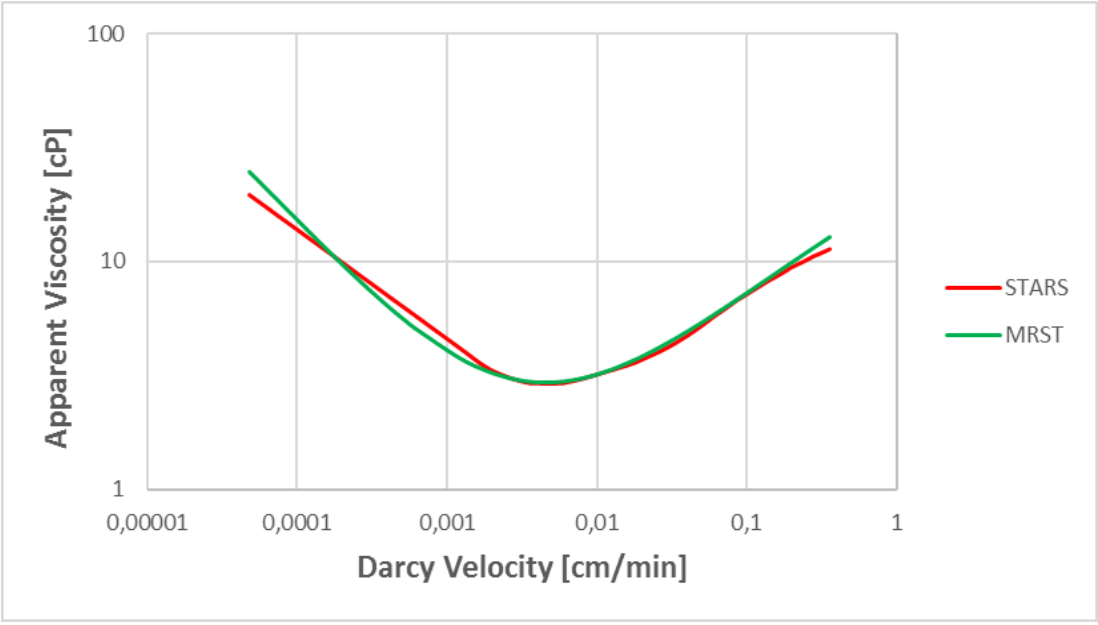

Figure 9.6: Rheology curve of 800ppm HPAM using STARS and MRST.

The rheology curve of 800ppm HPAM obtained by the two different simulators have a few minor deviations, where the most pronounced deviation is found in the lower Darcy velocity interval. Not surprisingly, this lower velocity intervall corresponds to the 0,1 mL/min injection rate that STARS found troublesome.

The overall trend of the rheology curves can be assessed based on the differential pressure match. Relative increase in differential pressure is decreasing with volumetric injection rates in the low to intermediate rate regime. This regime corresponds to the shear thinning region of the 800ppm HPAM rheology curve where apparent viscosity is decreasing and thus reduced resistance to flow results in lower relative differential pressures with increasing flux. The opposite phenonmenon is observed at intermediate to high injection rates where the shear thickening region of 800ppm HPAM results in relatively higher differential pressures at increasing flux.

800ppm HPAM injectivity as a function of volumetric injection rate using both STARS and MRST is shown in Figure 9.7.

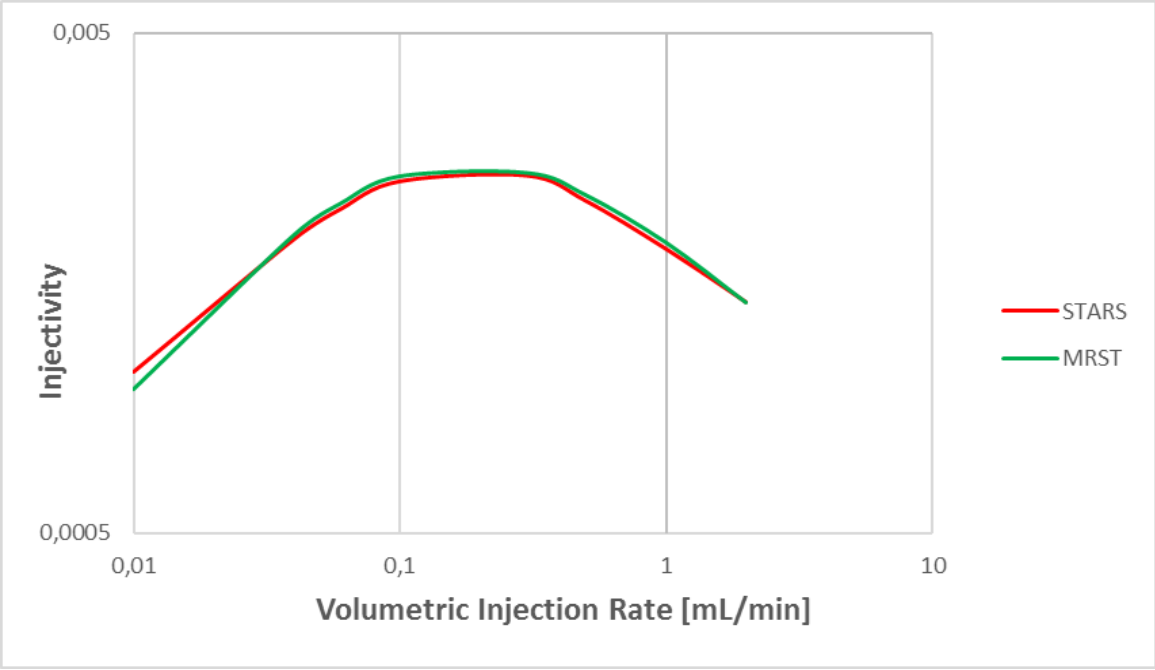

Figure 9.7: X4 experiment: 800ppm HPAM injectivity.

Since injectivity is defined as the ratio of volumetric injection rate to differential pressure, deviations in the history match will affect the injectivity deviations proportionally. Although discrepancies are generally insignificant, a pronouced deviation at an volumetric injection rate of 0,1 mL/min is clearly noticable, as expected from the differential pressure deviation.

9.1.3 History Match of Secondary Water Flood

Experimental values obtained from the secondary water flood did not contain any significant outliers. However, differential pressure at a volumetric injection rate of 10 mL/min seems to deviate from the general trend. Nevertheless, a satisfactory history match was obtained and the relationship between differential pressure and volumetric injection rate was linear. As mentioned, this linear behavior is expected since water is a Newtonian fluid. History match results obtained in both STARS and MRST is shown in Figure 9.8.

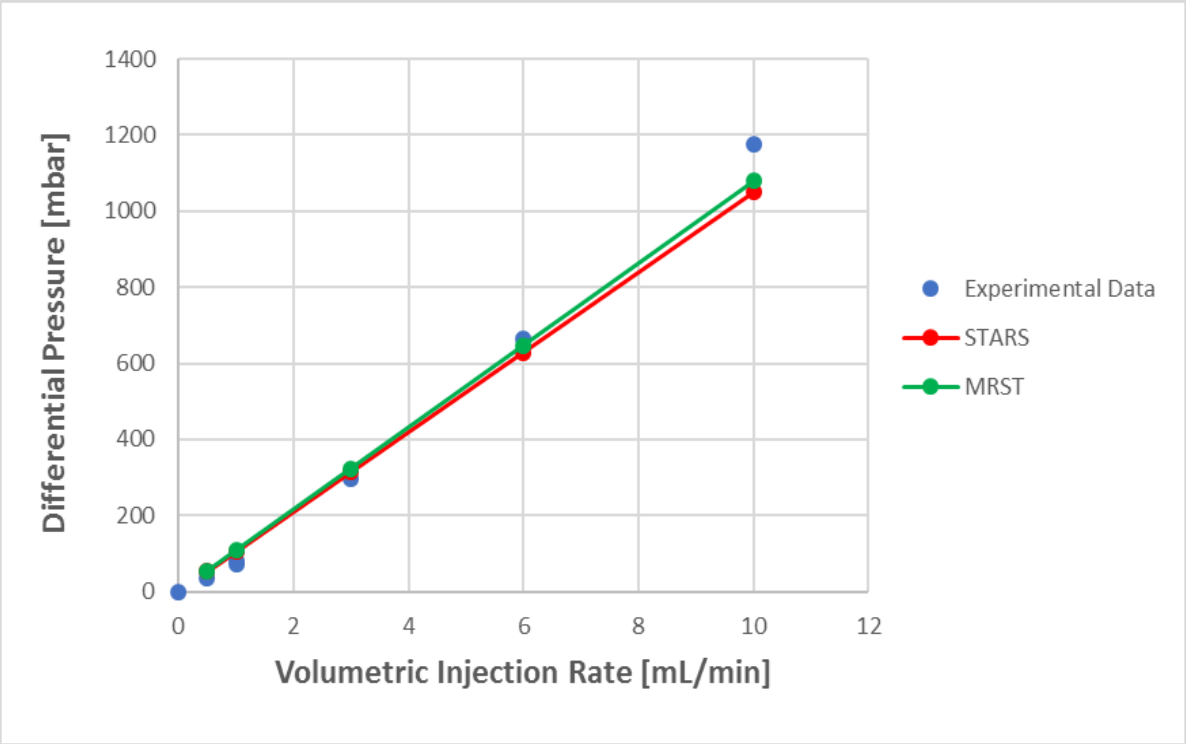

Figure 9.8: X4 experiment: History match of secondary water flood.

Absolute permeability of the porous media was estimated at 840 and 808 mD in STARS and MRST, respectively. Permeability reduction resulting from the precursory 800ppm HPAM flood amounts to 3,5% and 3,8% for STARS and MRST, respectively. This permeability reduction indicates that polymer retention occurred during the precursory polymer flood.

The permeability deviation between the two simulator tools is merely 4%. This deviation is a result of both the initial permeability deviation obtained in the initial water flood and the least squares versus manual approach used in MRST versus STARS, respectively.

History match deviations between STARS and MATLAB is small, but seems to become more pronounced at higher volumetric injection rates. In accordance with the initial water flood, these

deviations are assessed by plotting differential pressure deviation in percentage terms versus volumetric injection rate as shown in Figure 9.9.

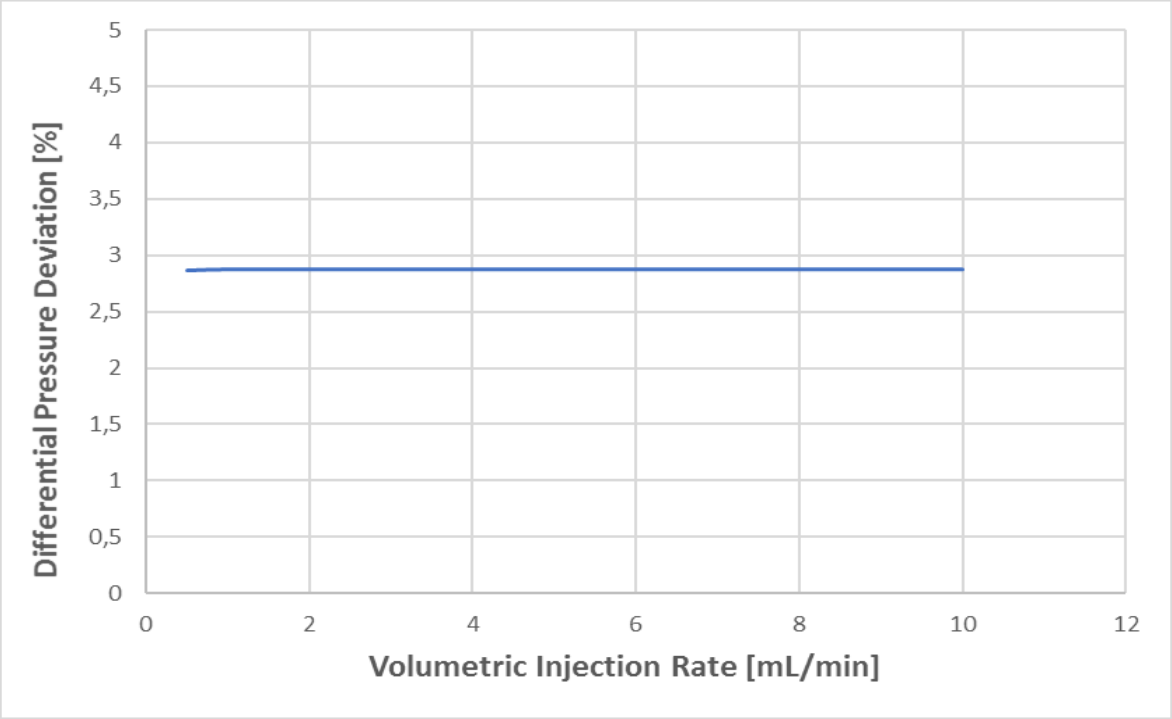

Figure 9.9: History match deviation of secondary water flood between STARS and MRST.

Differential pressure deviations between STARS and MRST is constant throughout the injection rates encountered and equal to about 2,9%.

9.1.4 History Match of 2000ppm HPAM Flood

Permeability values of 840 and 808 mD obtained from the secondary water flood was used in the 2000ppm HPAM flood simulations in STARS and MRST, respectively. History match results from both simulator tools are shown in Figure 9.10 and Figure 9.***11***, where Figure 9.11 depicts the history match for the lowest injection rates not readily observable from Figure 9.10.

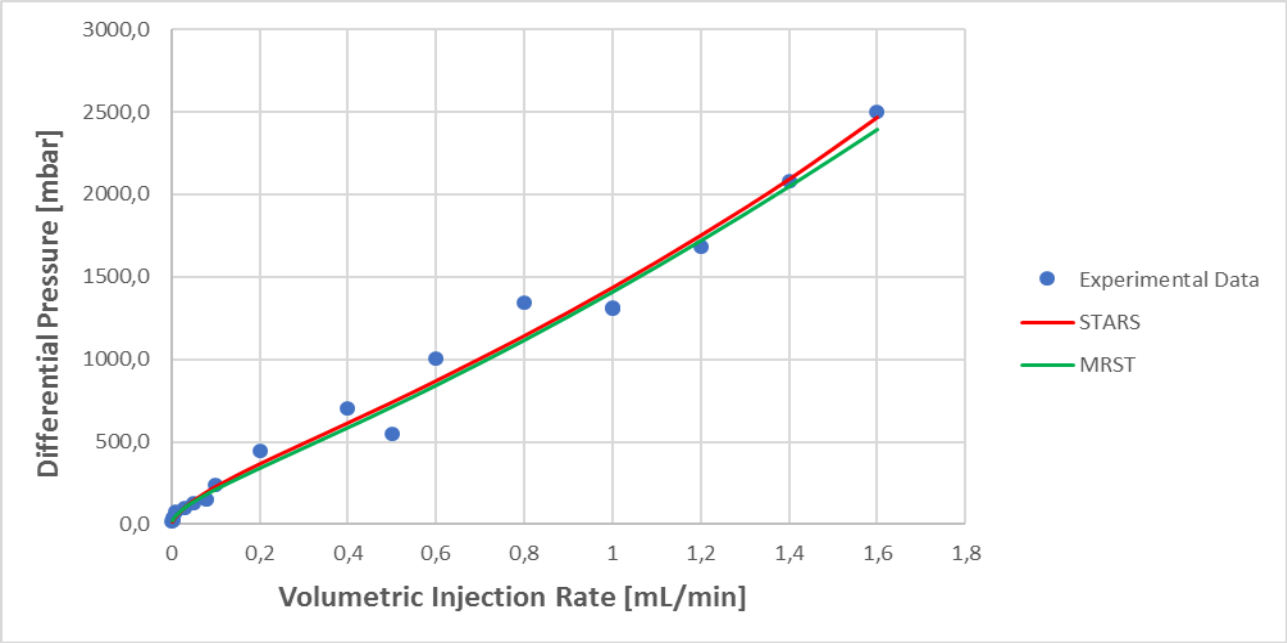

Figure 9.10: X4 Experiment: History match of 2000ppm HPAM flood.

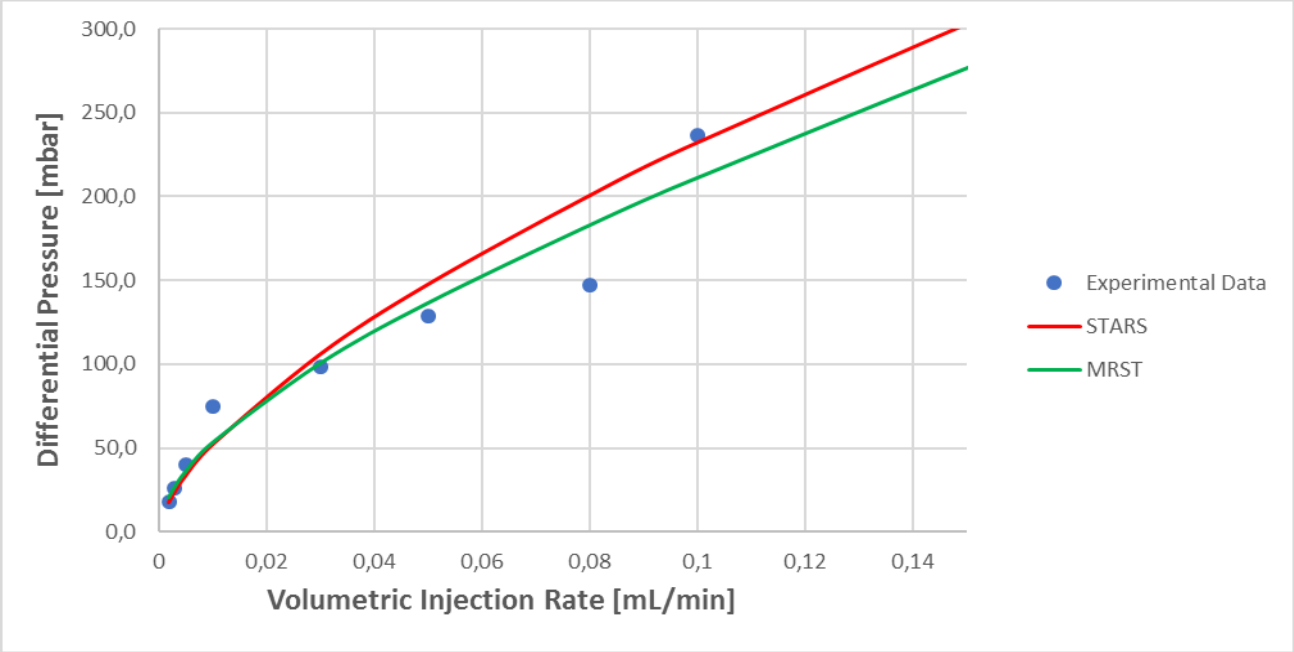

Figure 9.11: X4 Experiment: History match of 2000ppm HPAM flood (lower region).

History match results from both STARS and MRST are relatively similar although, deviations are more pronounced in the upper and lower flow rate regime. Because of deviating experimental data, especially at low to intermediate volumetric injection rates, some uncertainty will be impossible to avoid.

At first glance, experimental differential pressures at injection rates of 0,05 and 0,08 mL/min seems to be outliers, but since these deviations are not far enough from experimental values to be defined as outliers, they are collectively increasing the uncertainty of the history match.

In Figure 9.10 and Figure 9***.11*** both minor and seemingly significant deviations are observed. A comparison of differential pressure deviations between STARS and MRST in percentage terms are shown in Figure 9.12.

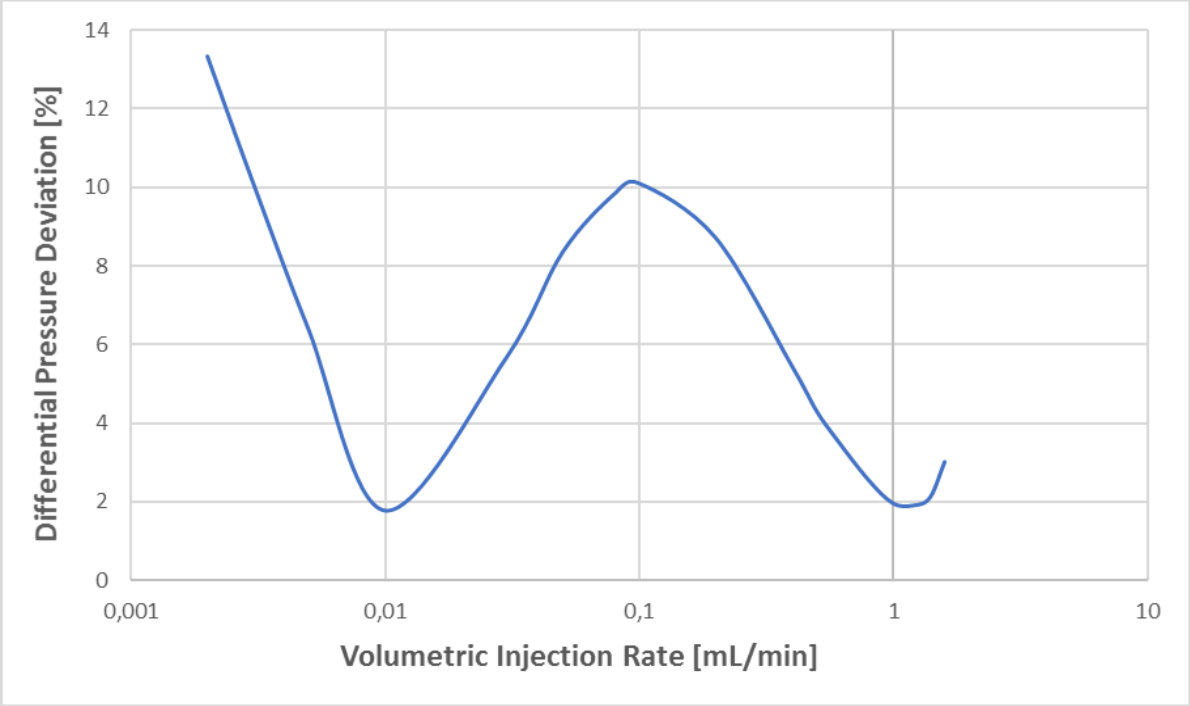

Figure 9.12: History match deviation of 2000ppm HPAM flood between STARS and MRST.

Percentage deviation between STARS and MRST range from about 3 to 13%. These significantly varying deviations can be explained in part by the two highly deviating experimental values described above, which are responsible for higher uncertainties and thus a larger interval of possible history matches.

The obtained rheology curves for the 2000ppm HPAM polymer using both STARS and MRST are shown in Figure 9.13.

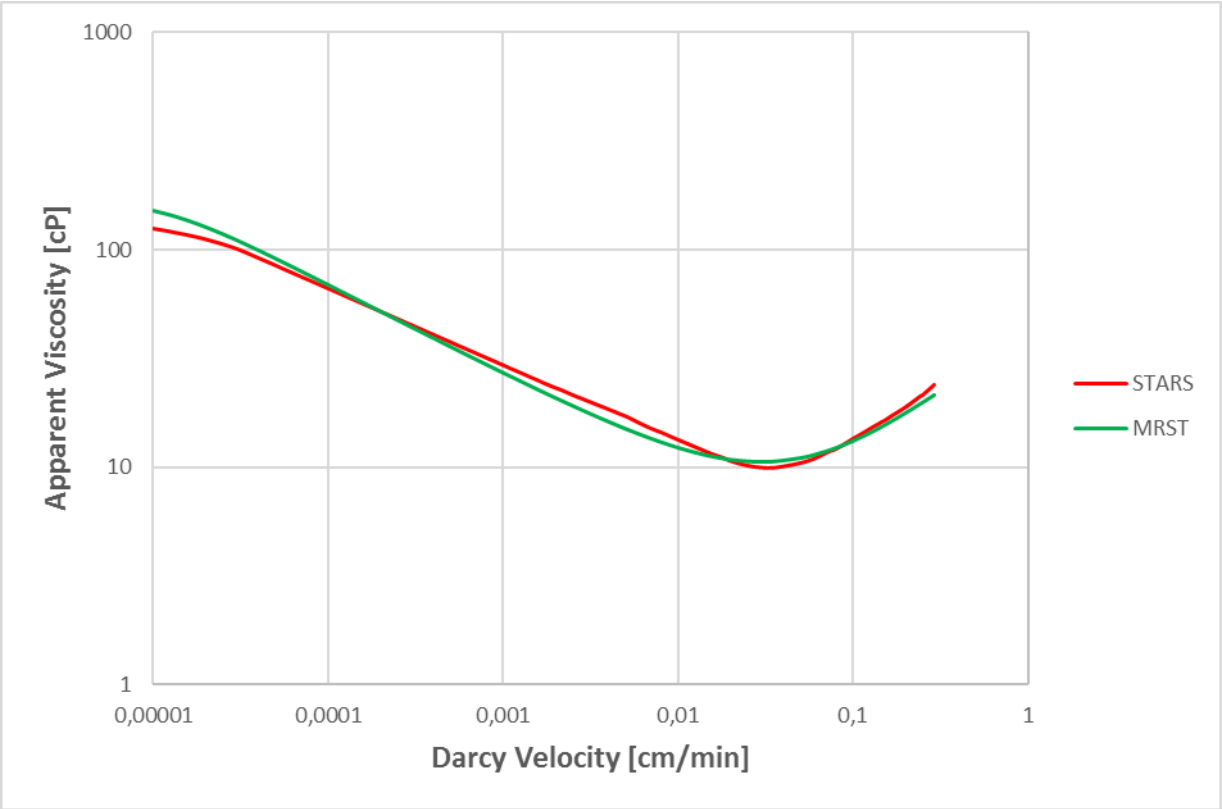

Figure 9.13: Rheology curve of 2000ppm HPAM using STARS and MRST.

The obtained rheology curves for 2000ppm HPAM using the two different simulator tools have a few minor deviations. The most pronouced deviation in absolute apparent viscosity is found at the lowest Darcy velocity. This region correspond to the lowest injection rate where differential pressure deviation was at its maximum value. STARS show higher apparent viscosity values at the highest Darcy velocities compared to MRST, but shows a lower apparent viscosity compared to MRST at the lowest Darcy velocities. The overall shape of the rheology curves and the slope of both shear thinning and shear thickening regions are relatively similar using STARS and MRST.

None of the curves exhibit a clear Newtonian plataeu at the transition between shear thinning and shear thickening behavior. Howver, the rheology curve obtained in STARS is leveling off when approaching the lowest velocities, thus indicating the presence of a low velocity Newtonian plataeu. This tendency is not as pronouced in the rheology curve obtained in MRST.

Injectivity as a function of flow rate using both STARS and MRST as simulator tools is shown in Figure 9.14.

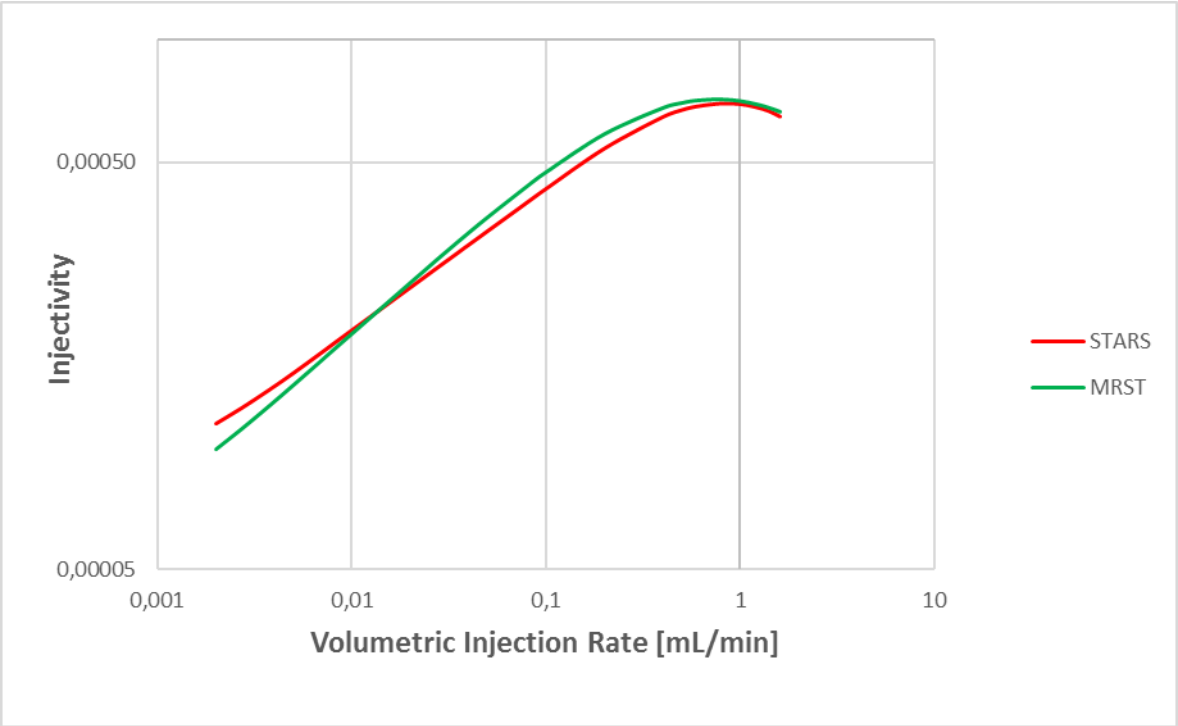

Figure 9.14: Injectivity of 2000ppm HPAM using STARS and MRST.

Since injectivity is defined as the ratio between volumetric injection rate and differential pressure, deviations in the history match will affect injectivity deviations proportionally. Injectivity is thus most pronouced in the low flow rate region where differential pressure deviations are highest. Because of its direct differential pressure dependency, percentage deviations between injectivity curves obtained will therefore follow deviations seen in Figure 9.12 exactly.

9.1.5 History Match of Tertiary Water Flood

To estimate absolute permeability of the porous media after the 2000ppm HPAM flood, the tertiary water flood was history matched in both STARS and MRST as shown in Figure 9.15.

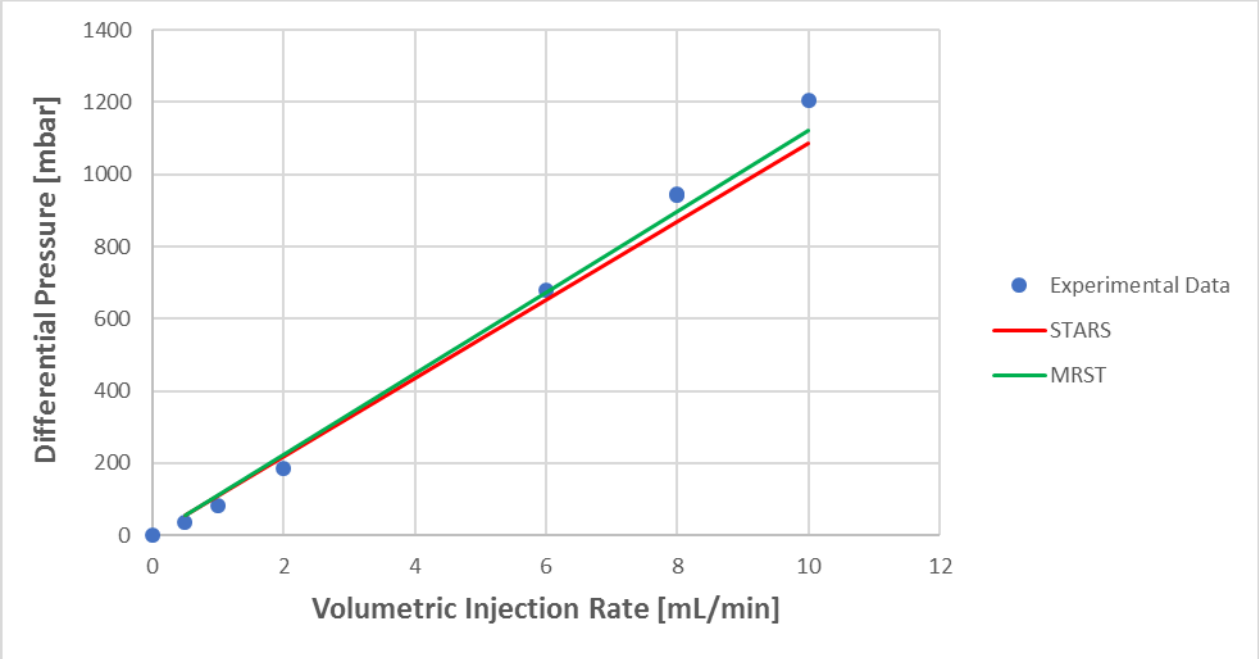

Figure 9.15: X4 experiment: History match of tertiary water flood.

Permeability values obtained from the history match of the tertiary water flood was estimated at 810 and 777 mD in STARS and MRST, respectively. This permeability deviation between the two simulator tools is just above 4 %.

Although no outliers from linear behavior was observed, there seems to be a non-linear deviation in the high volumetric injection rate regime. This behavior can also be seen in both initial and secondary water floods. Admittedly, differential pressure obtained in the initial water flood at a volumetric injection rate of 6 mL/min is too high to be called a deviation and is therefore classified as an outlier. However, in all three water floods, the differential pressure gradient as a function of volumetric flow rate seems to increase, while the linear trend appears to be maintained for volumetric injection rates up to about 4 mL/min.

Since water is a Newtonian fluid, the relationship between differential pressure and volumetric injection rate is assumed to be linear. The apparent flow rate dependent differential pressure gradient observed from experimental data contrasts this assumption. This behavior is not attributable to a turbulent flow regime since the value of Reynolds number for all sequential water floods is negligible and thus is clearly within the laminar flow regime. However, the apparent observation that differential pressure gradient increases with increasing volumetric

injection rate is a misguided observation. Figure 9.16 shows a plot of experimental differential pressures from all sequential water floods, fitted using least squares regression. Experimental differential pressures corresponding to a volumetric injection of zero is omitted from the plot.

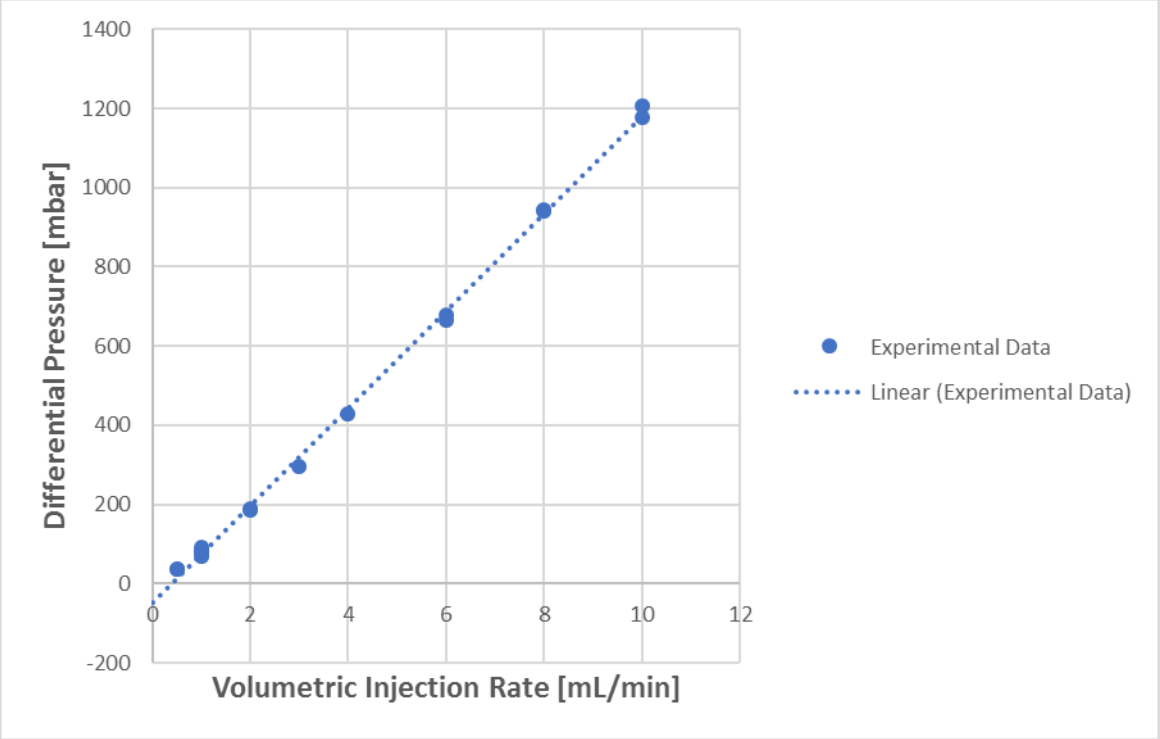

Figure 9.16: Linear trendline for all experimental water flood data.

The linear trendline shows a very good match with the experimental data. The question arises of why this linear relationship was not observed in the previously history matched water floods. This can be explained in terms of the differential pressure intersect with the y-axis, namely the differential pressure at zero volumetric injection rate. This differential pressure corresponds to the situation where no fluids are injected and should be equal to zero. As previously mentioned, the counter pressure from the production well is measured at zero injection rate and used for all successive measurements to calculate differential pressure at various injection rates. Based on the linear trendline in Figure 9.16, the suggestion made is that this counter pressure has been overestimated from experimental measurements and thus underestimated values of differential pressure are reported. In percentage terms, this offset will affect the low rate differential pressures to a greater extent than differential pressures at high flow rates. Therefore, the effect of an underestimated counter pressure induces an apparent velocity dependent pressure gradient.

Absolute permeability of the porous media decreased by 30mD after both 800ppm and 2000ppm HPAM floods in STARS, while the permeability reductions in MRST amounted to

32 and 31 mD, respectively. Consequently, the permeability reduction between successive water floods was approximately the same (3,5%) in both simulator tools even though two different polymer concentrations were flooded.

It was reported by Zhang and Seright (2014) [5] that if a porous media was first contacted with a dilute HPAM solution that satisfied retention, no significant additional retention occurs when exposed to higher concentrations. They also reported that retention is considered to be practically instantaneous. Since retention is assumed to instantaneous, polymer retention should have been satisfied after the 800ppm HPAM flood. Therefore, additional retention caused by the 2000ppm HPAM flood contradicts the conclusion made by Zhang and Seright.

History match deviations between STARS and MRST are minor, but seems to become more pronounced at the higher volumetric flow rates. The differential pressure deviation between the history match in STARS and MRST are compared in percentage terms, as shown in Figure 9.17.

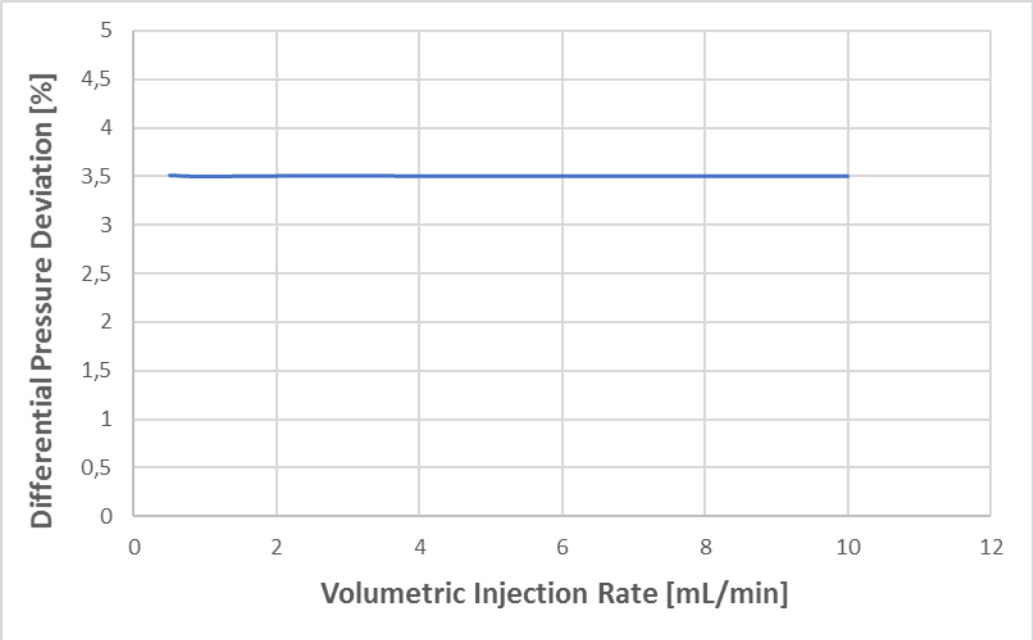

Figure 9.17: History match deviation of tertiary water flood between STARS and MRST..

In compliance with both precursory water floods, differential pressure deviations between STARS and MRST is rate independent. In the tertiary water flood this deviation amounts to about 3,5% as seen from Figure 9.17.

9.1.6 Summary of History Match results in STARS versus MRST

The conclusion drawn from the history match of the initial water flood was that since MRST uses a least squares method of minimizing the history match error, MRST obtains the most reliable result.

Since the subsequent 800ppm HPAM flood is affected by the permeability obtained in the initial water flood, the rheology curve of 800ppm HPAM obtained in MRST should also be the most representative.

In addition, the rheology curve obtained in MRST shows steadily increasing and decreasing values of viscosity in the shear thinning and shear thickening regimes, consistent with previously reported HPAM rheology [6], [7]. In contrast, 800ppm HPAM rheology obtained in STARS does not show this smooth viscosity behavior and its slope in both shear thinning and shear thickening regimes are alternating. This behavior is observed in the rheology curve of 2000ppm as well.

Also, STARS experienced difficulties at low rates when the slope of the specified rheology curve was too steep, thus a significant deviation in history matched differential pressure at an injection rate of 0,1 mL/min was obtained in the 800ppm HPAM history match. Therefore, the rheology curves obtained in MRST are selected as the most representative and will be used for the remainder of this thesis.

The permeability reductions resulting from polymer floods in the X4 experiment which were history matched in the water floods, are shown in Table 9.1.

Table 9.1: Permeabilities before and after polymer floods in the X4 experiment.

Initial Water Flood	Secondary Water Flood	Tertiary Water Flood
840mD	808mD	777mD

These permeabilities will be utilized when assessing the retention of 2000ppm HPAM in presence compared to absence of residual oil in chapter 9.4.

9.1.7 800ppm HPAM Rheology

Rheology of 800 ppm HPAM in presence of residual oil is shown in Figure 9.18 using the curve obtained in MRST.

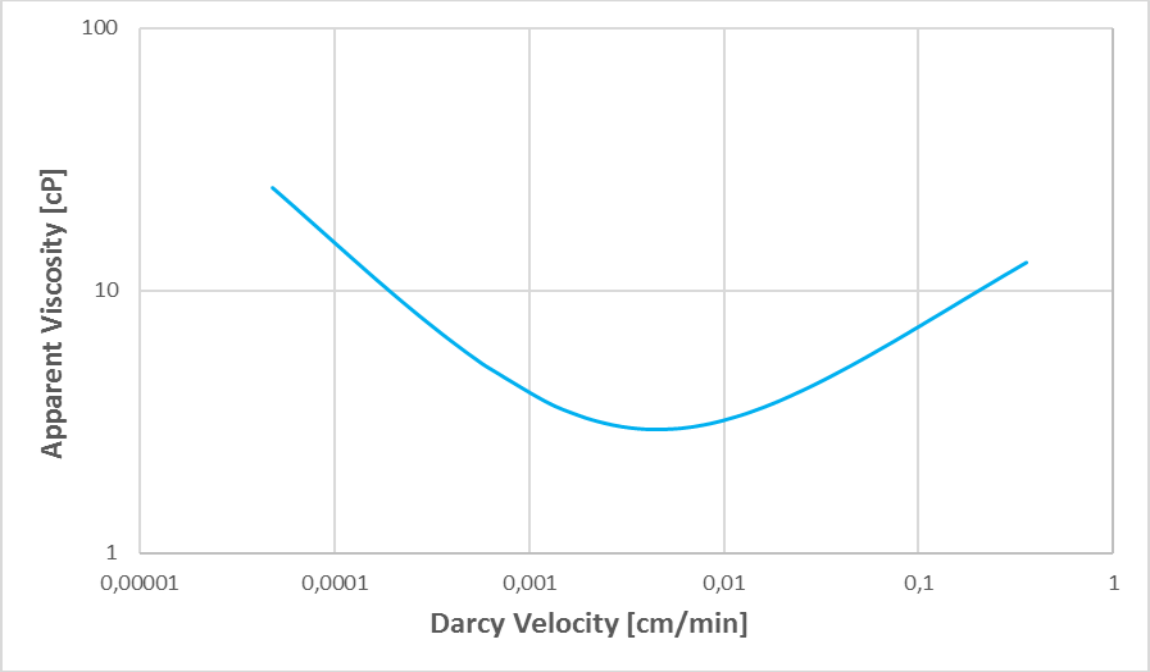

Figure 9.18: X4 experiment: 800ppm HPAM rheology.

It is evident that the 800ppm HPAM solution investigated exhibits a significant degree of shear thinning at low to intermediate Darcy velocities.

Occurrence of shear thinning in porous media has been debated. Seright et al. (2011) reported that only non-degraded polymer exhibit shear thinning behavior in porous media. This shear thinning behavior was attributed to high molecular weight species, which has a high propensity for mechanical degradation. They argued that degradation of high molecular species may occur due to high shear rates experienced near an injector, and that degraded polymer will consequently show Newtonian behavior in the low velocity regime [6].

In a more recent study by Skauge et al. (2016) [7], it has been suggested that polymers will be degraded to a lesser extent in radial floods compared to linear flow conditions. This discrepancy between polymer behavior in linear versus radial geometry is attributed to the radial transient flow pattern as opposed to the steady state conditions found in linear core floods.

In linear models at constant differential pressure, both volumetric injection rate and Darcy velocity remains constant. However, in radial models, Darcy velocity will not remain constant because the cross-sectional area of the flow path is increasing from the injection well towards

the circumferential outer boundary. A comparison of Darcy velocity as a function of distance from the injection well is shown for both linear and radial flow regimes in Figure 9.19.

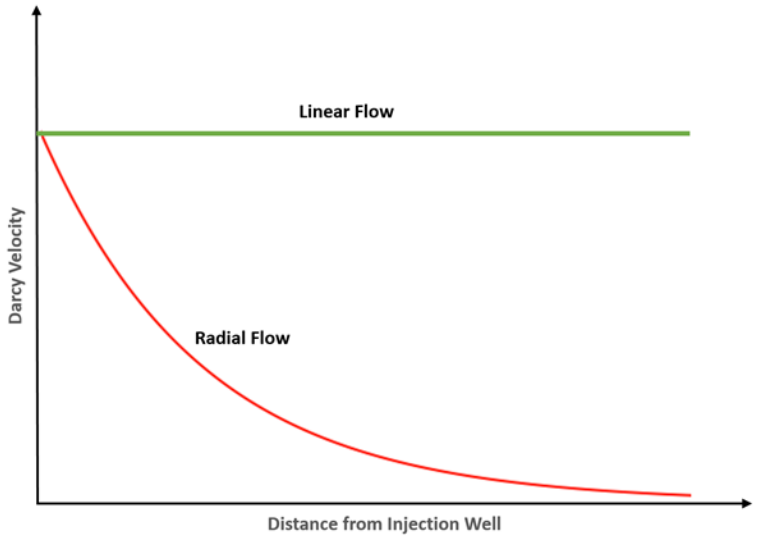

Figure 9.19: Darcy velocity as a function of distance from injection well in linear and radial models.

It has been suggested that the small amount of time that polymers are subjected to high flow velocities in radial models explains the absence of mechanical degradation compared to the linear flow regime. The elastic nature of viscoelastic polymers may therefore prevent mechanical degradation in radial flow regimes where they are subjected to high flux for a short time period.

In the X4 experiment, mechanical degradation of 800ppm HPAM can be ruled out based on bulk viscosity measurements (Table 7.3 and Figure 7.3). Effluent viscosity at the highest volumetric injection rate of 2 mL/min was 16 cP, compared to 15,1 cP of the injected solution. If mechanical degradation had occurred, effluent viscosity would have been significantly reduced compared to injected viscosity. Since mechanical degradation did not occur, the shear thinning behavior of 800ppm HPAM is consistent with previous literature.

At intermediate to high Darcy velocities, a shear thickening regime is observed. In polymer flooding, there exist a consensus in the scientific community that HPAM solutions exhibit shear thickening behavior at intermediate-to-high fluid velocities in porous media [6]. This shear thickening behavior is attributed to the viscoelastic character of HPAM and the elongational flow field encountered in porous media as mentioned in chapter 4.3.2.

In the entire interval of velocities investigated, 800ppm HPAM does not exhibit Newtonian plateau behavior.

9.1.8 2000ppm HPAM Rheology

Rheology of 2000 ppm HPAM in presence of residual oil is shown in Figure 9.20 using the curve obtained in MRST.

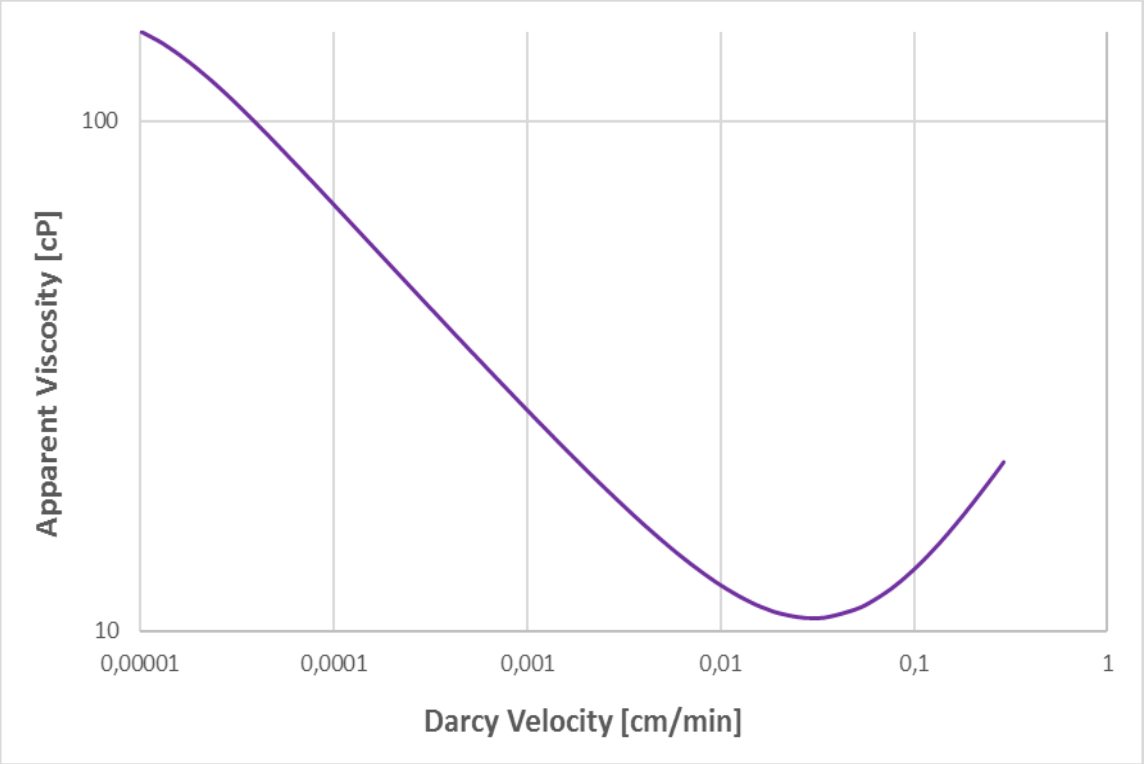

Figure 9.20: X4 experiment: 2000ppm HPAM rheology.

Shear thinning behavior is observed for low to intermediate flow rates, whereas shear thickening is observed at intermediate to high flow rates.

In the entire interval of velocities investigated, 800ppm HPAM does not exhibit Newtonian plateau behavior although, apparent viscosities seem to be leveling off when approaching the lowest velocity value in the interval investigated. Therefore, the proximity of a low velocity Newtonian plateau is suggested to be close to the lowest Darcy velocity in this interval.

As mentioned in chapter 9.1.7, Seright et al. (2011) reported that only non-degraded polymer exhibit shear thinning behavior in porous media [6]. It was established in chapter 7 that effluent viscosity was about 27% lower than injected viscosity and that this clearly demonstrates the occurrence of mechanical degradation. This contradicts the conclusions made by Seright et al. since the 2000ppm HPAM polymer in presence of residual oil clearly has a significant shear thinning regime.

As mentioned in chapter 4.3, rheology of polymers is different in porous media compared to bulk. To compare the in-situ and bulk viscosity of 2000ppm HPAM, a porous media effective shear rate can be calculated from equation (4.10), which was defined as:

$$\dot{\gamma}_{pm} = \alpha' \frac{4u}{\sqrt{8k_{e,i}\phi}} \tag{4.10}$$

Where $\dot{\gamma}_{pm}$ is porous medium effective shear rate, α' is a shape parameter of the pore structure, u is the Darcy velocity defined in equation (3.9), $k_{e,i}$ is effective permeability and ϕ is porosity.

The factor α' is generally determined by matching the critical shear rate for onset of shear thinning in bulk and porous media shear curves. In this case, onset of shear thinning was not observed and the power law model was therefore used instead to match bulk and porous media viscosities by fitting the parameter α', as seen in Figure 9.21.

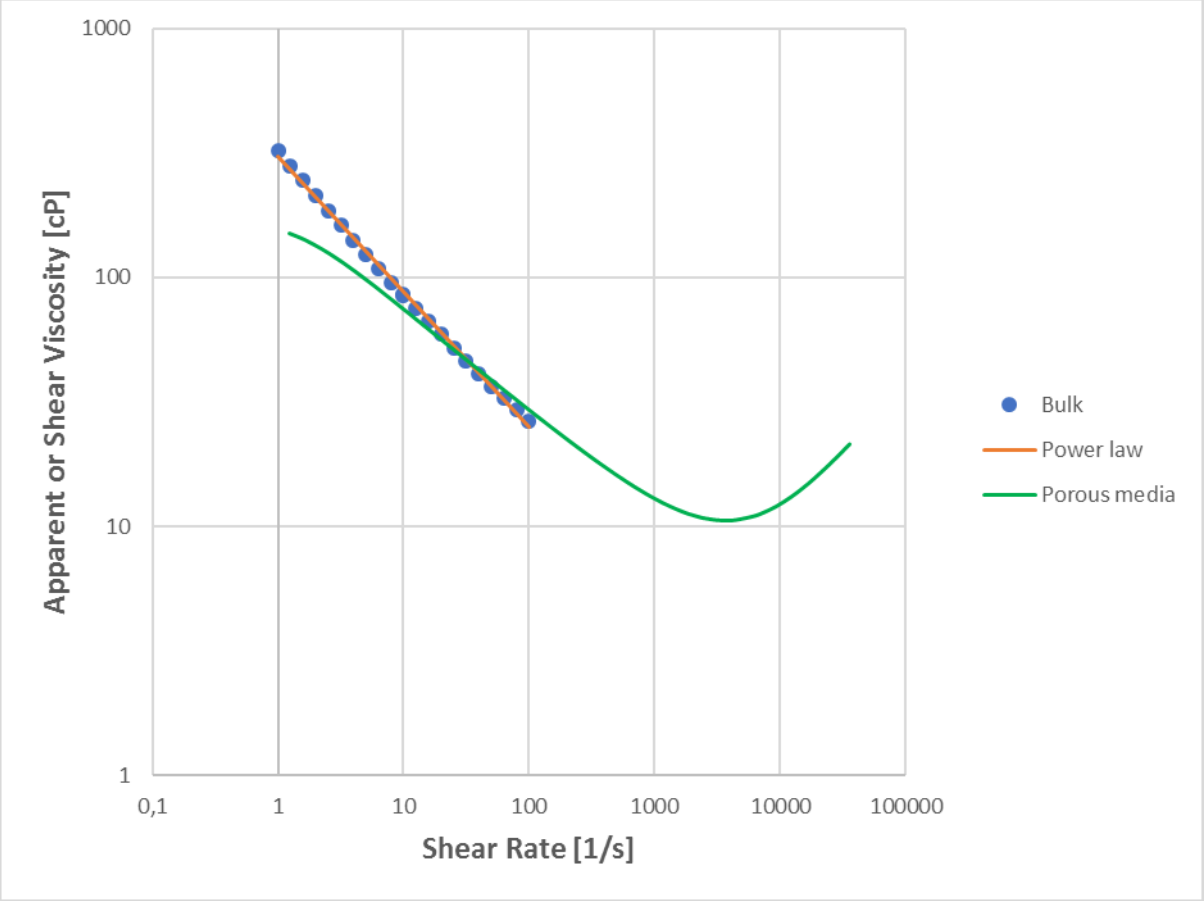

Figure 9.21: Comparison of bulk and in-situ rheology for 2000ppm HPAM (constant shape factor: α' = 50).

The power law model was defined in chapter 4.2 as:

$$\eta(\dot{\gamma}) = K\dot{\gamma}^{n-1} \tag{4.6}$$

Where η is shear dependent viscosity, $\dot{\gamma}$ is shear rate, and K and n are constants, where n is known as the power law index.

A least squares regression method was used to fit the power law model, which resulted in the parameters K and n being equal to 306 and 0,46, respectively. Based on the power law model and bulk viscosities, estimation of the shape parameter α' resulted in a value of 50. H. Færevåg (2014) [56] reported an identical value of the shape parameter ($\alpha' = 50$) when comparing bulk and in-situ rheology of the same polymer (2000ppm Flopaam 3630S) in approximately the same make up brine (TDS = 4758ppm). The experiment conducted by H. Færevåg was performed in radial Bentheimer sandstone in absence of residual oil.

At intermediate shear rates (10-100 s^{-1}), bulk and in-situ viscosities are very similar in both behaviour and absolute viscosity values. They both show shear thinning behaviour in this region and their slope is similar.

As mentioned in chapter 4.3.1, it was reported that in situ-viscosity of polymers in the dilute concentration regime at low shear rates was below the bulk viscosity due to an apparent slip effect [22, 23, 24, 25]. The opposite was reported for polymers in the semi-dilute regime [26].

For 2000ppm HPAM in presence of residual oil, bulk viscosities in the low shear rate region is higher than in-situ viscosities. Since concentration of 2000ppm in the experimental conditions of the X4 is considered to be in the semi-dilute regime, the obtained result contradicts previous literature. However, H. Færevåg (2014) reported the same behaviour in radial models where bulk viscosity was higher than in-situ viscosity at low shear rates. In fact, his results showed that in-situ viscosity was below bulk viscosity in the entire range of low to intermediate shear rates. The suggestion is therefore that the previously reported results in linear models are not comparable to radial geometry. It may seem that the radial geometry rather than presence of residual oil is responsible for the deviating result obtained in the low shear rate regime, compared to earlier literature.

9.1.9 Effect of Concentration on HPAM Rheology

The X4 experiment consists of two polymer floods, encompassing two different polymer concentrations. Since the permeability deviation of 30mD between PF800 and PF2000 only amounts to 3,8%, a direct comparison of their rheological behaviour as a function of concentration is assumed to be feasible. The rheology curves of both 800 and 2000ppm HPAM in presence of residual oil is shown in Figure 9.22.

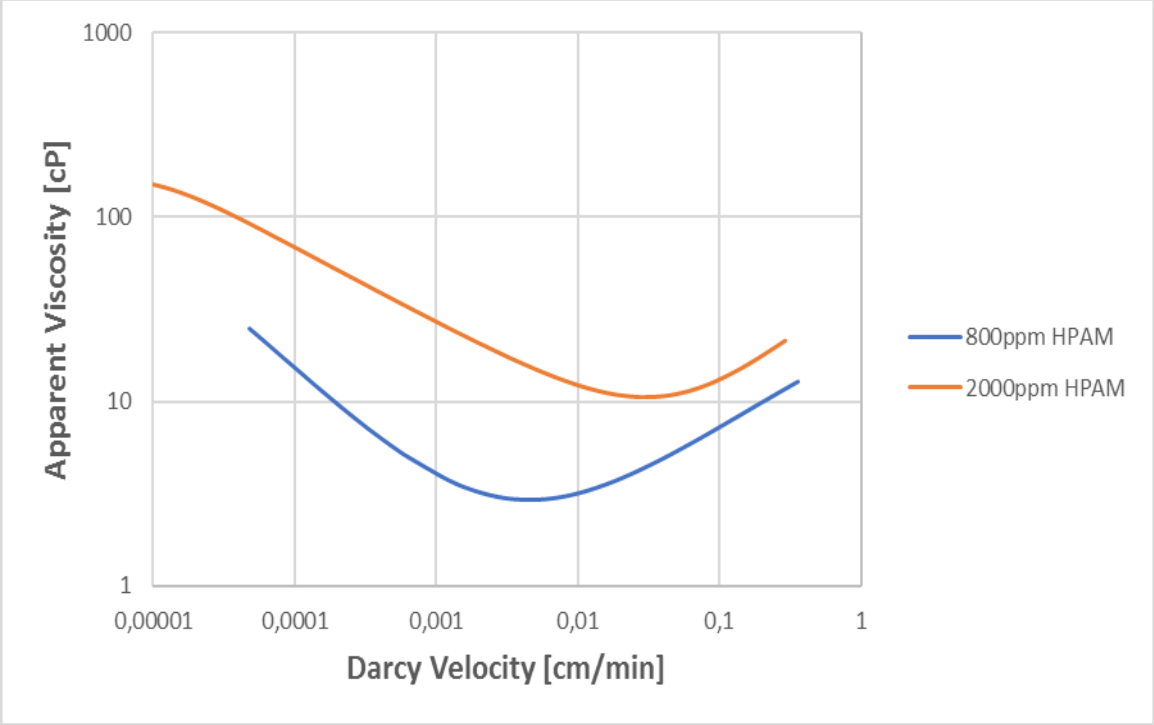

Figure 9.22: Effect of concentration on HPAM rheology.

As mentioned in chapter 4.8, the viscosity increasing feature of the large MW species present in HPAM will be accentuated with increasing polymer concentration. Therefore, a viscosity increase will be expected when increasing the polymer concentration of HPAM. Figure 9.22 confirms this expectation, where apparent viscosity values of 2000ppm HPAM is significantly greater than the 800ppm solution for all velocities within the investigated interval. However, since mechanical degradation of 2000ppm HPAM occurred, the offset in apparent viscosity values is suggested to have been significantly higher if the occurrence of mechanical degradation had been avoided.

It has been reported that onset of shear thickening for HPAM in both unconsolidated and consolidated sandstone shifts towards higher values with decreasing polymer concentration in linear models [33]. This was verified by Seright et.al (2011) [6]. The opposite is observed from Figure 9.22, where onset of shear thickening increases by one order of magnitude when

increasing the HPAM concentration from 800 to 2000ppm in presence of residual oil. This phenomenon could be attributed to either presence of residual oil or on radial flow conditions. However, it has been observed that onset of shear thickening increase with increasing concentration when performing polymer floods in radial models (in house experience). Therefore, this effect is attributed to radial flow regime rather than presence of residual oil.

To assess the relative slope of both shear thinning and shear thickening regions of 800 and 2000ppm HPAM, apparent viscosity as a function of Darcy velocity with non-logarithmic apparent viscosity axis is shown in Figure 9.23.

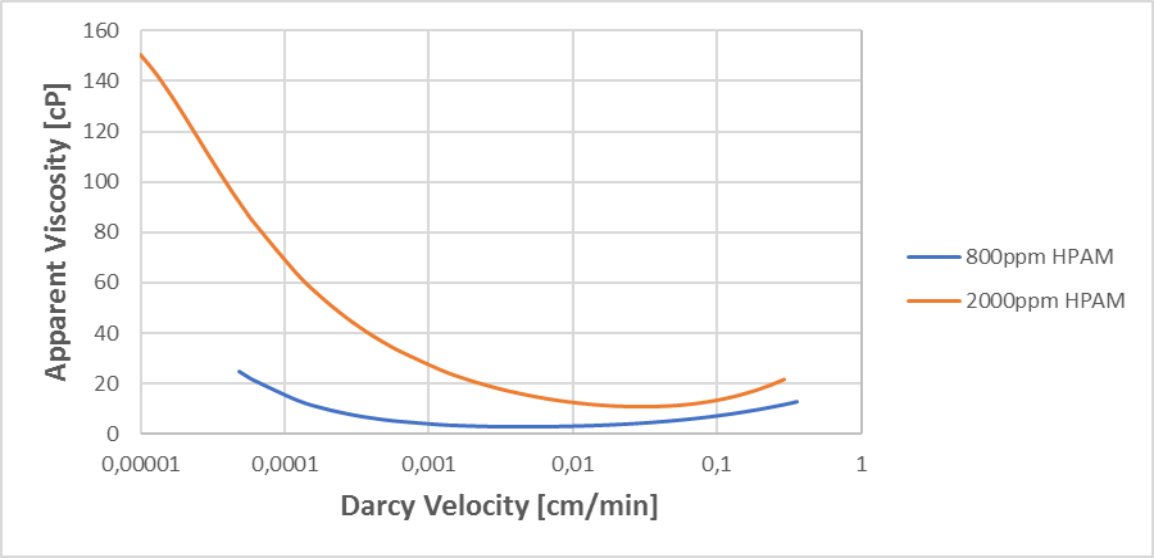

Figure 9.23: **Effect of concentration on HPAM rheology (non-logarithmic apparent viscosity axis).**

It is interesting to note the offset in apparent viscosity between the two HPAM concentrations in the shear thinning compared to the shear thickening regime. In the joint shear thinning regime, apparent viscosity of 2000ppm HPAM is between a factor of 3,7 and 6,2 higher than the 800ppm HPAM solution.

As previously mentioned, Seright et al. (2011) [6] attributed the shear thinning behavior of HPAM to the high molecular species present in the polymer solution. Since both 800 and 2000ppm HPAM in the X4 experiment was of the same molecular weight, an increasing concentration will contribute to an increased number of high molecular weight species. Since shear thinning behavior is attributed to these high molecular species the degree of shear thinning is expected to increase with increasing concentration. This is confirmed from Figure 9.22.

In the shear thickening regime however, the offset is between a factor of 1,8 and 2, thus the slopes of shear thickening regime for 800 and 2000ppm is very similar.

9.1.10 800ppm HPAM Injectivity

When a polymer flooding project is evaluated based on injectivity, the relative decrease in polymer injectivity compared to brine injectivity will be of concern. Therefore, 800ppm HPAM injectivity will be assessed based on the deviations from the corresponding brine injectivity.

Since injectivity is defined as the ratio between volumetric injection rate and differential pressure, Newtonian fluids such as water will exhibit a rate independent injectivity behavior. In contrast, non-Newtonian fluids such as HPAM will attain a rate dependent injectivity.

Figure 9.24 shows a plot of brine and 800ppm HPAM injectivity from the X4 experiment as a function of volumetric injection rate in presence of residual oil.

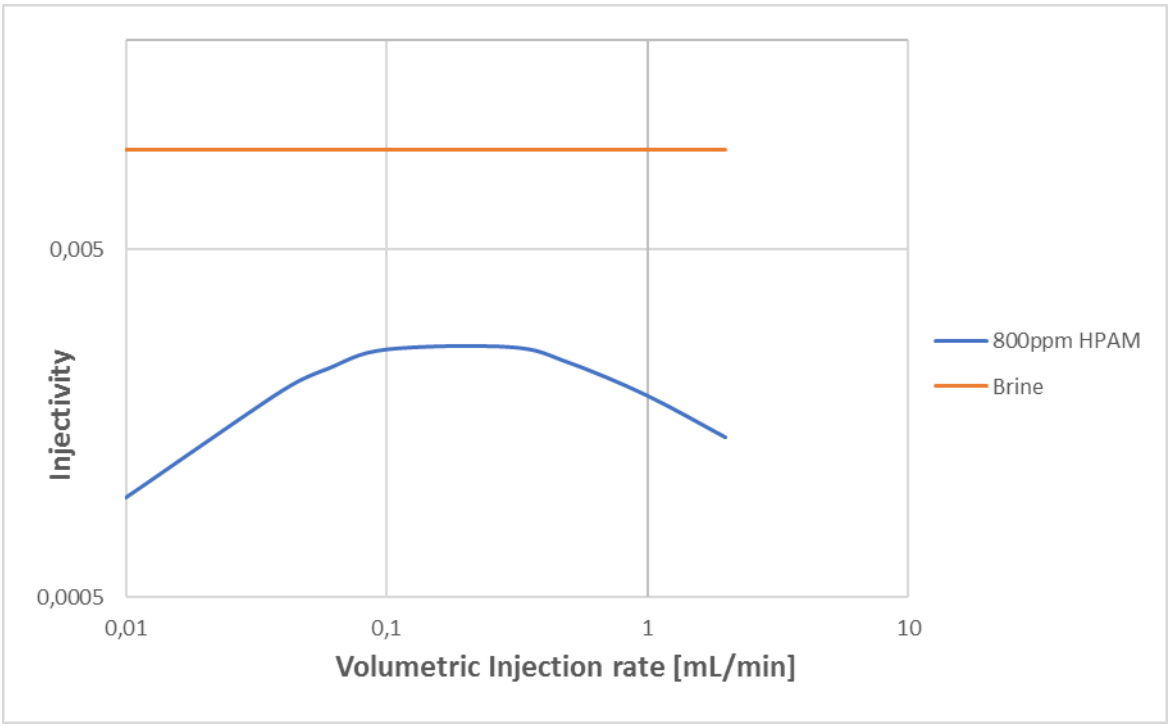

Figure 9.24: X4 experiment: 800ppm HPAM injectivity

Brine injectivity was calculated from the initial water flood, whereas 800ppm HPAM injectivity was calculated from the subsequent polymer flood. Thus, both injectivity values are obtained at the same value of permeability (840mD).

Figure 9.24 shows that an injectivity decrease between a factor of 3,5 and 10 is observed when adding 800ppm HPAM polymer to the injection brine. This is expected since the viscosity increase caused by polymers will induce larger differential pressures and thus by definition will decrease injectivity. Because the 800ppm HPAM solution exhibit rate dependent injectivity behavior, an optimum volumetric injection rate may be defined.

The HPAM injectivity is at a global minima value at the lowest volumetric injection rate of 0,01 mL/min. The injectivity increase with volumetric injection rate until a maximum injectivity value is reached at 0,3 mL/min. Increasing the velocity beyond the point of optimum injectivity results in decreasing injectivity values until a local minima value is attained at the highest volumetric injection rate investigated, i.e. at 2 mL/min.

Based on the injectivity values obtained for 800ppm HPAM in presence of residual oil, an injection rate in the range of 0,1 to 0,3 mL/min would be the optimal condition for polymer flooding. At the optimum polymer injectivity the reduction compared to brine is at its lowest value at 3,5. Some care should be taken to the relatively steep slope in both the low and high volumetric flow regimes, resulting in plummeting injectivity values.

9.1.11 2000ppm HPAM Injectivity

Figure 9.25 shows a plot of brine and 800ppm HPAM injectivity from the X4 experiment as a function of volumetric injection rate in presence of residual oil.

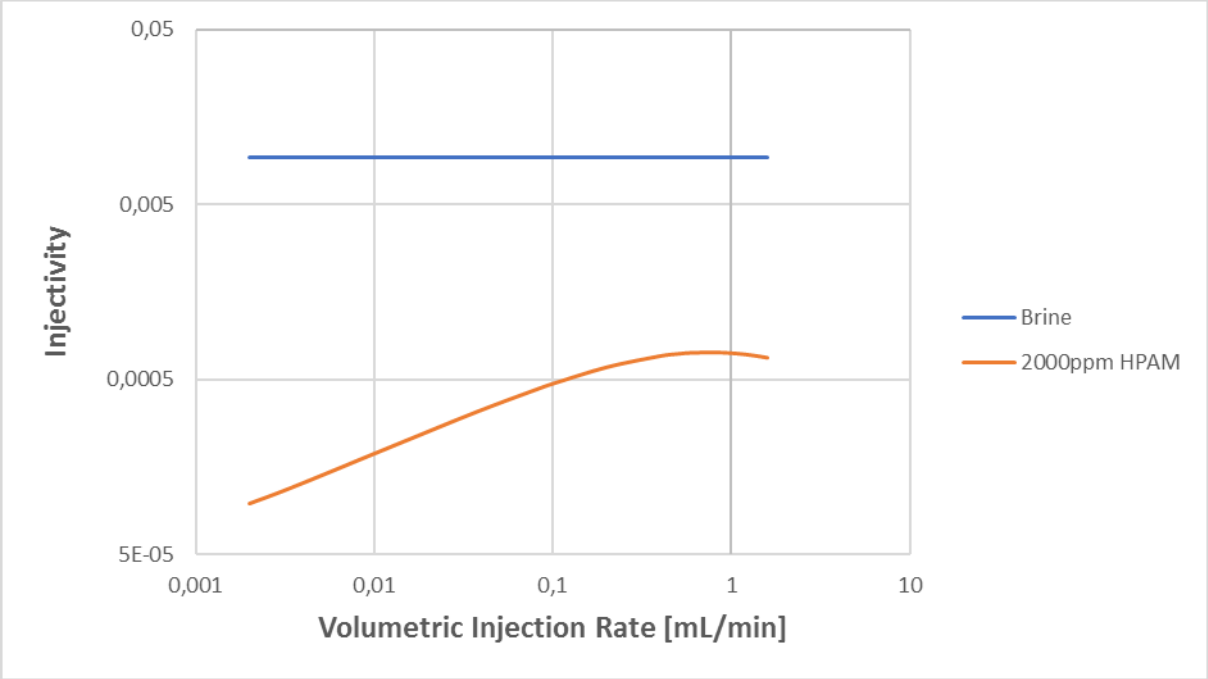

Figure 9.25: X4 experiment: 2000ppm HPAM injectivity.

Brine injectivity was calculated from the secondary water flood, whereas 2000ppm HPAM injectivity was calculated from the subsequent polymer flood. Thus, both injectivity values are obtained at the same value of permeability (808mD).

2000ppm HPAM injectivity is severely reduced compared to the brine solution and the deviation is most pronounced at low volumetric injection rates.

The injectivity of 2000ppm HPAM in presence of residual oil is at a global minima value at the lowest volumetric injection rate of 0,002 mL/min. A following injectivity increase is observed until a maximum value is attained at a volumetric injection rate of 0,8 mL/min. The injectivity then decreases slightly with at higher rates.

Based on these injectivity values, an injection rate of 0,8 would be the optimal condition for polymer flooding. However, the whole range of injection rates from 0,4 to 1,6 mL/min provides very similar injectivity values, thus a wide suboptimal range of injectivity values exist.

It is evident from Figure 9.25 that injectivity decreases very steeply when reducing the injection rate below 0,2 mL/min and this range should preferably be avoided.

9.1.12 Effect of Concentration on HPAM Injectivity

A comparison of polymer injectivity for both HPAM concentrations investigated in presence of residual oil is shown in Figure 9.26.

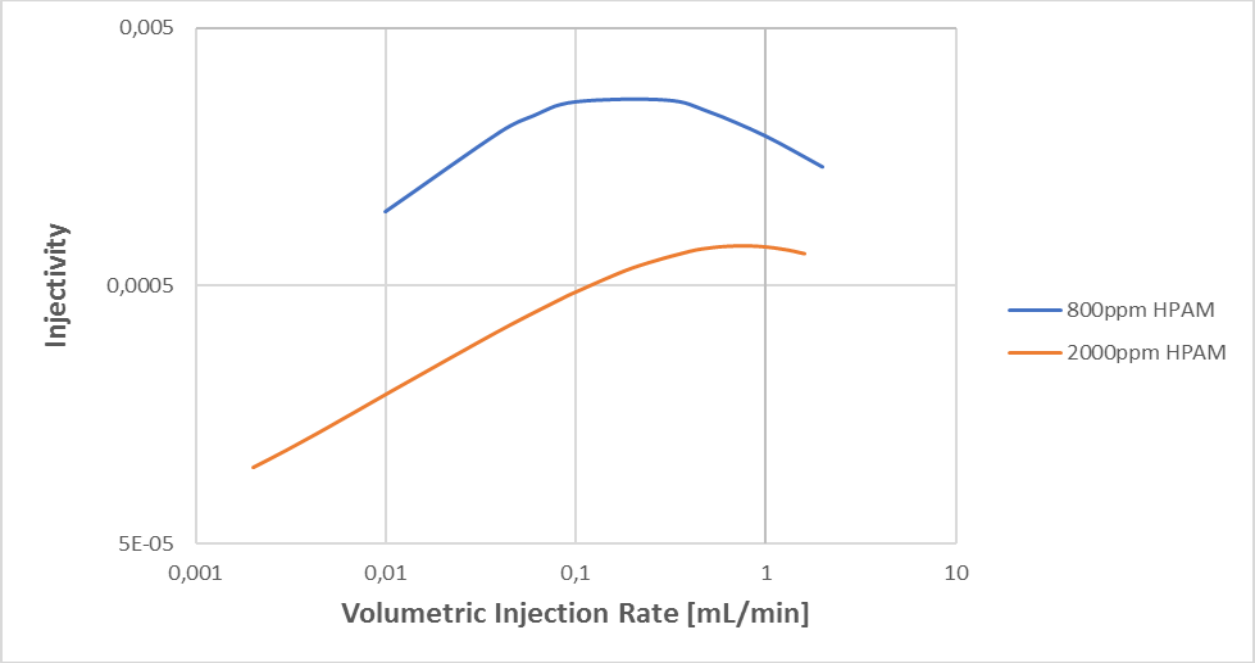

Figure 9.26: Effect of concentration on HPAM injectivity.

Effect of concentration on HPAM injectivity is to reduce injectivity with increasing polymer concentration. Since permeability only decreased by an additional 3,5% when the polymer concentration was increased, the effect of concentration on polymer injectivity was not higher than expected based on polymer rheology between the two concentrations.

The optimal injectivity for the 800ppm solution is almost a factor of four higher than the 2000ppm solution. This was expected based on their rheology curves where increasing viscosity values were observed when polymer concentration was increased. The injectivity offset between the two concentrations is at its maximum value at the lowest joint injection rate in the investigated interval, i.e. at 0,01 mL/min. Beyond this point, the injectivity offset is steadily decreasing. Injectivity of 800ppm HPAM is about a factor of 5 higher than 2000ppm HPAM at 0,01 mL/min and reaches its lowest offset at 1,0 mL/min where the ratio of 800 to 2000ppm HPAM injectivity is about 2,7. These offset values corresponds to the offset in shear thinning versus shear thickening regions discussed in chapter 1089.1.9.

The optimum injectivity values are also deviating, where 800ppm HPAM has an optimum injectivity at an injection rate of 0,3 mL/min, whereas this point is reached at 0,8 mL/min for 2000ppm HPAM in presence of residual oil.

9.2 X1 Experiment

A sequence of alternating floods, consisting of two water floods and one polymer flood serves as the basis for the X1 experiment used as a reference when 2000ppm HPAM in presence compared to absence of residual oil is investigated. A comprehensive description of the X1 experiment can be found in the article presented in chapter 6.1: Radial and Linear Polymer flow – Influence on injectivity [4]. Few differences other than presence versus absence of residual oil separates the two experiments compared in this thesis.

2000ppm HPAM flooded in both experiments are of the same polymer type (Flopaam 3630S) and composition of injection brine is identical. Also, both experiments are performed in a radial disc of Bentheimer sandstone. However, in the X4 experiment, 2000ppm HPAM was flooded after the precursor 800ppm HPAM flood, while no polymer flooding was conducted before the injection of 2000ppm HPAM in the X1 experiment.

A minor detail separating the X1 and X4 experiment is worth mentioning: In the X1 experiment, the radial disc was flooded with glycerol instead of water in the initial flood. In contrast to the X4 experiment where only one pressure transducer was placed in the injection well, 16 pressure transducers were distributed from the injection well towards the producer in the X1 experiment.

As previously mentioned, differential pressure in radial models decrease drastically from the injection well towards the circumferential outer boundary. The magnitude of differential pressures measured in the outermost pressure transducers are therefore much lower than in the injection well and may be immeasurable. Therefore, glycerol with a viscosity of 101,5 cP was used instead of water since differential pressure is proportional to viscosity and the measured pressures would be high enough to be registered. Since glycerol is a Newtonian fluid it could be used as a reference fluid of water. The differential pressure was downscaled to corresponding brine values by correcting it with the viscosity ratio between glycerol and water.

Because of the multitude of different pressure taps distributed along the propagation path of the radial disc, only two different injection rates had to be measured to estimate absolute permeability of the porous media. Since the initial glycerol flood was flooded with a Newtonian fluid, differential pressure drop as a function of volumetric injection rate is linear, and therefore an extrapolation could safely be performed to obtain the required values in the appropriate interval.

Two differential pressure measurements were reported at 2 and 5 mL/min in the injection well. Following the same procedure as for the X4 experiment, absolute permeability was

estimated at 2600mD before the 2000ppm HPAM flood. Also, the 2000ppm HPAM flood in absence of residual oil was flooded at injection rates of 2 and 5 mL/min. 2000ppm HPAM was history matched at these two injection rates and two rheology curves were obtained. These two history matched rheology curves did not cover the same flux interval as the rheology curve obtained from the 2000ppm HPAM flood in the X4 experiment. Therefore, the extended Carreau equation was utilized to extrapolate the rheology curve from X1 to the appropriate flux interval so that the rheology of 2000ppm HPAM in absence and presence of residual oil could be compared.

Figure 9.27 shows the two history matched rheology curves at 2 and 5 mL/min from the X1 experiment together with an extrapolated rheology curve obtained by employing the extended Carreau equation (equation (4.8)).

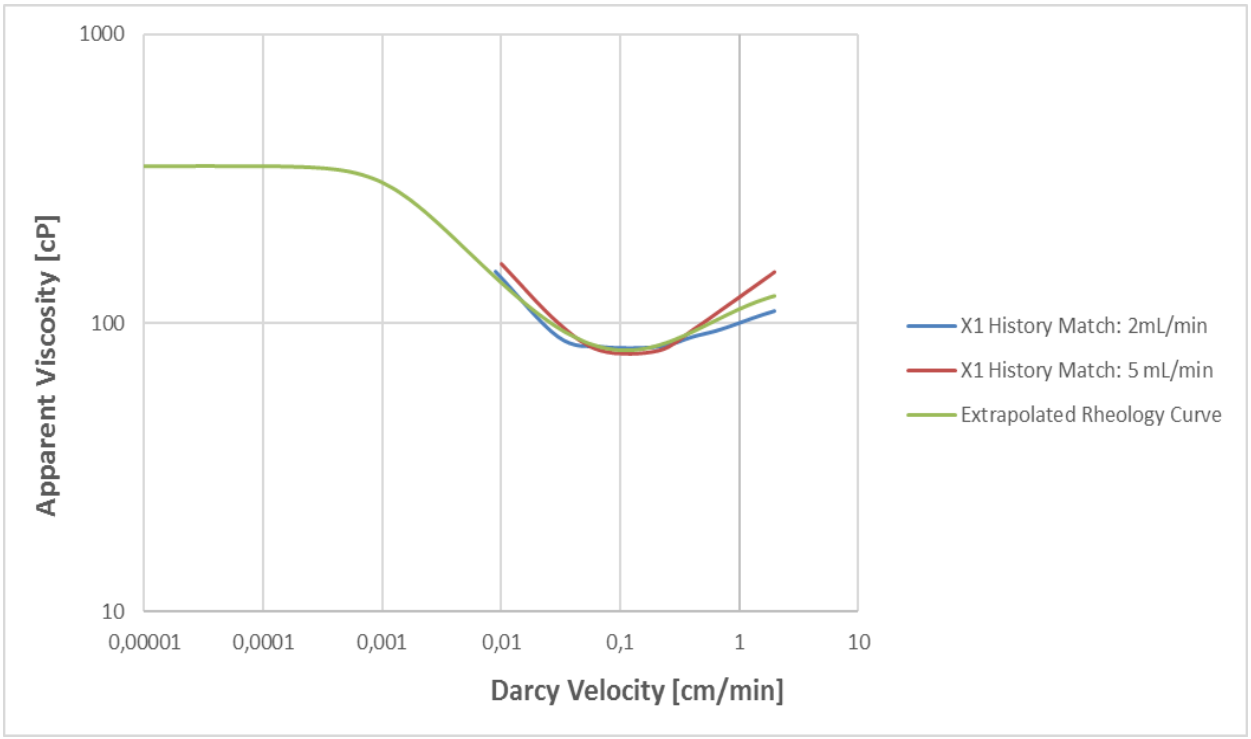

Figure 9.27: Extrapolated rheology curve from the X1 experiment using the extended Carreau equation.

The extrapolated rheology curve in Figure 9.27 is the average of the two rheology curves obtained in the X1 experiment, and should represent the approximate rheological behavior of 2000ppm HPAM in absence of residual oil. This curve will be used to compare the rheological behavior of 2000ppm HPAM in absence versus presence of residual oil. Only the part of the curve in the same velocity region as the 2000ppm HPAM curve from the X4 experiment will be utilized when the comparison is performed.

The Carreau parameters used to obtain the extrapolated rheology curve of 2000ppm HPAM in absence of residual oil is shown in Table 9.2:

Table 9.2: Carreau parameters from 2000ppm HPAM extrapolation.

μ_∞	μ_0	λ_1	n_1	μ_{max}	λ_2	n_2
1	**350**	$\mathbf{5,5 \cdot 10^6}$	**0,55**	**125**	$\mathbf{1,0 \cdot 10^4}$	**1,65**

After the 2000ppm HPAM flood in absence of residual oil, permeability was reduced from 2600 to 897 mD. This permeability reduction due to polymer retention amounts to about 65,5%.

9.3 Effect of Residual Oil on 2000ppm HPAM Rheology

Rheology curves of 2000ppm HPAM in absence and presence of residual oil are shown in Figure 9.28.

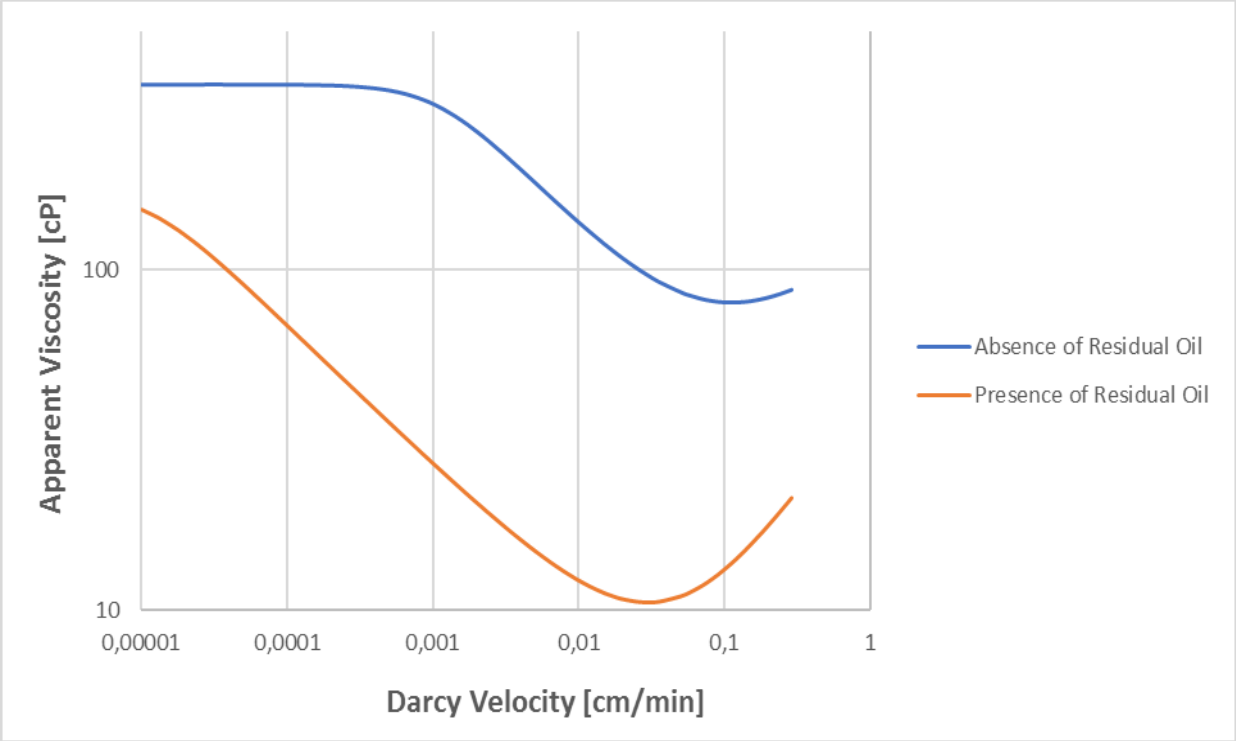

Figure 9.28: Effect of residual oil on 2000ppm HPAM rheology.

Apparent viscosity of 2000ppm HPAM in radial models in presence and absence of residual oil are significantly different in terms of shape and especially in terms of absolute viscosity values.

The apparent viscosity curve for the 2000ppm HPAM polymer in presence of residual oil shows a shear thickening region at high flux, followed by an extensive shear thinning region. However, the apparent viscosity curve for 2000ppm HPAM polymer in absence of residual oil shows a short shear thickening region followed by a steep shear thinning region before an extensive low flux Newtonian plateau is observed at intermediate-to-low flux.

The most interesting part of this comparison is the offset in absolute viscosity values. In fact, at the highest flux value, apparent viscosity of HPAM in the absence residual oil is a factor of four higher than in presence of residual oil. This difference is suggested to result from mechanical degradation of 2000ppm HPAM in presence of residual oil in contrast to 2000ppm HPAM in absence of residual oil where no significant mechanical degradation occurred. Effect of residual oil on polymer rheology may have had an effect, but since mechanical degradation occurred, this potential effect cannot be quantified.

Higher apparent viscosity values promote higher injection pressures. Since injectivity is defined as the ratio of volumetric flow rate and differential pressure, and the latter is proportional to viscosity, the isolated effect of reduced viscosity values will be to improve injectivity.

Both onset of shear thinning and shear thickening commence at lower flux values for 2000ppm HPAM in presence compared to in absence of residual oil. Effects of residual oil will be to effectively reduce the cross-sectional area of pores and thus the degree of shearing will be more extensive. Therefore, the HPAM polymer in presence of residual oil will be more influenced by shearing and polymer coils will start to align at lower flux, thus onset of shear thinning will commence at lower velocities.

Reduced cross sections resulting from a residual oil saturation will also influence onset of shear thickening. When flow channels in porous media are narrower, the extensional flow regime will be reached at lower flux and HPAM will exhibit viscoelastic behaviour at an earlier stage, thus onset of shear thickening will commence at lower flux.

Both shear thinning and shear thickening regimes of HPAM in presence of residual oil will be more extensive, while the low flux Newtonian plateau will be more extensive in absence of residual oil.

To assess the relative slope of both shear thinning and shear thickening regions of 2000ppm HPAM in presence and absence of residual oil, apparent viscosity as a function of Darcy velocity with a non-logarithmic apparent viscosity axis is shown in Figure 9.29.

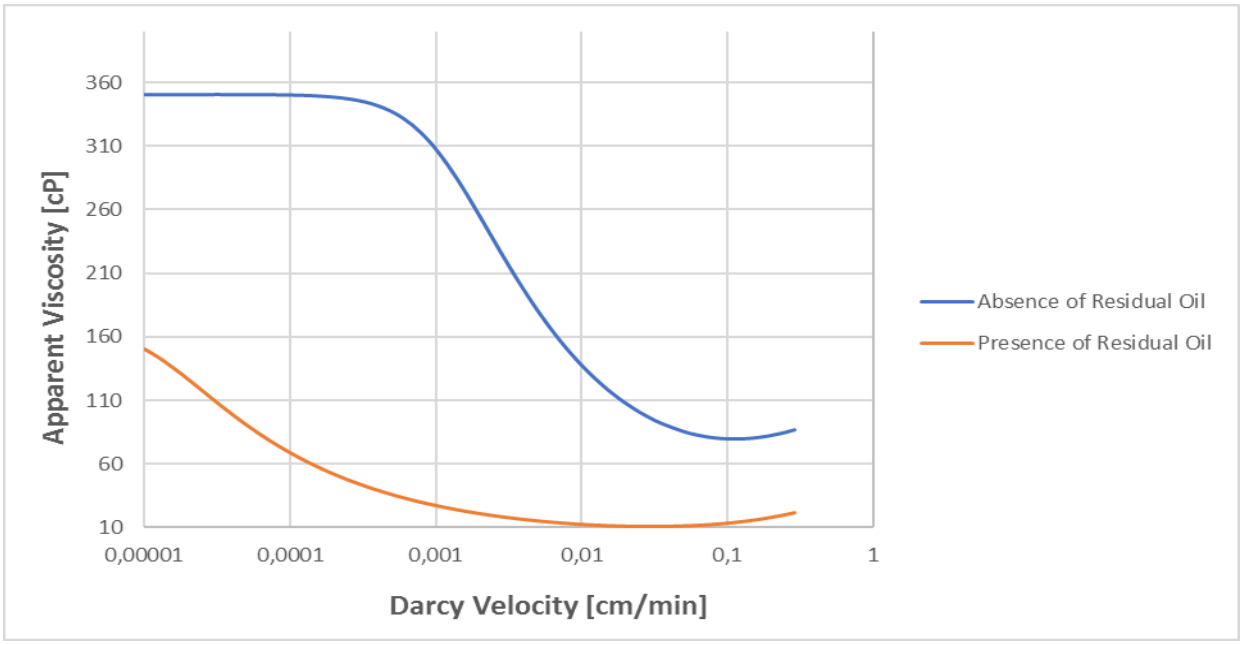

Figure 9.29: Effect of residual oil on HPAM rheology (non-logarithmic apparent viscosity axis).

It is interesting to note the offset in apparent viscosity between 2000ppm HPAM in absence and presence of residual oil in the shear thinning compared to the shear thickening regime. In the joint shear thinning regime, apparent viscosity of 2000ppm HPAM in absence of residual oil is between a factor of 10 and 12 higher than the polymer in presence of residual oil.

As previously mentioned, Seright et al. (2011) [6] attributed the shear thinning behaviour of HPAM to the high molecular weight species present in the polymer solution. Since 2000ppm HPAM in presence of residual was mechanically degraded, the degree of shear thinning is expected to be steeper for undegraded HPAM in absence of residual oil. Figure 9.29 confirms this expectation.

9.4 Effect of Residual Oil on Polymer Retention

The permeability reduction resulting from the 2000ppm HPAM flood in presence of residual oil amounted to about 3,5%. However, this was an additional permeability decrease after the 800ppm HPAM flood. It is suggested that if 2000ppm was injected after the initial water flood in the X4 experiment, the total permeability reduction would be equal to the sum of permeability reductions caused by both 800 and 2000ppm HPAM floods, i.e. the permeability reduction would be the same if both 800 and 2000pp HPAM were injected sequentially and if only 2000ppm HPAM was injected. This may be assumed because the rate and amount of retention will increase with polymer concentration [12]. Therefore, since stabilized pressure were obtained during flooding, maximum retention would be achieved and thus 2000ppm HPAM would have reached the same level of adsorption independent of precursory polymer floods of lower concentration. Therefore, a permeability reduction of 7,5% may be attributed to 2000ppm HPAM in presence of residual oil compared to 65,5% in absence of residual oil.

Permeability reductions caused by polymer flooding is attributed to polymer retention. As mentioned in chapter 4.5, three mechanisms are responsible for polymer retention during flow through porous media, and include: adsorption, mechanical entrapment and hydrodynamic retention. Since Zhang et al. (2015) concluded that almost all hydrodynamic retention is reversible and has limited effect on polymer flow behavior in porous media, hydrodynamic retention will not be included in the discussion.

Based on the conclusion of Zhang et al., retention is suggested to consist mainly of adsorption and mechanical entrapment. The permeability reduction per polymer molecule is much larger for mechanical entrapment than for polymer adsorption. As previously mentioned, mechanical entrapment may ensue as straining or concentration blocking [42]. Since straining is most likely to occur in the vicinity of the well bore region and mainly will reduce permeability by plugging pores in this region, the distribution of straining will show a peak close to the injection well and will be nearly negligible at considerate distances from the injection well if the pore size distribution is not severely heterogenous. In contrast, concentration blocking will most likely occur in both the near-well environment and deeper into the porous media. Thus, the concentration loss of polymers associated with concentration blocking is higher than the corresponding loss to straining given the same permeability reductions.

In contrast to straining and concentration blocking, adsorption will occur over the entire propagation path and thus the concentration loss associated with polymer adsorption is significantly higher than the two mechanisms of mechanical entrapment.

Which of these mechanisms is the dominating factor for the observed permeability reductions is not possible to establish because the effluent concentration was not measured. If straining was the dominating mechanism, only minor concentration loss of polymer would be observed, while permeability reductions dominated by adsorption would result in significant concentration loss of polymer.

However, it is possible based on the precursory 800ppm HPAM flood to suggest that straining was not accountable for the additional permeability reduction of 3,5% caused by the 2000ppm HPAM flood in presence of residual oil. Since both 800 and 2000ppm HPAM flood was flooded with the same polymer type, i.e. same molecular weight, straining should have been satisfied by the 800ppm HPAM polymer. This is because all pores that were too narrow for the large molecular weight polymer to penetrate was already blocked by the 800ppm HPAM polymer. In addition, since 2000ppm HPAM was mechanically degraded during flooding, a large fraction of the large molecular weights initially present in the polymer was fragmented and thus straining becomes less probable.

Therefore, it is suggested that for the 2000ppm HPAM polymer in presence of residual oil, the two dominating mechanisms of polymer retention was adsorption and mechanical entrapment in the form of concentration blocking.

Since 2000ppm HPAM in the absence of residual oil was not mechanically degraded and did not follow a precursory polymer flood, it is difficult to suggest the most likely retention mechanisms responsible for the permeability reduction observed since effluent concentrations are not available.

9.5 Effect of Residual Oil on 2000ppm HPAM Injectivity

When the implementation of a polymer flood project is considered, it is generally injectivity relative to brine which is of concern. This fact has major influence on the comparison of X1 and X4 when investigating the effect of residual oil on polymer injectivity. This is because presence of residual oil will not just hinder the flow of a polymer solution, it would have hindered the brine solution as well. Therefore, in the one-phase X1 experiment, differential pressures obtained for both brine and polymer floods will be much lower than the corresponding pressures obtained in the two-phase flow in the X4 experiment. Actually, if injectivity of 2000ppm HPAM is compared in the presence and absence of residual oil without taking into account the effects of one versus two phase flow, injectivity would be significantly reduced at residual oil saturation as depicted in Figure 9.30.

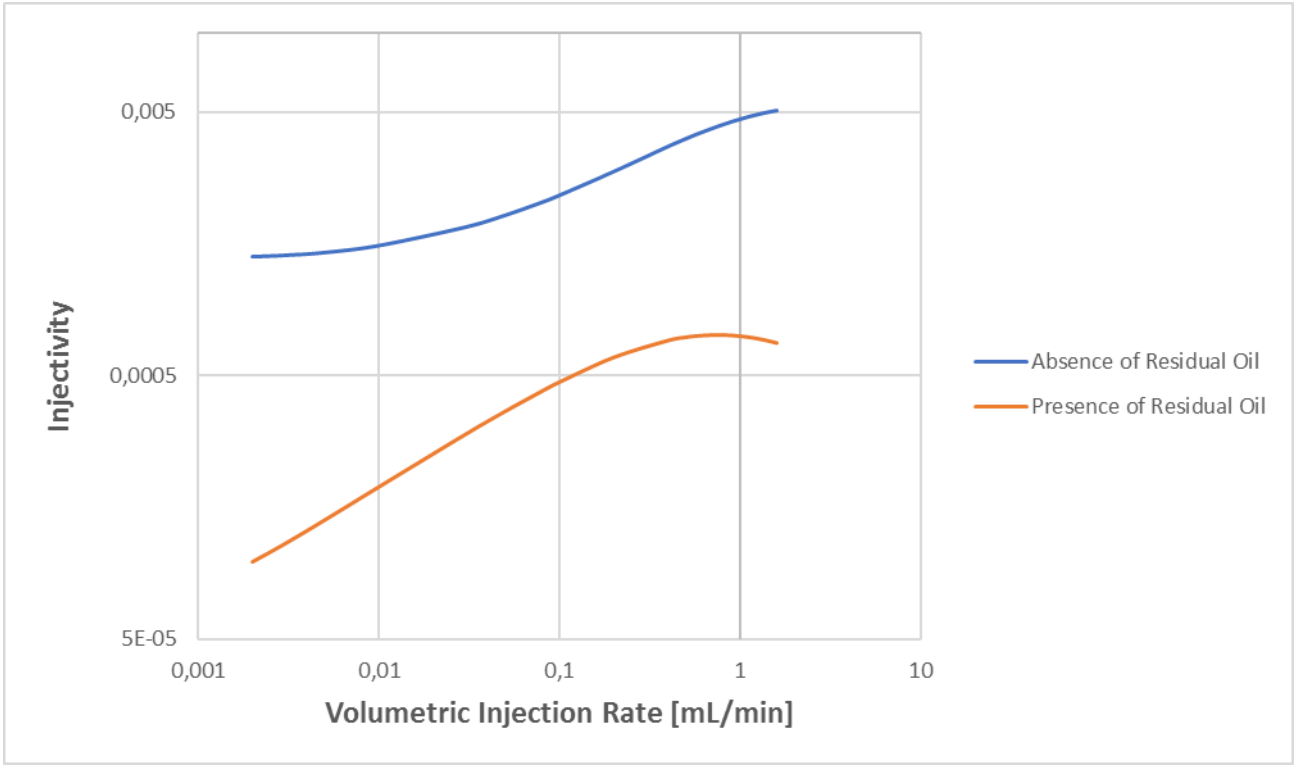

Figure 9.30: Effect of residual oil on polymer injectivity.

The offset between optimum injectivity values of HPAM in presence and absence of residual oil amounts to a factor of 5,5, which is about the lowest offset encountered in the interval of volumetric injection rates investigated.

Injectivity in absence of residual oil is about a factor of 14 higher than the corresponding injectivity observed when residual oil is present, and is the highest offset value observed in the interval of investigated velocities.

With regards to injectivity, the improved rheological properties of 2000ppm HPAM in presence of residual oil leads to an expectation of improved injectivity. However, since mobility of the injected polymer solution is greatly reduced by the presence of residual oil, the opposite is observed. Therefore, the governing factor for polymer injectivity will be two-phase permeability when the corresponding brine permeability is not considered.

However, to investigate isolated effects of residual oil on HPAM injectivity, the investigation should be performed relative to brine injectivity. Since injectivity of 2000ppm HPAM in absence of residual oil is obtained from one-phase flow in contrast to the two-phase flow conditions in presence of residual oil, injectivity will be dominated by the different flow conditions. Therefore, the brine permeabilities will accounted for by employing a definition of injectivity that consider the relative injectivity compared to brine at similar experimental conditions, i.e. equation (5.2) defined in chapter 5. The equation is repeated here for emphasis:

$$I = \frac{\Delta P_b}{\Delta P_p} = = \frac{\eta_b k_{e,p}}{\eta_p k_{e,b}} \qquad (5.2)$$

When brine injectivity is considered, i.e. the effect of residual oil on injectivity is compared and plotted as injectivity of polymer divided by brine injectivity, the result is completely altered, as shown in Figure 9.31.

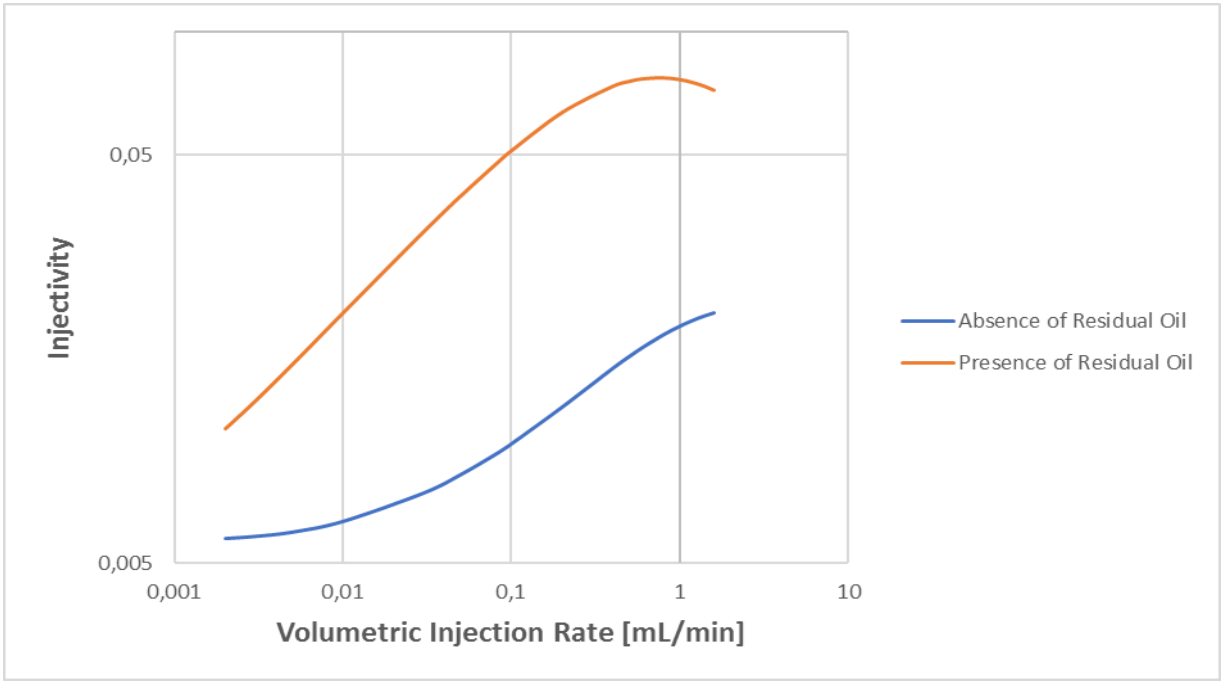

Figure 9.31: Isolated effect of residual oil on polymer injectivity.

The effect of residual oil is to increase HPAM injectivity in presence compared to absence residual oil by a factor of between 1,85 and 5,25. This is a more reasonable way to compare injectivity in polymer flooding because relative injectivities are compared and the difference between one phase versus two phase conditions between experiment X1 and X4 is deducted and thus the only difference between the two experiments is the presence versus absence of residual oil.

At the optimum injectivity value for 2000ppm HPAM in presence of residual oil (at 0,8 mL/min) injectivity is in excess of a factor of four higher than injectivity of 2000ppm HPAM in absence of residual oil.

A relevant part of the explanation to these contrasting injectivity values lies in the mechanical degradation of 2000ppm HPAM in the presence of residual oil which reduced absolute apparent viscosity values compared to the situation without residual oil. This is a result of disconnected oil ganglia in the middle of pores that hinders the flow of polymer and thus shearing becomes more prominent. The other influencing factor is the significantly larger permeability reduction in absence versus presence of residual oil caused by polymer retention. The permeability reductions caused by polymer retention in presence of residual oil was reduced by 85,5% compared to 2000ppm HPAM in absence of residual oil. This significant deviation in permeability reductions will have significant impact on injectivity.

Based on these results, injectivity is underestimated when core floods are conducted in the absence of residual oil.

Evident from equation (*5.2*), relative injectivity of polymer to brine depends on both apparent viscosity and permeability. Since 2000ppm HPAM in presence of residual oil was mechanically degraded, the effects of residual oil on apparent viscosity cannot be quantified. The increase in polymer injectivity in presence of residual oil may therefore be attributed to the significantly reduced permeability due to retention mechanisms.

9.6 Results Summary

The principal aim of this thesis was to investigate the effect of residual oil on polymer injectivity. History matches were performed, based on the X4 experiment in which a radial core plug was flooded sequentially by water and polymer to establish the permeability of the porous media and rheological properties of HPAM, respectively. These results were compared to a history matched experiment (X1) performed in absence of residual oil.

Two simulator tools were utilized when history matching the X4 experiment, STARS and MRST, and both showed quite similar results although, history matches obtained in MRST was selected as the most representative.

History match results from all water floods suggested a non-linear deviation from Newtonian behaviour in the high volumetric injection rate regime. This proved to be a misguided observation. By plotting differential pressure as a function of flow rate and omitting the values at zero flow rate, the relationship was linear in the entire rate interval investigated. The measured counter pressure was suggested to be overestimated, resulting in apparent non-Newtonian behaviour.

Permeability reductions after both polymer floods was observed even though the porous media was first flooded with a low concentration polymer. Zhang and Seright (2014) [5] reported that if a porous media was first contacted with a dilute HPAM solution that satisfied retention, no significant additional retention occurs when exposed to higher concentrations. They also reported that retention is considered to be practically instantaneous. Since retention was assumed to be instantaneous, polymer retention should have been satisfied after the 800ppm HPAM flood. Therefore, the additional retention caused by the 2000ppm HPAM flood contradicts the conclusion made by Zhang and Seright.

Mechanically undegraded 800ppm HPAM exhibited shear thinning behavior at low to intermediate flux. This shear thinning behavior was attributed to high molecular weight species. In the intermediate to high flow regime, 800ppm HPAM showed shear thickening behavior. This is also in agreement with previous literature and is attributed to the viscoelastic nature of HPAM and the elongational flow field encountered at sufficiently high flux in porous media.

2000ppm HPAM in presence of residual oil exhibited shear thinning behaviour at low to intermediate flux, whereas shear thickening was observed at high velocities. Even though no Newtonian plateau behaviour existed, apparent viscosity values levelled off when approaching lower velocities and proximity of a low velocity Newtonian plateau was suggested. Bulk

viscometric data indicated occurrence of mechanical degradation during propagation though porous media.

Bulk and in-situ viscosity was compared for the 2000ppm HPAM solution. Inconsistent with previously reported results for semi-dilute polymer solutions, in-situ viscosity was lower than bulk viscosity in the lower shear rate regime. However, an unpublished experiment conducted at the University of Bergen showed similar results. H. Færevåg (2014) investigated the same HPAM polymer as investigated in the X4 experiment (Flopaam 3630S) with the same concentration and molecular weight in similar make up brine. The experiment was conducted in a radial disc of Bentheimer sandstone, consistent with the experimental conditions of X4. The only difference between the X4 experiment and the experiment executed by H. Færevåg was the presence versus absence of residual oil.

Effect of concentration on HPAM rheology was to increase absolute viscosity values and to increase the slope of shear thinning because of increased number of high molecular weight species.

800ppm HPAM injectivity was assessed relative to brine injectivity of the precursory water flood at the same value of permeability. The optimum injectivity values were obtained at intermediate flux, whereas global and local minima value of injectivity were observed in the lower and upper velocity regime of the interval investigated.

Injectivity of 2000ppm HPAM increased with increasing flux from a global minima value at the lowest flux. An optimum injectivity was obtained at an injection rate of 0,8 mL/min followed by an injectivity decrease until a local minima value was attained.

Effect of concentration on polymer injectivity was to reduce injectivity. Since permeability only decreased by an additional 3,5% when increasing polymer concentration, polymer injectivity was not reduced more than expected based on rheology.

The X1 experiment was used as a reference to compare both rheology and injectivity in presence versus absence of residual oil. 2000ppm HPAM rheology in absence of residual oil was extrapolated using the extended Carreau equation.

Effect of residual oil on polymer rheology was to reduce absolute viscosities. However, since mechanical degradation occurred in presence of residual oil, this viscosity offset may not be attributed to presence of residual oil.

If brine permeability was not considered, polymer injectivity was reduced in the presence of residual oil. However, to investigate the isolated effects of residual oil on polymer injectivity, brine permeability must be accounted for. The relative injectivity of 2000ppm HPAM was therefore scaled with brine injectivity and compared in presence versus absence of residual. Isolated effect of residual oil was to significantly increase polymer injectivity. Since mechanical degradation occurred in presence of residual oil, the effect of residual oil is not quantifiable.

10 CONCLUSION

In this thesis, the principal aim was to investigate effects of residual oil on polymer injectivity in radial models. Also, polymer rheological behaviour in presence of residual oil was assessed. The investigations conducted were performed exclusively on the synthetic polymer partially hydrolyzed polyacrylamide (HPAM).

Consistent with previous literature, permeability reductions caused by 2000ppm HPAM in presence of residual oil exceeded corresponding values in absence of residual oil. Both Szabo (1975) [30] and Hughes et al (1990) [49] reported that retention was reduced in presence of residual oil by a few factors. However, permeability reductions caused by 2000ppm HPAM in presence compared to absence of residual oil was reduced by about 88,5%, which is far greater than previously reported in the literature.

Current literature suggests that if porous media is first contacted with a low concentration HPAM solution that satisfies retention, no significant additional retention occurs when exposed to higher concentrations. In contrast, permeability determination both before and after polymer flooding revealed that additional retention occurred when the porous media was exposed to a higher concentration solution. This observation may be attributed to the radial flow regime or presence of residual oil.

In agreement with current literature reported in absence of residual oil, mechanically undegraded 800ppm HPAM in presence of residual oil exhibits shear thinning behaviour in the lower flux regime. Mechanically degraded 2000ppm HPAM also shows extensive shear thinning at low flux. This is not in agreement with previously reported results in absence of residual oil. Presence of residual oil is suggested to be responsible for the behavioural discrepancy at low flux compared to previous literature.

In contrast to previous literature, onset of shear thickening was increased when increasing HPAM concentration from 800 to 2000ppm in presence of residual oil. However, this behaviour has been observed in radial core floods experiments performed in-house and was thus attributed to the radial flow geometry rather than prescence of residual oil.

Comparison of bulk and in-situ viscosities of 2000ppm HPAM shows higher bulk viscosity values at low shear rates and is not in agreement with previously reported results in the semi-dilute concentration regime. However, these observations validated results of H. Færevåg (2014) which investigated the same polymer type (Flopaam 3630S) at similar experimental

conditions although, in absence of residual oil. The principal deviation in experimental conditions between previous reported results and the results obtained by H. Færevåg, is the linear versus radial flow geometry. Therefore, it is suggested that this discrepancy may be attributed to differing flow conditions.

Effect of concentration on HPAM injectivity was to reduce injectivity when increasing the polymer concentration. Since permeability only decreased by an additional 3,5% when the polymer concentration was increased, the effect of concentration on polymer injectivity was not higher than expected based on polymer rheology.

A comparison of rheology curves of 2000ppm HPAM in presence versus absence of residual oil shows that absolute viscosity is reduced in presence of residual oil. This viscosity difference is suggested to result from mechanical degradation of 2000ppm HPAM in presence of residual oil in contrast to 2000ppm HPAM in absence of residual oil where no significant mechanical degradation occurred. The effect of residual oil on polymer rheology may have had an effect, but since mechanical degradation occurred this potential effect cannot be quantified.

Residual oil influenced both onset of shear thickening and shear thinning of 2000ppm HPAM. Onset of shear thinning commence at lower flux in presence of residual. The effect of residual oil is to effectively reduce the cross-sectional area of pores and thus the degree of shearing will be more extensive. Therefore, the HPAM polymer in presence of residual oil will be more influenced by shearing and the polymer coils will start to align at a lower flux, thus the onset of shear thinning will commence at lower velocities. Since the effect of residual oil will be to reduce cross section in the pores, flow channels in the porous media are narrower and the extensional flow regime will be reached at lower flux and thus HPAM will exhibit viscoelastic behaviour at an earlier stage, thus onset of shear thickening will be reduced.

Permeability reductions during polymer flooding was severely enhanced in absence compared to presence of residual oil. The permeability reduction decreased by 85,5% in presence compared to absence of residual oil. Since effluent concentrations were not measured, it was not possible to determine the dominant retention mechanism. If polymer adsorption was the main contributor to the observed permeability reductions in absence of residual oil, significant amounts of polymer loss will be avoided when flooding in presence of residual oil. Since polymer retention is a huge expenditure in polymer flooding, reduced retention and thus lower costs associated with polymer loss may improve the economics of polymer flood projects and may render some previously deemed uneconomic, economically feasible.

When the effects of residual oil on injectivity was investigated without considering the effects of different flow conditions, injectivity was reduced in presence of residual oil. However, when considering the implementation of a polymer floods project, it is the relative decrease or increase in injectivity relative to brine injection that is of concern. Injectivity was therefore assessed by investigating the isolated effects of residual oil.

Results shows that polymer injectivity is significantly increased in presence of residual oil. Over the entire injection rate interval investigated, injectivity was increased by a factor of about 1,85 at the lowest injection rate encountered and a maximum factor of 5 at the highest volumetric injection rate.

Based on these results, it is suggested that injectivity may be underestimated when core floods are conducted in absence of residual oil. Since 2000ppm HPAM in presence of residual oil was mechanically degraded, the effects of residual oil on rheology cannot be quantified. The increase in polymer injectivity in presence of residual oil may therefore be attributed to the significantly reduced permeability due to retention mechanisms.

11 FURTHER WORK

Polymer rheology and corresponding injectivities are not fully understood in radial models and especially the effects of residual oil should be focused on in future studies. Some suggestions to further work are presented in this section.

Since mechanical degradation of 2000ppm HPAM occurred in presence of residual oil, effects of residual oil on polymer rheology could not be established quantitatively. Therefore, an interesting next step would be to investigate the effects of residual oil on polymer injectivity in absence of mechanical degradation. This may be achieved by utilizing lower molecular weight polymers less prone to mechanical degradation.

Influence of residual oil on polymer retention should also be investigated further. Since effluent concentration was not measured during the experiments history matched in this thesis, the dominating mechanism of the observed permeability reductions and thus retention mechanisms were not quantifiable. Since permeability reductions in presence compared to absence of residual oil was estimated at 88,5%, the economic implications for polymer flood project economics if the responsible mechanism was adsorption would be immense.

Due to several contrasting results performed in radial models compared with current literature based on linear models, effects of radial versus linear flow could be investigated further. Since the effects of concentration on onset of shear thickening in radial models is observed to be the opposite of what is reported from linear models, the discrepancy should be investigated and the responsible mechanisms quantified.

Finally, it may be beneficial to separate the effects of radial flow versus influence of residual oil on polymer retention. Current literature suggests that if porous media is first contacted with a low concentration HPAM solution that satisfies retention, no significant additional retention occurs when exposed to higher concentrations [5]. In contrast, permeability determination both before and after polymer flooding revealed that additional retention occurred when the porous media was exposed to a higher concentration solution. It would be interesting to investigate whether this observation may be attributable to the radial flow regime or presence of residual oil.

12 REFERENCES

1. Gao, C.H., *Advances of Polymer Flood in Heavy Oil Recovery*. 2011, Society of Petroleum Engineers.
2. Gao, C., J. Shi, and F. Zhao, *Successful polymer flooding and surfactant-polymer flooding projects at Shengli Oilfield from 1992 to 2012.* Journal of Petroleum Exploration and Production Technology, 2014. **4**(1): p. 1-8.
3. Sheng, J.J., B. Leonhardt, and N. Azri, *Status of Polymer-Flooding Technology.* 2015.
4. Yerramilli, S.S., P.L.J. Zitha, and R.C. Yerramilli, *Novel Insight into Polymer Injectivity for Polymer Flooding*. 2013, Society of Petroleum Engineers.
5. Zhang, G. and R. Seright, *Effect of Concentration on HPAM Retention in Porous Media.* 2014.
6. Seright, R.S., et al., *New Insights into Polymer Rheology in Porous Media*. 2010, Society of Petroleum Engineers.
7. Skauge, T., et al., *Radial and Linear Polymer Flow - Influence on Injectivity*. 2016, Society of Petroleum Engineers.
8. Muggeridge, A., et al., *Recovery rates, enhanced oil recovery and technological limits.* Philosophical Transactions of the Royal Society A: Mathematical, Physical and Engineering Sciences, 2014. **372**(2006).
9. Teigland, R. and J. Kleppe, *EOR Survey in the North Sea*. 2006, Society of Petroleum Engineers.
10. Skarestad, M. and A. Skauge, *PTEK213 Reservoarteknikk II*. 2014, Bergen: University of Bergen. 220 p.
11. Jewett, R.L. and G.F. Schurz, *Polymer Flooding-A Current Appraisal.* 1970.
12. Sorbie, K., *Polymer-Improved Oil Recovery* 1991, Glasgow: Blackie CRC Press. 359 p.
13. Seright, R.S., *The Effects of Mechanical Degradation and Viscoelastic Behavior on Injectivity of Polyacrylamide Solutions.* 1983.
14. Glasbergen, G., et al., *Injectivity Loss in Polymer Floods: Causes, Preventions and Mitigations*. 2015, Society of Petroleum Engineers.
15. Thomas, A., N. Gaillard, and C. Favero, *Some Key Features to Consider When Studying Acrylamide-Based Polymers for Chemical Enhanced Oil Recovery.* Oil Gas Sci. Technol. – Rev. IFP Energies nouvelles, 2012. **67**(6): p. 887-902.
16. Green, D. and G. Willhite, *Enhanced Oil Recovery*. 1988: Society of Petroleum Engineers.
17. Zolotukhin, A. and J. Ursin, *Introduction to Petroleum Reservoir Engineering*. 2000: Høyskoleforlaget. 407 p.
18. Donaldson, E.C., G.V. Chilingarian, and T.F. Yen, *Enhanced Oil Recovery, II: Processes and Operations*. 1989: Elsevier Science. 603 p.
19. Tarek, A., *Reservoir Engineering Handbook (2nd Edition)*. 2001: Elsevier Science. 1454 p.
20. Donaldson, E.C., R.D. Thomas, and P.B. Lorenz, *Wettability Determination and Its Effect on Recovery Efficiency.* 1969.
21. Wang, D., et al., *Viscous-Elastic Polymer Can Increase Microscale Displacement Efficiency in Cores*. 2000, Society of Petroleum Engineers.
22. Lien, J., *PTEK211 Grunnleggende Reservoarfysikk*. 2004, Institutt for fysikk of teknologi: University of Bergen. 76 p.
23. Lake, L., *Fundementals of Enhanced Oil Recovery*. 2014: Society of Petroleum Engineers.

24. Chauveteau, G. and A. Zaitoun. *Basic rheological behavior of xanthan polysaccharide solutions in porous media: Effect of pore size and polymer concentration*. in *Proceedings of the First European Symposium on Enhanced Oil Recovery, Bournemouth, England, Society of Petroleum Engineers, Richardson, TX*. 1981.
25. Chauveteau, G., *Rodlike Polymer Solution Flow through Fine Pores: Influence of Pore Size on Rheological Behavior.* Journal of Rheology, 1982. **26**(2): p. 111-142.
26. Chauveteau, G., *Fundamental Criteria in Polymer Flow Through Porous Media*, in *Water-Soluble Polymers*. 1986, American Chemical Society. p. 227-267.
27. Chauveteau, G., M. Tirrell, and A. Omari, *Concentration dependence of the effective viscosity of polymer solutions in small pores with repulsive or attractive walls.* Journal of Colloid and Interface Science, 1984. **100**(1): p. 41-54.
28. Cannella, W.J., C. Huh, and R.S. Seright, *Prediction of Xanthan Rheology in Porous Media*. 1988, Society of Petroleum Engineers.
29. Zamani, N., et al., *Effect of porous media properties on the onset of polymer extensional viscosity.* Journal of Petroleum Science and Engineering, 2015. **133**: p. 483-495.
30. Carreau, P.J., *Rheological Equations from Molecular Network Theories.* Transactions of the Society of Rheology, 1972. **16**(1): p. 99-127.
31. Bird, R., R. Armstrong, and O. Hassanger, *Dynamics of Polymeric Liquids: Fluid Mechanics*. 1987, Chichester, UK: John Wiley & Sons. 672 p.
32. Delshad, M., et al., *Mechanistic Interpretation and Utilization of Viscoelastic Behavior of Polymer Solutions for Improved Polymer-Flood Efficiency*. 2008, Society of Petroleum Engineers.
33. Heemskerk, J., et al., *Quantification of Viscoelastic Effects of Polyacrylamide Solutions*. 1984, Society of Petroleum Engineers.
34. Szabo, M.T., *Some Aspects of Polymer Retention in Porous Media Using a C14-Tagged Hydrolyzed Polyacrylamide.* 1975.
35. Skauge, T., O. Kvilhaug, and A. Skauge. *Influence of Polymer Structural Conformation and Phase Behaviour on In-situ Viscosity*. in *IOR 2015-18th European Symposium on Improved Oil Recovery*. 2015.
36. Maerker, J.M., *Shear Degradation of Partially Hydrolyzed Polyacrylamide Solutions.* 1975.
37. Maerker, J.M., *Mechanical Degradation of Partially Hydrolyzed Polyacrylamide Solutions in Unconsolidated Porous Media.* 1976.
38. Seright, R., et al., *Rheology and mechanical degradation of EOR polymers.* SPE/British Society of Rheology Conference on Rheology in Crude Oil Production: London, UK, 1983.
39. Vela, S., D.W. Peaceman, and E.I. Sandvik, *Evaluation of Polymer Flooding in a Layered Reservoir With Crossflow, Retention, and Degradation.* 1976.
40. Gogarty, W.B., *Mobility Control With Polymer Solutions.* 1967.
41. Hughes, D.S., et al., *Appraisal of the Use of Polymer Injection To Suppress Aquifer Influx and To Improve Volumetric Sweep in a Viscous Oil Reservoir.* 1990.
42. Bolandtaba, S.F. and A. Skauge, *Network Modeling of EOR Processes: A Combined Invasion Percolation and Dynamic Model for Mobilization of Trapped Oil.* Transport in Porous Media, 2011. **89**(3): p. 357-382.
43. Marker, J.M., *Dependence of Polymer Retention on Flow Rate.* 1973.
44. Zhang, G. and R.S. Seright, *Hydrodynamic Retention and Rheology of EOR Polymers in Porous Media*. 2015, Society of Petroleum Engineers.
45. Pye, D.J., *Improved Secondary Recovery by Control of Water Mobility.* 1964.

46. Xie, D., et al., *Application of Organic Alkali for Heavy-Oil Enhanced Oil Recovery (EOR), in Comparison with Inorganic Alkali.* Energy & Fuels, 2016. **30**(6): p. 4583-4595.
47. Floerger, S. *FLOPAAM For Enhanced Oil Recovery*. Available from: http://snf.com.au/downloads/Flopaam_EOR_E.pdf.
48. Zaitoun, A., et al., *Shear Stability of EOR Polymers.* 2012.
49. de Gennes, P., *Scaling Concepts in Polymer Physics*. 1979: Cornell University Press. 324 p.
50. Ying, Q. and B. Chu, *Overlap concentration of macromolecules in solution.* Macromolecules, 1987. **20**(2): p. 362-366.
51. Smith, F.W., *The Behavior of Partially Hydrolyzed Polyacrylamide Solutions in Porous Media.* 1970.
52. Lee, K., C. Huh, and M.M. Sharma, *Impact of Fractures Growth on Well Injectivity and Reservoir Sweep during Waterflood and Chemical EOR Processes*. 2011, Society of Petroleum Engineers.
53. Skauge, A., et al., *2-D Visualisation of Unstable Waterflood and Polymer Flood for Displacement of Heavy Oil*. 2012, Society of Petroleum Engineers.
54. Ltd, C.M.G., *STARS User Guide - Advanced Process & Thermal Reservoir Simulator*. 2016, Calgary, Alberta, Canada: CMG.
55. Evensen, G., *The Ensemble Kalman Filter: theoretical formulation and practical implementation.* Ocean Dynamics, 2003. **53**(4): p. 343-367.
56. Færevåg, H., *Experimental Study of Polymer Rheology in Radial Models*, in *Department of Physics and Technology*. 2014, University of Bergen: Bergen. p. 171.

APPENDIX: STARS DATA FILES AND PARAMETERS

The STARS data files utilized for the initial water flood and 800ppm HPAM flood parts of the X4 experiment are shown in this appendix. While the initial water flood data file can be used to history match all water floods in the X4 experiment with appropriate changes, the same can be done for both polymer floods using the 800ppm HPAM flood data file.

Initial Water Flood Data File

```
** Radial lab model with one well in the middle

** Geometry 30cm diameter and 2.205 cm thickness

** Injection well 0,3 cm thick

** 2016-12-07, 15:06:31, Jørgen

** 2016-12-07, 15:19:55, Jørgen

RESULTS SIMULATOR STARS 201410

** ============== INPUT/OUTPUT CONTROL ========================

TITLE1 'Radial 2-Phase Model'

TITLE2 'Polymer Injection HPAM 800ppm and 2000ppm'

INUNIT      LAB

OUTUNIT LAB

SHEAREFFEC SHV

WPRN        GRID TIME

OUTPRN      GRID PRES SW W X VISW

OUTPRN      WELL ALL

WPRN        ITER TIME

OUTPRN      ITER NEWTON

WSRF        WELL 1
```

```
WSRF           GRID TIME

**WSRF         SECTOR 1

**Limits what well data, grid data and reservoir data are printed

OUTSRF GRID MASS ADSORP MOLE ADSORP PPM ADSPCMP KRO KRW KRW
MASDENW MOLDENW PRES RFW SHEARW

          SW VISCVELW VISW W X Y

OUTSRF WELL MOLE COMPONENT ALL

**OUTSRF SPECIAL

**$  Distance units: cm

**RESULTS XOFFSET          0.0000

**RESULTS YOFFSET          0.0000

**RESULTS ROTATION          0.0000  **$  (DEGREES)

**RESULTS AXES-DIRECTIONS 1.0 -1.0 1.0

** ========= RESERVOIR DESCRIPTION ================================

GRID  RADIAL        148 1 1          RW 0.30

KDIR  DOWN

DI       IVAR 147*0.1 0.3

DJ       CON 360

DK       CON 2.205

DTOP 148*1

NULL CON 1

POR ALL

 147*0.228  0.99

PERMI ALL

147*870 1000000
```

PERMJ EQUALSI

PERMK EQUALSI

** 0 = pinched block, 1 = active block

PINCHOUTARRAY CON 1 **Defines pinch outs using an array input format

END-GRID

** ============= COMPONENT PROPERTIES ============================

MODEL 3 3 3 2

COMPNAME 'Water' 'Polymer' 'Res_Oil' **Name of components in system

CMM

0.018 8 0.456

PCRIT

0 0 0

TCRIT

0 0 0

PRSR 101

PSURF 101

MASSDEN

0.001 0.001 0.001

CP

0 0 0

AVISC

0.96 32.6 250

VSMIXCOMP 'Polymer'

VSMIXENDP 0 4.5089977e-006

VSMIXFUNC 0 0.1 0.2 0.3 0.4 0.5 0.6 0.7 0.8 0.9 1

** Use the following keywords for a smooth shear effect that fits the data in SHEARTAB:
SHEARTHIN 0.97285 4.535e-008

**Shear velocity **Viscosity

SHEARTAB

** ================ ROCK-FLUID PROPERTIES ======================

ROCKFLUID

**RPT = Rock type number

RPT 1 WATWET

** Sw krw krow

SWT

0 0 1

0.78 0.0500000 0

ADSCOMP 'Polymer' WATER **ADSCOMP = Adsorbing component

ADSPHBLK W **

ADSTABLE

** Mole Fraction Adsorbed moles per unit pore volume

** Mole Fraction Adsorbed moles per unit pore volume

0 0

4.508997705e-006 9.969376504e-008

ADMAXT 9.96938e-008

ADRT 2.49234e-009

PORFT 1

RRFT 1

** ============== INITIALIZATION ================================

```
INITIAL

VERTICAL OFF

INITREGION 1

PRES  CON 101.1

TEMP CON 22

SW CON 0.78

SO CON 0.22

MFRAC_WAT 'Water' CON           1

** ============  NUMERICAL CONTROL ================================

NUMERICAL

TFORM ZT

ISOTHERMAL

MAXSTEPS 50000

RUN

** ============  RECURRENT DATA  ==================================

TIME 0

DTWELL 1e-4

DTMIN 1e-8

DTMAX 0.1

WELL 'Injector'

**INCOMP  WATER  0.999995491  4.5089977e-006  0.0

INJECTOR MOBWEIGHT EXPLICIT 'Injector'

INCOMP  WATER  1.0  0.0  0.0

TINJW  22.0
```

```
PINJW  101.1
OPERATE  MAX  STW  6.0  CONT REPEAT
**          rad  geofac  wfrac  skin
GEOMETRY  K  0.30  0.2    1.0    0.0
     PERF       GEO  'Injector'
** UBA             ff          Status  Connection
   1 1 1         1.0  OPEN    FLOW-FROM  'SURFACE'
WELL  'Producer1'
PRODUCER 'Producer1'
OPERATE  MIN  BHP  101.1  CONT REPEAT
**          rad   geofac  wfrac  skin
GEOMETRY  K  0.075  0.2    1.0    0.0
     PERF       GEO  'Producer1'
**    UBA         ff   Status    Connection
   148 1 1       1.0  OPEN    FLOW-TO  'SURFACE'
TIME 2
TIME 5
TIME 10
**DTMAX 1
TIME 20
TIME 40
TIME 60
**WSRF         GRID 1
TIME 80
```

```
WELL 'Injector'
INJECTOR MOBWEIGHT EXPLICIT 'Injector'
INCOMP  WATER  1.0  0.0  0.0
OPERATE  MAX  STW  4.0  CONT REPEAT
TIME 100
TIME 120
TIME 140
TIME 160
TIME 180
WELL 'Injector'
INJECTOR MOBWEIGHT EXPLICIT 'Injector'
INCOMP  WATER  1.0  0.0  0.0
OPERATE  MAX  STW  2.0  CONT REPEAT
TIME 200
TIME 220
TIME 240
TIME 260
TIME 280
WELL 'Injector'
INJECTOR MOBWEIGHT EXPLICIT 'Injector'
INCOMP  WATER  1.0  0.0  0.0
OPERATE  MAX  STW  1.0  CONT REPEAT
TIME 300
TIME 320
```

TIME 340

TIME 360

TIME 380

STOP

800ppm HPAM Flood Data File

**========== INPUT/OUTPUT CONTROL ========================

TITLE1 'Radial 2-Phase Model'

TITLE2 'Polymer Injection HPAM 800ppm and 2000ppm'

INUNIT LAB

OUTUNIT LAB

SHEAREFFEC SHV

WPRN GRID TIME

OUTPRN GRID PRES SW W X VISW

OUTPRN WELL ALL

WPRN ITER TIME

OUTPRN ITER NEWTON

WSRF WELL 1

WSRF GRID TIME

**WSRF SECTOR 1

OUTSRF GRID MASS ADSORP MOLE ADSORP PPM ADSPCMP KRO KRW MASDENW MOLDENW PRES RFW SHEARW SW VISCVELW VISW W X Y

OUTSRF WELL MOLE COMPONENT ALL

**OUTSRF SPECIAL

**$ Distance units: cm

**RESULTS XOFFSET 0.0000

**RESULTS YOFFSET 0.0000

**RESULTS ROTATION 0.0000 **$ (DEGREES)

**RESULTS AXES-DIRECTIONS 1.0 -1.0 1.0

** ========= RESERVOIR DESCRIPTION============================

```
GRID  RADIAL       148 1 1          RW 0.30
KDIR  DOWN
DI       IVAR 147*0.1 0.3
DJ       CON 360
DK       CON 2.2
DTOP 148*1
NULL CON 1
POR ALL
147*0.218  0.99
PERMI ALL
147*870 1000000
PERMJ EQUALSI
PERMK EQUALSI
**  0 = pinched block, 1 = active block
PINCHOUTARRAY CON   1
END-GRID
** ================== COMPONENT PROPERTIES=======================
MODEL 3 3 3 2
COMPNAME 'Water' 'Polymer' 'Res_Oil'
CMM
0.018 8 0.456
PCRIT
0 0 0
TCRIT
0 0 0
PRSR 101
PSURF 101
MASSDEN
0.001 0.001 0.001
CP
0 0 0
AVISC
```

0.96 3.15 250

VSMIXCOMP 'Polymer'

VSMIXENDP 0 1.8e-006

VSMIXFUNC 0 0.1 0.2 0.3 0.4 0.5 0.6 0.7 0.8 0.9 1

	**Darcy velocity	**Apparent Viscosity
SHEARTAB	0.0095	3.15
	0.01	3.18
	0.012	3.3
	0.014	3.4
	0.016	3.49
	0.018	3.59
	0.02	3.7
	0.025	3.95
	0.03	4.2
	0.035	4.45
	0.04	4.7
	0.045	4.95
	0.05	5.2
	0.055	5.45
	0.06	5.7
	0.065	5.9
	0.07	6.1
	0.075	6.3
	0.08	6.5
	0.085	6.7
	0.09	6.85
	0.1	7.15
	0.12	7.7
	0.14	8.2
	0.16	8.6
	0.18	9
	0.2	9.4

```
                0.24                9.95
                0.28                10.5
                0.32                10.9
                0.36                11.3
** ================= ROCK-FLUID PROPERTIES ========================
ROCKFLUID
RPT 1 WATWET
SWT
**      Sw              krw             krow
        0               0               1
        0.78            0.0500000       0
ADSCOMP 'Polymer' WATER
ADSPHBLK W
ADSTABLE
**      Mole Fraction   Adsorbed moles per unit pore volume
**      Mole Fraction   Adsorbed moles per unit pore volume
          0                             0
        1.8e-006                1.656273168e-008
ADMAXT 1.656273168e-008
ADRT 1.656273168e-008
PORFT 1
RRFT 1
** ============== INITIALIZATION ================================
INITIAL
VERTICAL OFF
INITREGION 1
PRES  CON 101.1
TEMP CON 22
SW CON 0.78
SO CON 0.22
MFRAC_WAT 'Water' CON           1
** ============  NUMERICAL CONTROL ================================
```

```
NUMERICAL
TFORM ZT
ISOTHERMAL
MAXSTEPS 500000
RUN
** ============  RECURRENT DATA  ================================
TIME 0
DTWELL 1e-4
DTMIN 1e-8
DTMAX 0.1
WELL 'Injector'
INJECTOR MOBWEIGHT EXPLICIT 'Injector'
INCOMP  WATER  0.9999982  1.8e-006  0.0
TINJW  22.0
PINJW  101.1
OPERATE  MAX  STW  2.0  CONT REPEAT
**          rad  geofac  wfrac  skin
GEOMETRY  K  0.30  0.2    1.0    0.0
     PERF       GEO  'Injector'
** UBA             ff          Status  Connection
   1 1 1         1.0  OPEN    FLOW-FROM  'SURFACE'
WELL  'Producer1'
PRODUCER 'Producer1'
OPERATE  MIN  BHP  101.1  CONT REPEAT     **BHP = Bottom hole pressure
**          rad   geofac  wfrac  skin
GEOMETRY  K  0.075  0.2    1.0    0.0
     PERF       GEO  'Producer1'
**    UBA         ff   Status    Connection
   148 1 1       1.0  OPEN    FLOW-TO  'SURFACE'
TIME 2
TIME 5
TIME 10
```

**DTMAX 10

TIME 20

TIME 40

TIME 60

**WSRF GRID 1

TIME 80

TIME 100

TIME 200

TIME 300

TIME 400

TIME 500

TIME 1000

TIME 1500

TIME 2000

TIME 2500

TIME 3000

TIME 3500

TIME 4000

TIME 4500

TIME 5000

TIME 5500

TIME 6000

TIME 6500

TIME 7000

TIME 7500

TIME 8000

TIME 8500

TIME 9000

TIME 9500

TIME 10000

TIME 10500

TIME 11000

TIME 11500

TIME 12000

TIME 12500

TIME 13000

TIME 13500

TIME 14000

TIME 14500

TIME 15000

TIME 15500

TIME 16000

TIME 16500

TIME 17000

TIME 17500

TIME 18000

TIME 18500

TIME 19000

TIME 19500

TIME 20000

STOP

STARS Data File

A STARS data file can contain a maximum of nine different data groups in the keyword input system, whereas these groups must follow a specific input order [47]:

- Input/Output Control
- Reservoir Description
- Other Reservoir Properties
- Component Properties
- Rock-fluid Data
- Initial Conditions
- Numerical Methods Control
- Geomechanical Model
- Well and Recurrent Data

Each keyword in the data file belongs to a specific group, and cannot appear in other groups, unless it is specifically indicated.

STARS General Flooding Parameters

Several parameters in the STARS data file had to be specified in order to history match the sequence of water and polymer floods performed in the X4 experiment.

The specified input and output units was defined in the data file by the keywords INUNIT and OUTUNIT, where lab units were chosen. In order to define the porous media grid blocks, the keywords GRID, KDIR, DI, DJ, DK, DTOP was specified. The radius of the injection well was assigned by specifying RW, which followed directly after grid blocks in the data file. The porosity and permeability corresponding to the various blocks was assigned by using the POR ALL and PERM ALL keywords. To mark the end of the radial disc, i.e. the production well, porosity and permeability was set equal to 0,99 and 1000000, respectively, in the last grid block at the rim of the disc.

The molecular weight of the species involved also had to be specified by the CMM keyword. Brine viscosity was assigned in the AVISC keyword. Only endpoint relative permeability values were assigned in the data file since the history matches were performed at constant saturation, and is identified as SWT in the Rock-fluid data group.

Initial conditions such as pressure, temperature, initial water and oil saturation was defined by using the PRES, TEMP, SW and SO keywords, respectively.

The timestep size of individual iterations were selected by specifying DTWELL, DTMIN and DTMAX, whereas DTWELL is the first timestep used, DTMIN is the smallest allowed timestep and DTMAX is the maximum allowed timestep size. To ensure that the duration of the simulation corresponded to the duration specified, MAXSTEPS, which specifies the maximum allowed timestep number, had to be specified a higher value than the product of DTMAX and the simulation duration. If not, the simulation will not run to completion.

Injected species by mole fractions was specified by the INCOMP keyword and the injection pressure and injection temperature was determined using the keywords PINJW and TINJW, respectively.

The volumetric injection rate was specified by the keywords OPERATE MAX STW (injection rate) CONT REPEAT.

The last part of the data file consists of the timesteps saved for investigation of simulation results and the last time specified is the simulation lifetime, i.e. the duration of the simulation performed by STARS.

STARS Polymer Flooding Parameters

In addition to the parameters specified in general, and that would suffice for the water floods, several additional parameters had to be specified when simulating a polymer flood. These include:

- MODEL: Specifies the number of components in the model and consist of four entries, e.g. as in the data file submitted: MODEL 3 3 3 2. The first entry corresponds to the total number of components included in the model, and may consist of both fluids and rocks. The second entry is the total number of fluid components (water, oil, gas). The third entry is equal to the total number of components in only the water and oil phases, and the last entry is the total number of components in the water phase.
- COMPNAME: This keyword is followed by the name of the components in the system, where the order of components must be specified in a specific sequence: Components in water phase, components in oil phase, components in gas phase and rock type components, respectively.

- VSMIXCOMP, VSMIXENDP and VSMIXFUNC denotes the solute component, i.e. polymer when mixed with water to form a polymer solution, the lower and upper mole fraction of polymer being mixed with water and the linear or non-linear mixing rule of the polymer solution, respectively.
- SHEARTAB and SHEAREFFEC: While SHEARTAB specifies the polymer viscosity as a function of either shear rate or Darcy velocity, SHEAREFFEC specifies which of the two former parameters that is chosen. In the polymer floods performed in this thesis, the SHEAREFFEC SHV option was selected, indicating Darcy velocity dependent viscosities.
- ADSCOMP: Specifies the adsorbing component, chosen among the components specified in COMPNAME.
- ADSTABLE: Consists of the upper and lower mole fractions and corresponding adsorption values, where the relationship between polymer concentration and adsorption is linear.
- ADMAXT: Is the maximum adsorption capacity of the polymer.
- ADRT: Specifies the level of residual adsorption, and where ADRT equal to zero indicates completely reversible adsorption and completely irreversible adsorption corresponds to a ADRT value equal to ADMAXT. All ADRT values chosen in the range between zero and ADMAXT corresponds to partially reversible adsorption.
- PORFT: Denotes the accessible pore volume of the system. An IPV value of zero corresponds to PORFT being equal to unity, and a PORFT value of zero corresponds to IPV being equal to one.
- RRFT: Specifies the residual resistance factor for the adsorbing component.
- INCOMP WATER: Injected components should be specified by mole fractions in the same order as they were defined in the COMPNAME keyword.